

Please note that the links in the PEARL logotype above are “live” and can be used to direct your web browser to our site or to open an e-mail message window addressed to ourselves.

To view our item listings on eBay, [click here](#).

To see the feedback we have left for our customers, [click here](#).

This document has been prepared as a public service . Any and all trademarks and logotypes used herein are the property of their owners.

It is our intent to provide this document in accordance with the stipulations with respect to “fair use” as delineated in Copyrights - Chapter 1: Subject Matter and Scope of Copyright; Sec. 107. Limitations on exclusive rights: Fair Use.

Public access to copy of this document is provided on the website of Cornell Law School at <http://www4.law.cornell.edu/uscode/17/107.html> and is here reproduced below:

Sec. 107. - Limitations on exclusive rights: Fair Use

Notwithstanding the provisions of sections 106 and 106A, the fair use of a copyrighted work, including such use by reproduction in copies or phono records or by any other means specified by that section, for purposes such as criticism, comment, news reporting, teaching (including multiple copies for classroom use), scholarship, or research, is not an infringement of copyright. In determining whether the use made of a work in any particular case is a fair use the factors to be considered shall include:

- 1 - the purpose and character of the use, including whether such use is of a commercial nature or is for nonprofit educational purposes;
- 2 - the nature of the copyrighted work;
- 3 - the amount and substantiality of the portion used in relation to the copyrighted work as a whole; and
- 4 - the effect of the use upon the potential market for or value of the copyrighted work.

The fact that a work is unpublished shall not itself bar a finding of fair use if such finding is made upon consideration of all the above factors



Development of the B&W 800D

Contents

Introduction	3
Project brief	3
Overview	3
Drive units	4
Enclosures	8
Crossover.	12
Performance.	13
Industrial Design	13
Appendices	
I Diamond Dome Tweeter.	14
II The FST Midrange Driver	21
III The use of Rohacell® in loudspeaker cones	24
IV Tapered tube theory	26
V Sphere/tube midrange enclosure	28
VI Matrix™ cabinet	30
VII Decoupling	32
VIII Finite Element Analysis.	34
IX Laser Interferometry.	36



Introduction

Bowers and Wilkins' 800 Series first saw the light of day in 1979 with the introduction of the original Model 801. Its radical shape, composed of separate enclosures for each drive unit, was to remain relatively constant for almost 20 years, proving, like so many concepts to come from the R&D division at Steyning, that good ideas, based on sound principles stand the test of time.

The development of the flagship Nautilus speaker, launched in 1993, introduced a raft of new ideas that clearly warranted adaptation to a broader range of products, the result of which was the Nautilus 800 Series. That Series was to redefine the high-end audio speaker market and the development of the then top model in the range – the Nautilus 801 – was covered in a previous paper. The subsequent development of the Signature 800, which refined and extended some of the principles used in the Nautilus 801, was also the subject of a paper.

This paper describes the development of a new generation 800 Series, using the top model 800D to describe the principles and techniques to be found in the range. There are significant new developments, but there is much in the new models that carries over from the old. These existing techniques are discussed here once more, so that this paper may be read in isolation, without reference to the previous publications.

Project Brief

High-end audio products are about performance. The investigation of new ideas, materials and processes is a continual process, sometimes coming as small steps and sometimes as significant leaps. In this case, our engineers had been pursuing several projects that promised a significant improvement in performance and the brief was simply to incorporate the results into products.

Overview

A loudspeaker system can be divided into three basic constituent parts:

- The drive units
- The crossover
- The enclosures and supporting structure

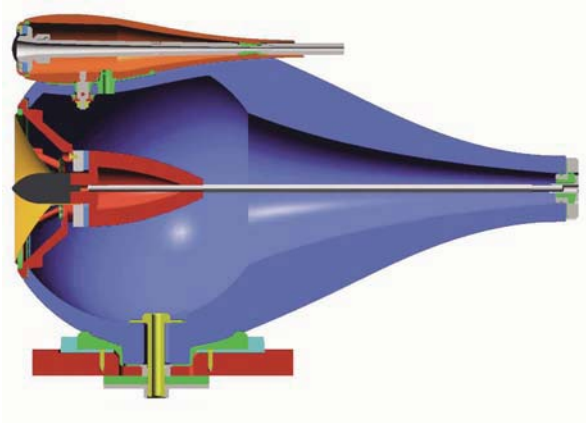
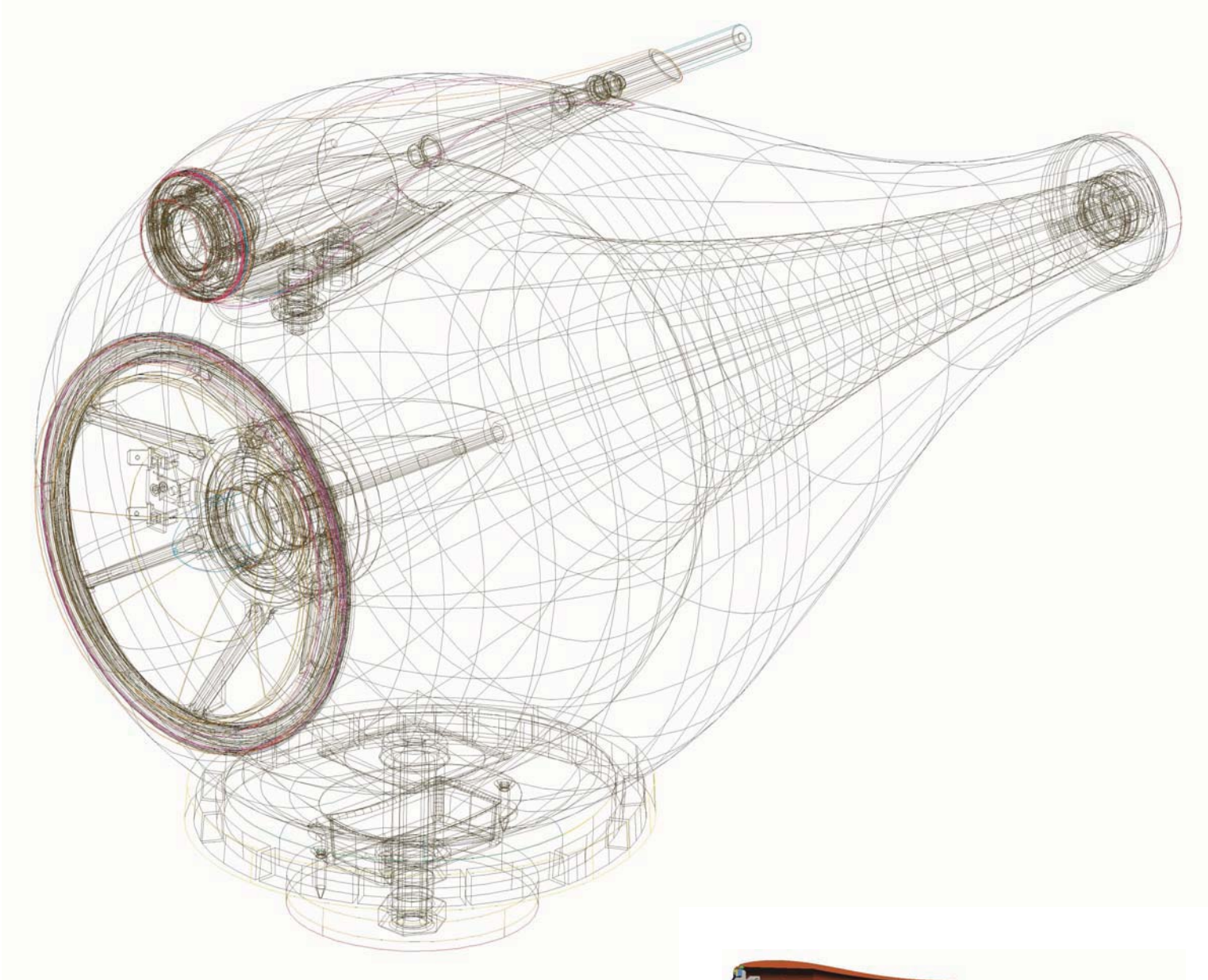
In an ideal situation, the drive units, seamlessly blended by the crossover, should transmit a perfect audio replica of the electrical input signal. The rest of the structure should remain perfectly stationary and serve only to support the drive units, absorb the unwanted radiation radiated from the rear side of each drive unit diaphragm and be shaped to aid even distribution of the sound away from the loudspeaker. How good a speaker sounds can be measured by how close the designer can get to this ideal. In the real world, of course, we fall somewhat short. Drivers suffer from distortions of all kinds and enclosures vibrate and add their own coloration to the sound. Crossover components add unwanted artifacts to the electrical signal before it even reaches the drivers.

We shall examine our design philosophy to all these categories separately, but in fact, in the design process, they must be treated as a whole, because they all interact. The choices the designer makes in one area are affected by what he has to work with in another. Inevitably, choices have to be made and it is down to the skill of the design engineer to make a balanced judgement and optimise the whole. It is a skill that combines science with art. The science provides understanding and points the way forward. For as long as the scientific understanding is incomplete, however, an understanding of the art of music is essential. In high-end audio, it is not sufficient simply to achieve a pleasant sound, the designer must strive to recreate as closely as possible the impression of being at an event, of being able to imagine performers in front of the listener, of raising the goose bumps on the skin and hair on the back of the neck. That is the target, and virtually impossible to describe by a set of numbers.

The listener must be the final arbiter of how well the target has been met. All we can do within the scope of this paper is to examine the science. In the sections immediately following there is a general overview of each of the techniques used and they are covered in greater detail in the Appendices at the end of the paper.



Drive Units



Perhaps the most radical of the new technologies used in the speaker is the diamond dome of the tweeter. The acoustic development is covered in detail in Appendix I.

One of the surprising outcomes of the new design when compared with the existing aluminium dome design is that the -6dB frequency is lower (The blue horizontal line in figure 4 represents the -6dB level after the tweeters are equalised flat to 90dB by the crossover). This may at first glance seem strange, considering that diamond is much stiffer and has a significantly higher break-up frequency than aluminium. The answer is simply to be found in the 'ideal' response of an infinitely stiff dome of the same shape, which suffers a deep dip in the response around 70kHz because of the difference in arrival times of sound generated at different parts of the dome (Represented by the green shaded area in figure 1). At 70kHz , the wavelength of sound in air is 4.9mm (0.19in) at 20C , which is comparable with the height of the dome. That the aluminium dome has the higher -6dB frequency is simply because the response is on the way down from a high amplitude resonance at 30kHz .

We took the view that the diamond dome should follow this ideal as closely as possible and we should not attempt to achieve a flatter acoustic response through various devices that would either cause the total radiating area to deliberately deviate from piston-like behaviour at a lower frequency or by engineering cavity effects in front of the diaphragm.

Our listening experience had repeatedly and consistently shown that the most important criterion affecting the sound quality was how closely the radiating surface remained piston-like in the accepted range of human hearing below 20kHz . We were therefore not tempted by any perceived marketing need to follow popular (mis)conceptions of what is required to properly convey the improvements offered by high sampling rate digital recording formats. We kept the acoustic response of the infinitely stiff dome as our target. If one removes the acoustic time delay effects by examining the structural acceleration response of the dome,

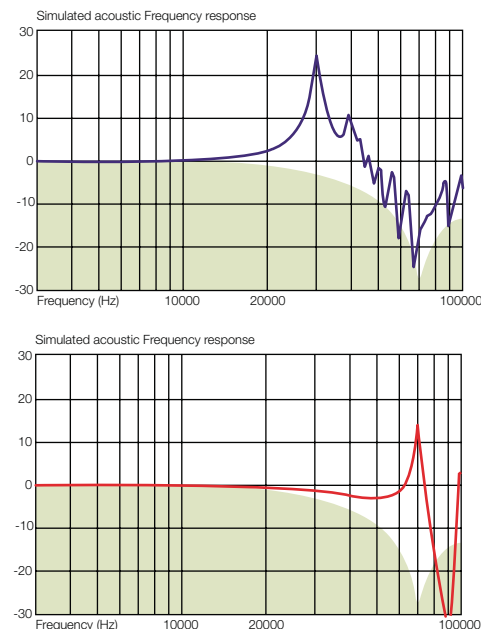
one sees that it is flatter and more extended, as expected (see Appendix I).

It should be remembered that deviation from piston-like behaviour does not suddenly happen when the break-up resonance frequency is reached. It builds up from a much lower frequency. It is similar to the effect of anti-aliasing filters used in digital recording. Those used in the standard 44.1kHz CD format may have cut-off frequencies above the accepted limit of human hearing, but deviations in the phase and associated group delay begin well below 20kHz . It is the shifting of these build up effects well above the limit of hearing that is most important, not necessarily maintaining a flat acoustic amplitude response to 100kHz or whatever, although, of course, the two are related.

That it is possible to produce a diamond dome at all is due to relatively recent developments in the production of industrial diamonds.

The standard technique for synthesising diamond is to simulate the conditions that occur in nature, ie the high pressures and temperatures that are found inside a volcano. The technical difficulty in achieving temperatures as high as $2,100\text{C}$ ($3,800\text{F}$) and pressures exceeding 50 kbar limits the size and shape of the diamond components that can be manufactured by this process.

In the 1980s, the invention of a chemical vapour deposition (CVD) technique for growing diamond overcame this limitation: the deposition temperature was halved and, more critically, growth could now be achieved at sub-atmospheric pressures. The technique succeeds in producing diamond under conditions for which graphite is the thermodynamically stable form of carbon by creating a carefully balanced chemical environment that stabilises the diamond surface as it grows; in effect, the kinetics win over the thermodynamics. This very specific environment is generated by exciting a gas mixture of hydrogen with a small percentage of an alkane (carbon source gas) and other gases (such as argon and oxygen). The resultant plasma contains alkyl radicals, hydrogen atoms and



1 FEA simulated acoustic responses of aluminium (top) and diamond (bottom) domes. The response of an 'ideal' dome is shown shaded in each case.



2a



2b



2c

2 Diamond dome manufacture.

a Domes awaiting removal from the forming substrate.

b Laser cutting the outside diameter.

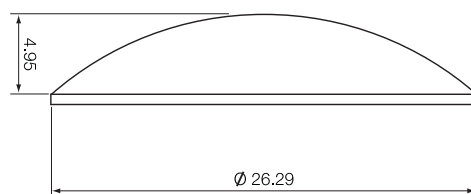
c Checking material thickness.

high-energy electrons. A range of power sources can be used to excite the plasma, the most common being microwaves, heated filaments and arc discharges. The diamond is deposited directly onto a suitable substrate material, for instance tungsten, molybdenum or silicon. This substrate can be removed after deposition to leave a freestanding diamond layer. The layers produced can be millimetres or microns thick with areas greater than 100 cm². It is also possible to replicate complex shapes machined into the substrate. The diamond itself is polycrystalline and of high purity and, because the properties are selected and controlled, diamond materials grown by the CVD process can actually outperform natural diamond in many applications.

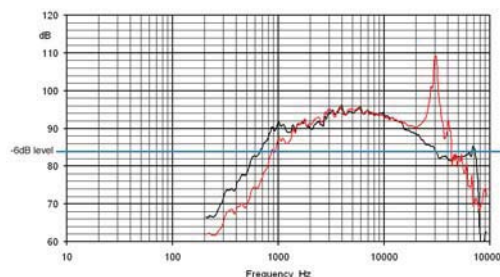
In developing the tweeter dome, B&W worked closely with one of the world's foremost producers of industrial diamonds, Element 6, based in Ascot, UK. As in so many industrial applications, although the basic process was well established, there were practical difficulties peculiar to this application that had to be overcome. Depositing diamond to the profile of the spherical section of the dome itself was fairly straightforward, but the vertical ring location for the voice coil (see figure 3) proved particularly tricky. Forming and ejecting with parallel sides and maintaining material thickness at the sharp corner were difficult. This part of the profile is crucial both in ensuring repeatable accurate location of the voice coil and also in increasing the dome's stiffness to raise the first break-up frequency. This is the first time such a profile has been manufactured and the design is patented.

The dome itself does not constitute the whole of the radiating surface. The supporting surround plays an important role in determining the tweeter's response.

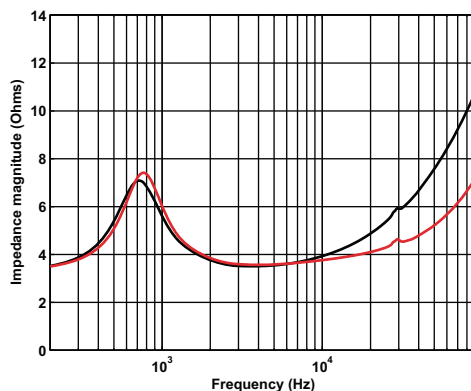
During the development of the Nautilus 800 Series, deficiencies in the plastic film half roll surround used on the then standard tweeter design were ameliorated by using a flat foam polymer surround. Its motion remained better phase matched to that of the aluminium dome and gave a smoother overall response. However, in the new systems, we wanted to use crossover filters with more gradual roll-off



3 Diamond dome profile



4 Responses of new diamond dome tweeter (black) and Nautilus 800 Series tweeter (red)



5 Tweeter impedance with (red) and without (blue) a silver layer on the magnet centre pole.

Midrange

rates (see the subsequent section on the crossover) and this necessitated lowering the tweeter's fundamental resonance frequency. This could only be achieved by reverting to a half roll profile to increase compliance, but we were able to take advantage of a new synthetic rubber material that avoided the shortcomings of the original plastic film. We were thus able to achieve good phase coherence with the dome and usefully lower the fundamental resonance frequency.

Frequency response deviations from the ideal are not dependent solely on the dome and surround. Any moving coil drive unit is a current driven device, with the force on the voice coil represented by the formula:

$$F = Bli$$

where F = force, B = magnetic flux density, l = length of coil in the magnetic gap and i = current.

Yet for various reasons, mainly to do with controlling bass response, amplifiers are voltage sources. The high frequency response of a drive unit is therefore affected by the inductance of the voice coil and, in order to maintain high frequency response, the inductance should be minimised. To that end, not only does the tweeter employ a single layer ribbon wire voice coil to minimise the number of turns, it also uses a silver plated centre pole in the magnet structure.

Copper is more usually used for this purpose. The electrically conducting layer acts as a shorted turn in the secondary windings of what is in effect a transformer and reduces the inductance of the primary windings (the voice coil). Accommodating a layer of non-magnetic material widens the magnetic gap, with a resultant decrease in flux density and hence drive unit sensitivity. Silver, having a higher conductivity than copper, is effective with a thinner layer and is used here to maximise sensitivity.

Both the tweeter and bass drive unit diaphragms of the 800D are designed following the 'stiff is good' principle. However, good reproduction in the midrange has a particular requirement that precludes this approach if a single drive unit is to be used to cover the whole range. With stiff diaphragms, the dispersion progressively narrows as the frequency increases and the wavelength becomes similar to or smaller than the diameter of the diaphragm. With bass units, this factor is never a problem, because the wavelength is always significantly greater than the size of the drive unit. At 400Hz, the wavelength is just under 860mm (34 in), compared to, say, 380mm (15 in) or 250mm (10 in) or less for the bass drive unit. At 4kHz, the wavelength is 86mm (3.4 in) and so with any drive unit of a size large enough to give high output levels with low distortion at the bass-to-midrange crossover frequency, beaming is likely to be a problem. Off centre listeners are going to hear a sound with a significantly different balance from that on axis, and image precision will suffer.

Having established that we do want to achieve high sound levels and do not want to use more than one drive unit, the best option is to use a drive unit with a more flexible cone material. That does mean that the cone is virtually certain to be operating in its break-up region for much of its usable range, but the usual deleterious effect of this (delayed resonances colouring the sound) is ameliorated greatly if the correct material is chosen.

Woven Kevlar® has been used by B&W since 1974. For the Nautilus 800 Series, the way we used Kevlar in midrange-only (as opposed to bass/midrange) drive units was improved by the use of a new design of outer cone support or surround. Such drive units go under the name FST, standing for Fixed Suspension Transducer.

For the Signature 800 and Nautilus 800, the magnet structure was improved by using a Neodymium-Iron-Boron (NeFeB) magnet driving a thicker top plate. The use of a short coil in a long magnetic gap lowered harmonic distortion and improved detail retrieval. The reduced bulk of the magnet had a minor secondary benefit in reducing the bulk of obstructions behind the cone and hence the amount of sound energy from the rear of the cone being reflected back through the cone to add delayed coloration. This approach is carried over to all models in the new 800 Series. Completely new to this Series is the chassis (basket), which provides greater strength than before without compromising the open area of the original. The use of Kevlar® in the FST drive unit is discussed in detail in Appendix II.



Bass Unit



The 800D uses two 250mm (10-in) diameter bass drive units. At B&W, we have long promoted the use of stiff, rigid cones for bass drivers. Bass/midrange drivers are a different matter, because of the same bandwidth conditions that apply to the FST midrange driver, but for bass-only drivers in 3-way systems, the ability to withstand deformation when subjected to the high pressure differences inside and outside the cabinet is the best way of achieving that dynamic performance often described as 'slam'. The stiffness also pushes the onset of break-up to higher frequencies, extending this piston-like behaviour.

At B&W, we have commonly used two materials for this application – aluminium and a fibre pulp mix of kraft paper and Kevlar, further stiffened by resins. Both materials are stiff, but metals in particular suffer high Q resonances outside their working range, due to their low inherent damping. They must be well attenuated by the time the break-up region is reached to avoid intrusive coloration. In the Nautilus 800 Series, the paper/Kevlar® mix was chosen over aluminium for two reasons:

- It was difficult in practice to form aluminium cones of large diameter that fulfilled the bass alignment criteria. Either they split during forming or the thickness had to be increased such that they became too heavy.
- Paper/Kevlar® has higher internal damping and break-up resonances were better controlled.

However, even paper/Kevlar® is fairly dense and results in relatively thin section cones if a reasonable sensitivity is to be achieved. This can allow a certain amount of sound energy from inside the cabinet to pass through and cause low levels of coloration. As general driver, cabinet and crossover quality has improved in recent times, even this very low level of coloration deserves corrective attention and the sandwich construction of our PV1 subwoofer driver has shown that a thick cone construction can have benefits in this area.

Simply adding thickness, however, is not a universal panacea. In a passive speaker, we cannot afford to add mass at the same time. The choice of alignments becomes too

restricted and one cannot make up for lost sensitivity by adding amplifier power, as is the case with a powered subwoofer. So, work began on finding a material that would add further stiffness, increase inherent damping and act as a better sound barrier than the materials we had used in the past.

The material chosen has a composite sandwich construction. Sandwich construction cones are not new. The famous Leak Sandwich speaker of the 1960s used a bass cone having an expanded polystyrene core bounded by thin aluminium skins, as did the flat fronted, oval B139 from KEF that followed shortly after. Both these diaphragms were thick and were a better sound barrier than the paper cones common at the time. However, they were fairly heavy and expanded polystyrene as a core material can now be improved on in terms of stiffness and internal damping to achieve higher break-up frequencies and better-controlled resonances.

The core material chosen was Rohacell®, again an expanded foam material and one that is commonly used in aircraft construction, due to its light weight and relatively high strength. This is bounded on both sides by carbon fibre skins in woven mat form with a high level of resin to add stiffness. Neither Rohacell® on its own nor a Rohacell®/carbon fibre sandwich is a new cone material, although the introduction of both is relatively recent. What is novel in the 800 Series is the cone thickness that has been achieved through improvements in the manufacturing process. Most Rohacell® cones are in the 1-2mm thickness range. In the 800 Series, the core thickness is 8mm, which aids the suppression of sound transmission considerably.

The audible result of the new cone material, with its enhanced stiffness and reduced sound transmission is to improve what is referred to as bass attack or dynamic bass. Most bass lines in music do not consist of steady tones. The waveforms have an extended frequency range and the reduction in coloration in the upper bass/lower midrange cleans up the presentation significantly.

A detailed discussion of Rohacell®/carbon fibre sandwich cones is to be found in Appendix III.

Enclosures Tweeter

The Tweeter incorporates Nautilus™ technology through the use of a tapered tube, filled with wadding attached to the rear of the unit and matching the hole through the pole (See appendix V). The exponential profile has been designed to ensure that the cut-off frequency of the tube is low enough to absorb all the energy in the operational bandwidth of the tweeter, but allowing a shorter tube than in the Nautilus™. It also allows the absorptive wadding to be packed loosely at the mouth of the tube and to become gradually compressed towards the end. This allows the sound energy radiating from the rear of the dome to pass through the pole piece and into the tube without being reflected back up towards the dome. This variation in packing density ensures that the acoustic impedance is varied smoothly, and that there are no sudden changes that would cause such a reflection of energy. As the passband of the tweeter is similar to that in Nautilus™, the onset of cross modes in the tube is not a problem, occurring well above audibility in the human ear.

A secondary use for the tube is as a heat sink. The small dimensions of the magnet assembly result in a low thermal mass. Making the tube of zinc alloy and ensuring a good thermal bond to the magnet back plate significantly reduced the operating temperature of the unit. When fed music from a 600W amplifier run just below clipping, the operating temperature is reduced by around 20C. In fact the tweeter was found to be capable of withstanding unclipped high frequency peaks from an amplifier rated up to 1kW, without the coil burning out. The tweeter/tube combination is housed in an outer die-cast shell which defines the outer housing of the unit. The tweeter diaphragm only moves a maximum of 0.5mm. Therefore, it is crucial



to isolate it from mechanical energy arising elsewhere in the system. To this end, the tweeter and tube are held in the housing with rings moulded with a Shore 1A hardness elastomer. The housing in turn is decoupled from the midrange enclosure below by the use of two isolator pads of high compliance gel material.

The top isolator has been shaped to sit in the scallop of the midrange head enclosure and cradle the underside of the tweeter housing. Raised ribs have been designed into this isolator to create maximum compliance at this interface, in order to absorb any energy transmission between the midrange head enclosure and tweeter body. The bottom isolator sits between the connector and the underside of the midrange head enclosure to ensure that both the sections of the Molex cable connector are isolated from the midrange head enclosure. The tweeter is allowed to float free and reproduce the input signal without any external interference.

The midrange enclosure is carried over from the Nautilus 800 Series with a small change to the exterior design where the tweeter is mounted. The tweeter is more enveloped, but this is an aesthetic development with no acoustic significance, except that the tweeter is mounted further forward (see the section Crossover).

The unique sphere/tube design overcomes the bandwidth limitations of simple tube loading and is described in Appendix VI.

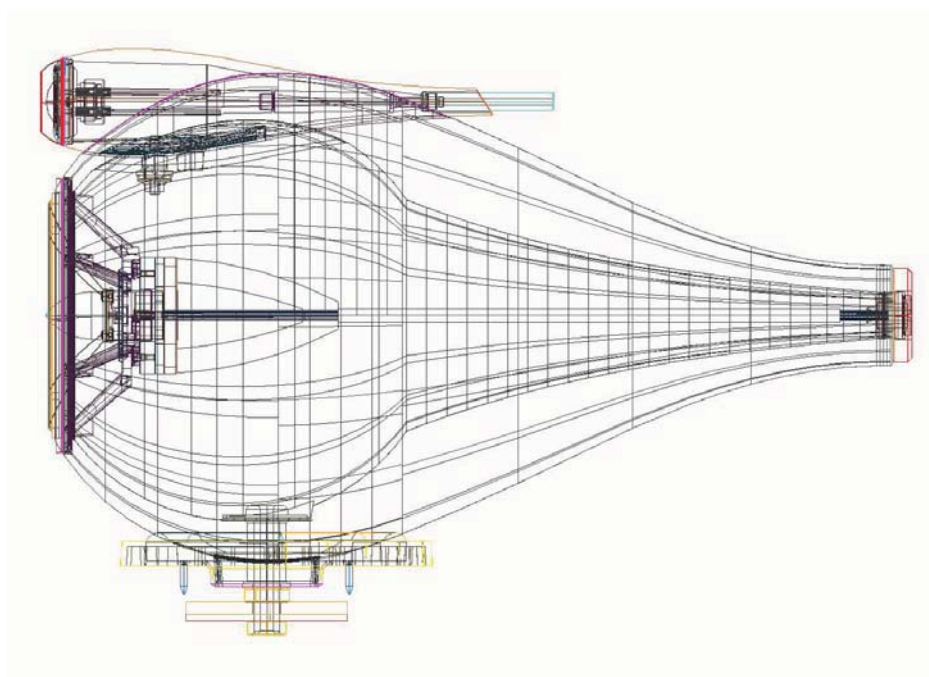


6 Forming curved cabinet sides at B&W Denmark

Because tube loading results in an overdamped high-pass alignment, it is not applicable to passive system bass cabinets because of the inability to add boost equalisation. Therefore, like the Nautilus™800 Series products, the 800D employs a Matrix™-braced vented-box enclosure (see appendix II).

The inertness of the cabinet is further enhanced by using 38mm thick panels, also contributing significant mass. In addition, smoothly curving the rear surface greatly adds to the stiffness of the cabinet and gives an interior shape that modifies the internal acoustic resonance modes, since there are fewer parallel surfaces. The combination of an internal Matrix™ construction, together with both a massive and stiff external 'skin', makes the combination uniquely resistant, not only to sound transmission from inside to outside, but also to intrinsic cabinet structural modes.

Bending thin wood laminations under heat and pressure is widely used in the furniture industry for the manufacture of chairs. However the ability to accurately match and join two such curved panels together without a witness groove and to maintain the accuracy required to fit the Matrix™ panels inside is beyond the capability of many suppliers. Special storage conditions for the raw laminations, with controlled temperatures and humidity are essential and sophisticated CNC 5-axis routing machines are required to shape the edges and cut-outs of the curved panels.



The movement of air in and out of tuning ports, which may represent quite a considerable physical displacement, often causes ‘chuffing’ noises as the air interacts with the discontinuities found at the internal and external ends of the port tube. These noises occur as turbulence is formed at the discontinuities. Even when the inside and outside ends of the tube are given smoothly rounded profiles, the problem is not totally cured, though it is mollified.

The reflex port is a well-established device to improve the bass response of a transducer in an otherwise sealed box of finite dimensions. As the power handling, excursion and linearity of bass drivers have steadily improved over the years, the limitations of a simple tuned port have become apparent. At low levels the behaviour of the air in the tube can be correctly approximated to a solid piston bouncing on a known air volume and at a specific tuning frequency; a readily predictable and essentially acoustic problem. At higher levels, aerodynamic effects become increasingly important and the associated loss means that a given rise in bass driver input level will yield a smaller rise in clean port output level. This also means that the port is not reducing the excursion of the bass driver as effectively and the system will thus behave increasingly like a lossy sealed box design; the combined effect is known as ‘port compression’ and can often create an ultimate ceiling to achievable bass levels.

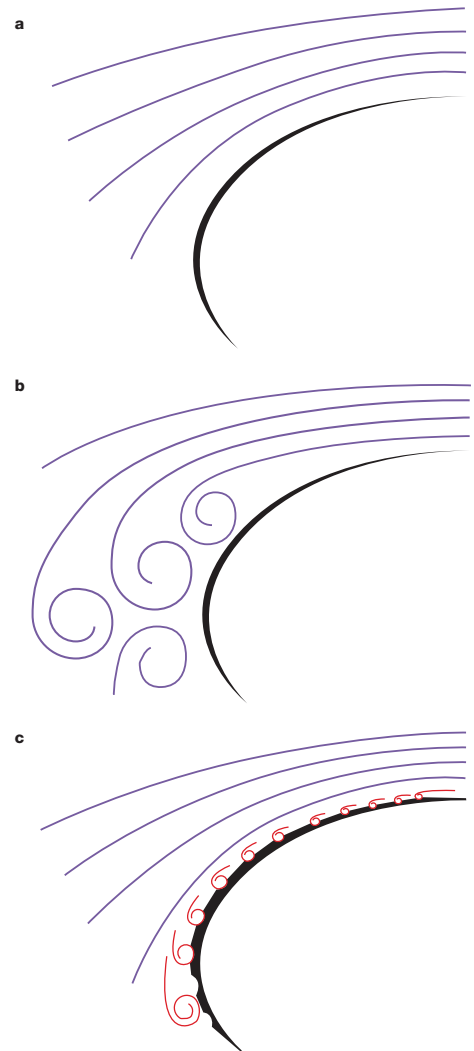
Well before any ceiling is reached, the energy losses associated with port compression cause problems and it is the way energy is lost rather than the amount lost that causes serious acoustic problems. At very low velocities, and with a perfect entry, air travelling through a real port tube will pass smoothly along streamlines, which do not interfere with one another. Close to the walls of the tube is a thin boundary layer caused by skin friction, with a relatively high velocity gradient. It provides the transition between the stationary walls and the moving air. Laminae of air rub against each other causing pressure drag through noiseless viscous losses. These are minimal at low levels but increase at a geometric rate in proportion to velocity. At high enough velocities, if the tube is excessively long and rough (or just very rough), the high shearing energies in the boundary layer can

make it turbulent, which may be heard as wind noise, particularly because it can excite the organ-pipe resonances of the tube.

Far more serious problems occur when laminar airflow tries to leave the tube at high velocities. If the curvature of the diffuser (flare) is too sharp, the minimal momentum of the air at the base of the laminar boundary layer is insufficient to pass the resulting sharp, adverse pressure gradient without stopping or stagnation. Slightly downstream, the pressure gradient (higher velocity with lower pressure to lower velocity with higher pressure) causes the flow at the base of the boundary to reverse and a turbulent eddy is created in the form of a rotating torus (this is how smoke rings can be blown). The boundary layer now becomes the region that is between the eddy and the main flow, but it has now separated from the surface of the diffuser. It tries to follow the pressure gradient formed by the turbulence, but may form more eddies trying to do so, and so on.

The turbulent wake thus created is responsible for the ‘chuffing’ noises that even gently flared ports can produce under some conditions. The separation can sometimes be so extreme that a turbulent jet can hit a listener at some distance from a speaker. The aerodynamics of reflex ports is actually rather complex and somewhat unusual in that it involves alternating flow in two different pressure regimes (at and below port resonance), three octaves of the frequency spectrum (different systems have different tunings), completely indeterminate starting conditions and well over 100dB of level difference.

Aerodynamics research into reflex ports at B&W is still in its infancy. Classical wind tunnel work is very difficult because the alternating flow makes a mockery of smoke trails. Recent work with Computational Fluid Dynamics has shown that ports are very difficult to model accurately. This is partly because of the large number of variables, and also because the flow regime is influenced so heavily by small-scale turbulence creation, which is less well understood than large-scale fully-developed turbulence (more is known about how aircraft stay in the air than how midge flies do). Therefore, work has been largely empirical, using comparative rather than



7 Representation of streamlines exiting port flare.

- a** Laminar airflow following curvature of flare
- b** Higher velocity turbulent airflow separates from surface of flare causing large scale eddy formation
- c** Small scale turbulence due to dimples encourages laminar streamlines to remain attached to boundary

absolute benchmarks, because it is difficult to make reliable measurements of turbulent noise.

Theoretical predictions of air velocities down the port were checked with a new Doppler measurement system, to establish the kind of flow regime operating around chuffing levels in terms of the Reynolds number (a dimensionless indicator of turbulence levels). This showed that, with care, it was possible to maintain laminar

flow down the port tube, but that air could detach from the flares at fairly modest levels. Simply making the flares more gentle would not guarantee silence.

Anyone studying aerodynamics will soon learn that turbulence is not always a problem. In fact, many aerodynamicists engineer turbulence to their advantage (indeed, some aircraft would not stay in the air without it). If a boundary layer is turbulent prior to the stagnation point it will be less inclined to separate because the base layer has increased kinetic energy. This means that the surface flow can be swept further downstream before pressure conditions stagnate it and the lower pressure in the layer that results from the higher velocities within the eddies adheres the main flow to the surface profile better. Thus, small-scale turbulence can be used to delay the large-scale turbulence caused by separation.

Artificially creating turbulence in the air moving down the tube can delay the onset of chuffing to higher bass unit input levels, but problem wind noise happens far earlier, especially when turbulent air is sucked back in to the port as the flow alternates. In addition, the thickened boundary layer effectively constricts the flow, causing pressure drag and thus airflow compression. This constriction also alters the effective area of the port, which in turn affects the Helmholtz tuning. Thus it is otherwise desirable to delay the onset of turbulent flow down the tube to as high a level as possible. A more optimal solution would thus be to use a smooth tube and limit artificial turbulence creation to the problematic stagnation area. (figure 7)

It is quite easy to produce turbulence where it is needed; aircraft use vortex generators, (vertical strakes) ahead of separation points. These strakes project into the main flow and are very effective, but when the same technique is applied to port flares it creates too much wind noise at lower levels.

Enter the golf ball. It can travel twice as far as an equivalent smooth ball because of its distinctive dimpled surface. The dimples are very carefully shaped to produce tiny separation points and favourable conditions for the creation of vortices within them. The ball is thus covered

by a thin turbulent boundary layer that moves the separation point further round the ball. This decreases the ball's wake and hence its drag, and it was this technology that was used to improve the performance of the port flares. Because a round port flare is axisymmetric, it was first thought that a series of rings with the cross section of a dimple might work (and be easier to prototype). However, the regular vortices formed simply became the new separation points and at lower levels there was audible wind noise because they were so abrupt. So real, pseudo random dimples were tried on the surface of the flare. These immediately improved the chuffing phenomenon as predicted, but there was still wind noise caused by deep dimples at the edge of the tube where flow velocities were highest. These were filled but at the expense of earlier separation levels.

A process of experimentation refined the size, shape and distribution of the dimples to maximise headroom and minimise wind noise. Small, smooth dimples are thus used where velocities are highest and larger, more abrupt dimples are used where velocities are lower. This greatly refines the exit flow regime and also ensures that a minimum of turbulence is carried back down the tube when the flow is reversed. It was found unnecessary to make the dimples totally random over the whole flare, but as long as they are locally irregular, perceptible wind noise is incoherent and unobtrusive.

In the case of the 800D, the port is down firing, so more wind noise is acceptable and the dimples are optimised for maximum high level flow. In use, the dimpled ports delay the nuisance chuffing noise to significantly higher levels. However, and perhaps of even greater importance, when large-scale separation does occur the resulting turbulence is far more incoherent and thus less apparent. A reduction of 6dB in certain regions of the noise spectrum was measured, particularly around the problem organ pipe frequencies. Port compression is also decreased and the tuning frequency is more stable at higher levels.

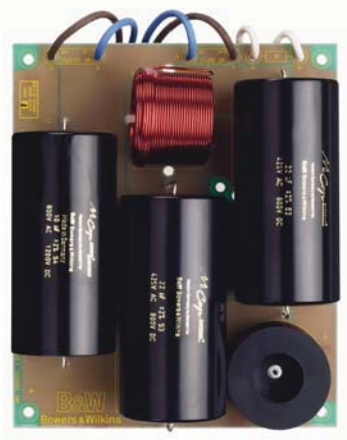
Having achieved excellent cabinets for each of the drive units independently, it is important that vibrations and radiation from each driver do not leak into the enclosures of others. Decoupling has been used extensively in the 800D to isolate drive units, apart from bass units, from their enclosures and the individual enclosures from one another. A discussion of the technique can be found in Appendix VIII.

Decoupling was not used for bass or bass/midrange units in the Series. While it has the potential for reducing vibration in cabinet walls, listening tests have always confirmed that this is more than offset by a reduction in the speaker's ability to portray 'slam'. A similar effect is noticed if the bass cabinet is not firmly anchored to the floor, for example using spikes. It should be noted that it is only bass drive units that are required to operate in the stiffness region, below their fundamental resonance frequency. All others operate entirely in the mass controlled region.



8 Gel gasket used for vibration isolation between tweeter and midrange enclosures

Crossover



Every effort was made to specify crossover components of the highest calibre. The science behind why certain crossover components sound better than others is not fully understood. That polypropylene capacitors sound better than electrolytics is well accepted and can be explained by the behaviour of the dielectric properties as the signal changes. What is not so clear-cut is why different capacitors, with ostensibly the same specification, can sound so different from one another. The difficulty in mapping physical properties to the perceived performance characteristics further compounds this problem. Whilst we understand some of the criteria, extensive listening tests are virtually the only tool at our disposal to ensure that the final choice of components is correct.

For the new 800 Series, we worked closely with one of the foremost European capacitor manufacturers to further optimise one of their existing designs. All inductors are air core for minimal distortion and thin film non-inductive resistors were used in critical applications. Where necessary for increased power handling, the resistors are thermally bonded to the cast aluminium plinth, which houses the crossover.

One of the notable things that comes from critical listening tests is that, no matter how good the crossover components are, all other things being equal, the fewer of them there are the better. That statement should be tempered by the qualification that the response of the speaker should be relatively flat with a good phase relationship between the drive units, but basic signal quality is never enhanced by putting in an extra component. To that end, one should try to minimise the component count whenever possible.

The simplest filter configuration is 1st-order, with a single series inductor for the low-pass and a single series capacitor for the high-pass. The fact of the matter is, however, that it is nigh impossible to have a truly 1st-order crossover in a passive loudspeaker system. One cannot simply look at the component count. Drive units themselves are inherently bandpass devices. They have a 2nd-order high-pass characteristic and usually a very high-order low-pass characteristic. These shapes must be added to the transfer function of the electrical network

and, even though the drive units' natural cut-off frequencies may be well removed from the crossover frequency, the phase response associated with the drive unit magnitude response usually intrudes through the frequency range of the crossover to disrupt the way the outputs of the two units add together.

In any case, a true 1st-order filter (assuming one had drive units with perfectly flat responses) is not particularly desirable. The two parts add together in quadrature (constant 90° phase difference) and, while this is of no consequence in the one-dimensional world of current flowing in a wire, when you have two drive units separated in space, things are rather different.

On the reference axis, the responses add together to give perfectly flat amplitude and phase response. (figure 9)

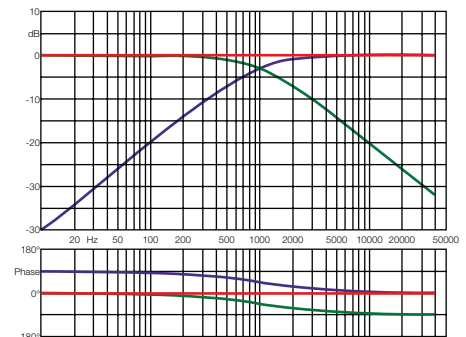
As you change the measuring axis to move downwards towards the lower drive unit, the upper unit becomes delayed in time. The two units become more in phase at crossover and there is a peak in the response of up to 3dB. (figure 10)

As the measuring position is moved up, the lower unit becomes delayed and the units become more out of phase, with a corresponding dip in the response at crossover that reaches a complete null when a 180° phase difference is realised. (figure 11)

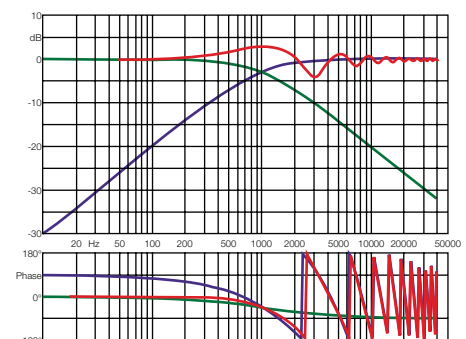
In both off-axis cases, the response oscillates as the units go in and out of phase due to linear time delay.

This situation of a lobe asymmetrically placed around the reference axis is not ideal, leading as it does to rapid changes in response with relatively little height change. A preferable situation is created when the units are in phase at crossover. The lobe is aligned with the reference axis and the same changes in listening height result in much smaller changes in response shape.

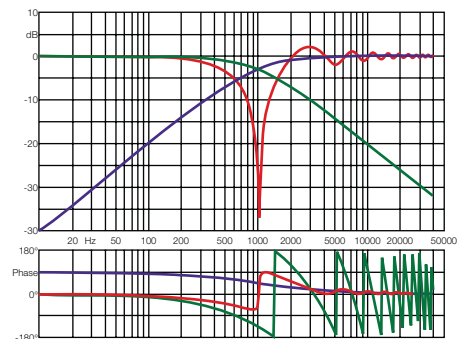
In the case of the midrange to tweeter crossover, we were able to use a single capacitor in series with the tweeter and achieve a response shape very close to a 2nd-order Linkwitz-Riley. Like



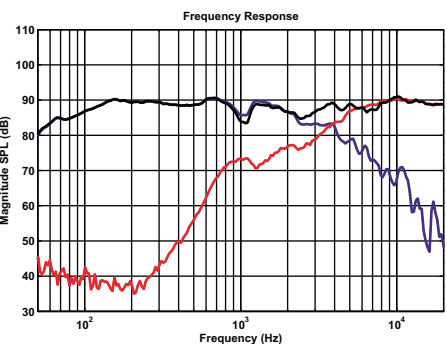
9 1st-order filter on axis



10 1st-order filter below axis



11 1st-order filter above axis



12 graph of midrange (blue), tweeter (red) and sum (green) responses

that theoretical shape and with the units nominally time aligned, it required the tweeter to be connected in reverse polarity for the units to be acoustically in phase with one another.

Reverse polarity connection of drive units has always been avoided at B&W in recent years, it being felt that the sound lacked coherence and focus. There is inevitably phase distortion and its associated group delay through any practical crossover, but it has been deemed preferable to restrict waveform distortion to the limited frequency range immediately each side of the crossover frequency rather than impose a broadband change through polarity reversal of any drive unit. In this case, positive polarity connection would have led to a sharp null at crossover, so this was avoided by realigning the relative time delay of the drive units. Rather than them being truly time aligned, the tweeter is advanced by half a wavelength at the upper crossover point of 4kHz to bring it in phase with the midrange unit when fed with the simple filter configuration. The addition of the drive units is illustrated in figure 12. The tweeter sits noticeably further forward than on the previous series models. (figure 13)

It was strongly felt that this approach – sacrificing true time alignment for a less complex crossover – gave superior results in terms of definition and imaging.

However, the bass drive unit's high voice coil inductance and the fact that the midrange drive unit's fundamental resonance frequency was fairly close to the desired crossover frequency meant that a higher component count was the best solution for the bass to midrange crossover. Nevertheless, the same in-phase drive unit relationship and positive polarity connection was followed.



13 side view of tweeter on head.

Several aspects of the speaker's performance are shown in figures 14 and 15, but many aspects of performance cannot be represented simply by a series of numbers or graphs; they can be assessed only through careful listening tests.

The Nautilus 800 Series products always had exceptional imaging, especially the 'headed' Nautilus 800, Nautilus 801 and Nautilus 802, which was in no small measure a function of the geometry of the enclosures. It is, for example, quite easy to locate a central image from a stereo pair, even when listening from outside the area between the speakers. The new 800 Series improves on this by adding still better stability with a better impression of height information. This last first became noticeable when the simple electrical filter between midrange and tweeter was incorporated.

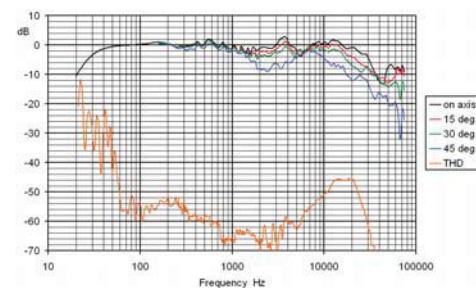
The new Rohacell® sandwich cone material delivers cleaner bass from a combination of its higher transmission loss blocking sound escaping from inside the cabinet more effectively and having a more extended piston range.

However, no matter what other features the new products employ, it is the diamond dome tweeter that captures the imagination. What it does not do is capture one's attention when listening. Rather it is an awareness that things simply sound more natural. Bright sounds do not become harsh, just bright. Everything is there in correct proportion and the nuances in the finest of detail in the input signal can be discerned and appreciated.

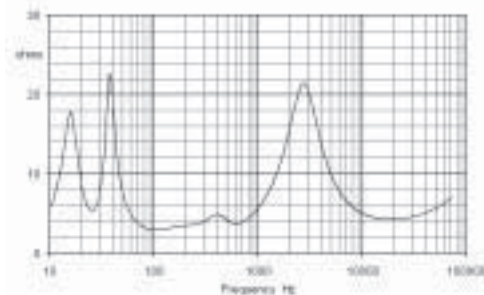
Certainly the simple crossover design coupled with the improvement in component quality has helped bring out the full potential of the diamond dome tweeter. It has also helped combine the component parts of the speaker into a coherent whole.

The styling of the 800D follows closely that of its predecessor, the Nautilus 800. That latter system's bass cabinet was in fact styled somewhat differently to the other two 'headed' products, the Nautilus 801 and Nautilus 802 in that the front baffle was curved round to the base and the cabinet was supported on the cast aluminium plinth by short pillars. That general style has now been carried through to the 801D and 802D. The bass grille has a more sculpted outline compared to the original Nautilus 800.

The Marlan 'head' design has altered slightly in the way the tweeter is more enclosed by the midrange cavity and, as mentioned above, the tweeter is mounted further forward for acoustic reasons.



14 800D – Horizontal responses and total harmonic distortion



15 800D – Modulus of impedance

Appendix I

Diamond Dome Tweeter

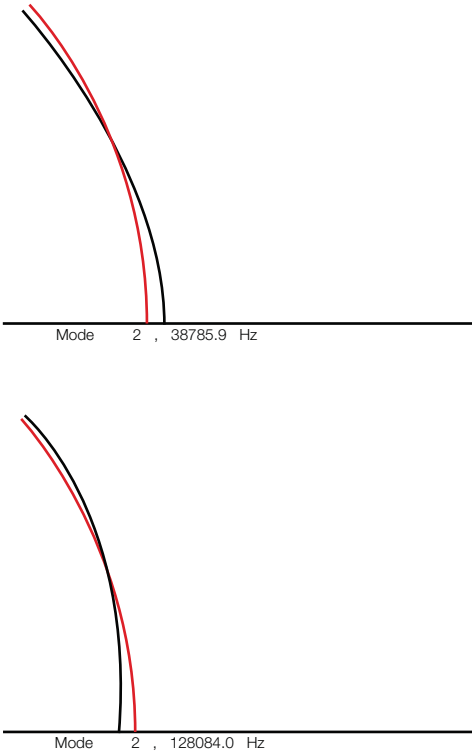
Introduction

B&W's standard 26mm diameter aluminium dome tweeter has gradually evolved over the years to give a higher and higher break-up frequency. The original tweeters had the first break-up at a frequency of approximately 26kHz whereas the latest tweeters, as used on the Signature 800 Series, have a 30kHz break-up. This improvement in break-up frequency has resulted from minor modifications in the design of the voice coil former (bobbin) such as swaging the top edge inwards to follow the dome profile (often referred to as crowning) or changing its length.

There are, of course, various different flavours of the standard tweeter in production, for example those using neodymium-iron-boron (NeFeB) and those using barium ferrite magnets, those with silver coating to the pole and those without, those with short and those with long rear tapered tubes. Also over the years we have used different surrounds (half roll plastic film and flat section foam polymer), different lead-outs (beryllium copper strip and tinsels) and a host of other variations in the quest to make the most revealing tweeter possible.

Thus the increase in subjective performance resulting from any increase in break-up frequency had to be judged against a background of many changing factors. However, it is generally accepted within B&W that a tweeter having its first resonance at 30kHz sounds better than one having its first resonance at 26kHz. This is perhaps a little surprising when the normal audible limit is generally considered to be 20kHz. However, as discussed throughout this paper, there are good reasons for pushing the break-up to very high frequencies.

So, within B&W, there has always been a motivation to increase the break-up frequency of tweeters. However, over recent years, provoked by high resolution audio formats such as SACD and DVD-A with effective sampling rates of 192kHz, the market has started to demand so called Super Tweeters, tweeters that are capable of reproducing frequencies up to 96kHz.



AI.1 First break-up mode shape and frequency for a 50µm Al (top) and diamond (bottom) dome.
Note: In all simulations, the red profile represents the dome's static shape.

The area of ultra high frequency audio in general is somewhat controversial and debates rage over which format is more accurate, whether and why either format is better than standard 44.1kHz sampling rate CD, whether humans can hear above 20kHz and so on. The resulting lack of clarity has led the market to believe that humans can hear above 20kHz and that a supertweeter is therefore required to do this. There is no credible scientific evidence at present, that the author knows of, that proves that frequencies above much 20kHz are audible, and experiments to clarify this area are very difficult to carry out.

Materials

In recent times, all B&W tweeters have used aluminium domes. Aluminium is a comparatively light and stiff material. This is beneficial because, for simple structures such as domes without formers, the break-up frequency is directly proportional to $\sqrt{(E/\rho)}$, where E = Young's Modulus and ρ = density. Clearly the stiffer or lighter a material is the better. Although aluminium and titanium are good, better materials are available. A comparison of some relevant materials is shown below.

Material	E (GPa)	ρ (kgm ⁻³)	$\sqrt{(E/\rho)}$	Relative
Aluminium	71	2700	5128	1.0
Titanium	120	4500	5164	1.0
Beryllium	318	1850	13111	2.6
Diamond	1000	3500	16903	3.3

Aluminium and titanium will give similar performance, but beryllium is approximately 2.6 times better than aluminium and diamond 3.3 times better than aluminium in terms of break-up frequency. To qualify this claim the simulated (using Finite Element Analysis, FEA) first break-up mode shape and frequency for a 50µm aluminium and diamond dome is compared in figure AI.1.

It is clear from the table above that diamond is a better material to use than beryllium from a break-up point of view. In fact diamond is the best material to use from this point of view. Beryllium does have the advantage, though, of being almost half the density of diamond. It is also claimed that beryllium has quite high damping for a metal, though at present data are not available to verify this claim.

Basic Tweeter Simulations

In Section 1, the superiority of diamond over any other material from a break-up point of view was discussed and simple simulations of domes were used to illustrate the performance improvements. However, what happens when diamond is used in tweeters?

The Model

In figure AI.2 the Finite Element Model of a tweeter is shown. In this case the surround is not included in the model to simplify the analysis and interpretation. Addition of a surround generally causes a small and consistent decrease in break-up frequency and therefore for comparative purposes this simplified model is justified. In addition the surround may introduce features in the SPL response caused by pure surround resonances (that are largely decoupled from the rest of the tweeter). These surround resonances will be common, regardless of the material used in the dome.

Modal Analysis

In figure AI.3, the first break-up frequency and mode shape for an aluminium tweeter and a diamond tweeter are compared. Taking each in turn, the aluminium tweeter is shown to have a break-up of approximately 28.5kHz. This is a little lower than for the best current tweeters used on the 700 Series mainly because a crown has not been modelled. However, the result is broadly representative of what is to be expected of aluminium tweeters.

The diamond tweeter has a first break-up frequency of approximately 80.8kHz. Here the diamond tweeter is modelled with a 40µm dome and 'Skirt'. A 40µm thickness design (cf 50µm aluminium dome) was chosen so as to compensate for the increase in density of diamond compared to aluminium (3500kgm⁻³ cf 2700kgm⁻³).

In Section 1 it was discussed that the break-up frequency of a diamond dome should be 3.3 times higher than an aluminium dome. Clearly for the complete diamond tweeter, less of an improvement has been achieved (approx 2.8 times). This compromised improvement results partly because the dome thickness is less in the diamond than the aluminium. However, a more

important factor is that the vibrational behaviour of a complete tweeter is more complex than for a simple dome and is partly dictated by the former, which in this case is common to both designs.

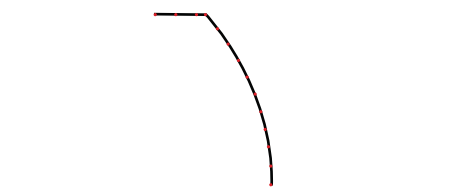
However, diamond domes clearly offer a means of considerably increasing the break-up frequency of a tweeter (at least in a virtual world).

Sound Pressure Level Response

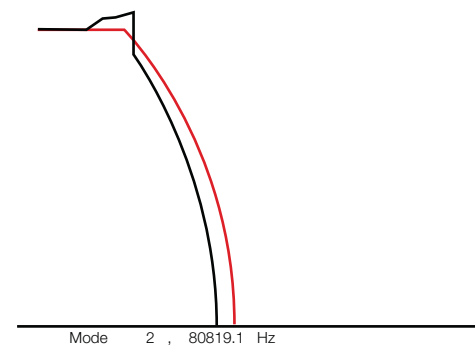
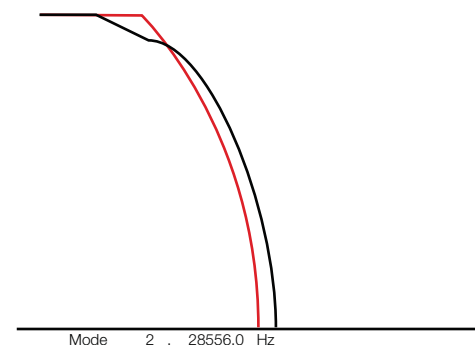
Before comparing the aluminium and diamond tweeters, some justification for the simulation method will be made. Two approaches are available: the Simple Source Method (SSM) and the Boundary Element Method (BEM). The SSM is the simpler, computationally cheap technique that relies upon the assumption that the vibrating surface is composed of a number of simple sources, each set in an infinite baffle. The BEM gives an approximate solution to Helmholtz' equation and is therefore a more complete solution than the SSM, but at increased computational expense. When using the BEM there is no infinite baffle assumption, so some kind of enclosure is required and in this work a sphere of radius 100mm was used.

In figure AI.4, a comparison is made between the SPL response from 1-100kHz of a standard aluminium tweeter calculated using the SSM and the BEM. The first thing to note is that, with both methods, the low frequency response is clearly wrong, as the surround and interior acoustics have not been modelled. Secondly, below 10kHz the BEM and SSM differ because only the BEM incorporates the effects of the enclosure. However, at higher frequencies, although there are small differences between the responses, use of the SSM is justified at least for comparative purposes.

In figure AI.5, three tweeter responses are shown. These are the responses of the aluminium and diamond tweeters (with first break-up modes corresponding to those shown in figure AI.3) together with the response of an infinitely rigid tweeter. The rigid response shows a characteristic roll off and deep null at approximately 70kHz caused by the interference effects owing to path length differences, commonly referred to as phase loss. The response of the diamond tweeter is much closer to that of the perfect



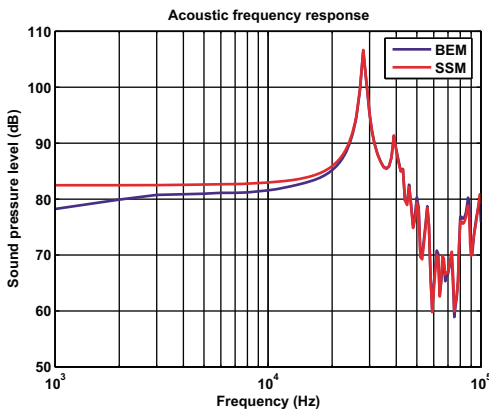
AI.2 Finite Element Model of a simplified tweeter



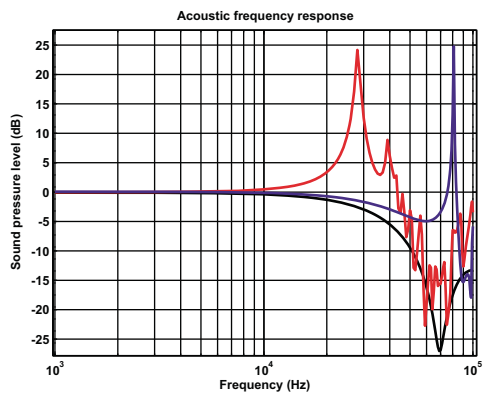
AI.3 Break-up frequency and mode shape for a standard AI tweeter and a diamond tweeter

Appendix I continued

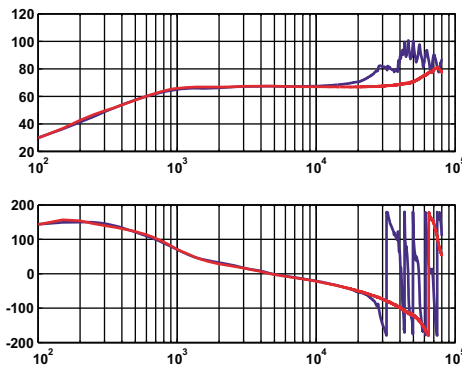
Diamond Dome Tweeter



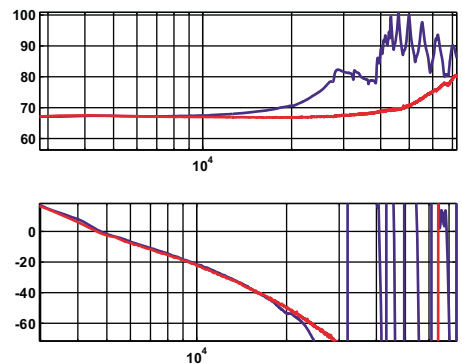
AI.4 The SPL response of an AI tweeter calculated using the SSM and the BEM



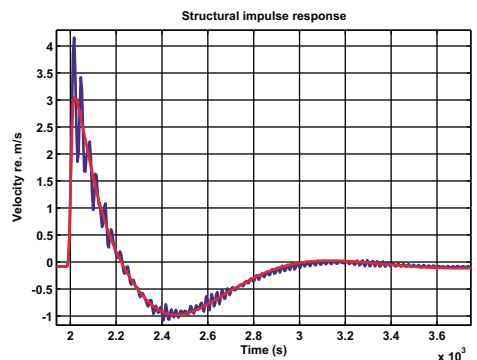
AI.5 The SPL response of aluminium, diamond and perfect, rigid tweeters



AI.6 Diamond (red) versus aluminium (blue) magnitude (upper) and phase (lower) responses



AI.7 Zoomed version of figure 6. Diamond (red) versus aluminium (blue) magnitude (upper) and phase (lower) responses



AI.8 Diamond (red) versus aluminium (blue) Structural Impulse Response

rigid tweeter below 20kHz than the aluminium tweeter. More specifically, at 10kHz, the response of the aluminium tweeter is approximately 0.8dB higher than the rigid tweeter whereas the diamond tweeter's response differs by only 0.1dB. At 20kHz, the difference is increased to approximately 4.6dB for the aluminium tweeter but is less than 0.5dB for the diamond tweeter. As discussed latter in the report, this absence of coloration in the diamond tweeter when compared to the perfect tweeter with a rigid response is thought to be the reason for the improved subjective performance.

Structural Acoustic Measurements

In the Section 2, the FEA was used to compare the performance of aluminium and a diamond tweeter. In this section structural measurements are presented.

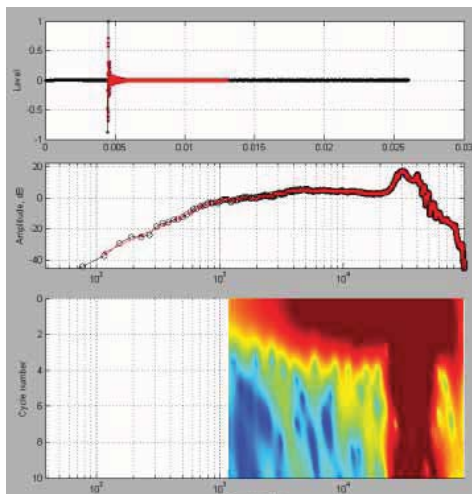
Structural Acceleration

In figure AI.6 the magnitude and phase response for the diamond and aluminium tweeter measured at the centre of the dome is shown and in figure AI.7 a zoomed version is shown. The aluminium tweeter, as expected, breaks up at 30kHz and above this frequency a number of resonances are apparent. The diamond tweeter's magnitude response is flat to approximately 40kHz before rising to a break-up frequency of approximately 74kHz.

Note: this flatness of acceleration response is really what should be quoted in specifications; it indicates a purity in real performance which is not obscured by acoustic effects such as phase roll-off. A flat acoustic frequency response can only be achieved by utilizing break-up.

Before 74kHz a number of small features are evident, the most pronounced being a small peak at approximately 65kHz. The cause of these secondary features is not clear though they could be as a result of surround resonances, tube resonances, rocking of the dome, etc.

The phase responses of the two tweeters start to deviate from approximately 15kHz (figure AI.7) with approximately 4 degrees difference at 20kHz. Though the phase responses are similar to 15kHz, the magnitude responses for the two tweeters show a far greater difference (approx



AI.9 Time-Frequency plots of aluminium and diamond

0.5dB at 10kHz and 3dB at 20kHz) and differences are evident from approximately 10kHz. As the simulations show in figure AI.5, we expect the output of the diamond tweeter to be lower than the aluminium tweeter – though care must be taken as here we are comparing an acoustic simulation with a structural measurement.

Structural Impulse Response

Figure AI.8 shows the structural impulse response of a point at the centre of the two types of tweeter (sampling rate 204.8kHz). Both responses show approximately the same rise time and overall low frequency response (to be expected) but the response of the aluminium tweeter is characterised by a high frequency ripple which results from the 30kHz resonance of the structure. When both responses are low pass filtered to exclude information above 20kHz no significant difference is evident (not shown). This makes sense because, as has been shown in Section 3.1, below 20kHz the phase responses show only very small differences at relatively high frequencies (though there is some magnitude difference).

Structural Time-Frequency Plots

In figure AI.9 the time-frequency responses (created using a Wavelet transform) for diamond and aluminium tweeters are shown. There are obvious differences in the transforms above 20kHz owing of course to the change in frequency of the break-up frequency. However below 20kHz the responses are largely the same.

Note: the apparent small resonant tails below 20kHz are thought to artefacts of the analysis method. It is uncertain whether the resonant tails between 20kHz and 60kHz in the diamond tweeter are artefacts or not. The increased amplitude of these tails compared to those below 20kHz suggests they are genuine. It is possible that like the small features apparent in the structural frequency response they are caused by surround or tube resonances.

Acoustic Measurements

In section 3, structural measurements were presented that highlight the differences between diamond and aluminium tweeters. In this section acoustic measurements are presented.

On-Axis SPL response

In figure AI.10, the on-axis SPL response for an aluminium and diamond tweeter are compared. The aluminium tweeter breaks-up at approximately 30kHz as expected. However, it is not so clear from this plot at what frequency the diamond breaks-up. The response of the diamond rolls off smoothly to approximately 45kHz owing to 'phase loss' (this effect is apparent in the simulations). Above this frequency the response rises before exhibiting two small peaks at approximately 63kHz and 74kHz. Above 74kHz the response of the diamond tweeter rolls off sharply.

As was shown in section 3 the actual break-up frequency of the diamond tweeter is at 74kHz, which compares to approximately 80kHz in the simulation (see figure AI.3). The lower frequency in the real tweeter is due to the effect of the surround and uncertainty of the material properties of the former/dome glue joint.

The peak in practice is much lower than in the simulation. This is thought to be in part because damping properties of the surround at any frequency but especially high frequencies are not known. Another explanation may be that the peak is superimposed on a sharply falling response so it appears to be lower than it is. Another factor is likely to be the effect of air absorption.

The degree of absorption is highly dependent on factors such as humidity, temperature and, of course, frequency. However, to illustrate the effect, at 80kHz, 70% humidity and at 20 degrees, attenuation is approximately 3dB/metre. See (1) for a detailed discussion of the effect of air absorption.

In figure AI.11 the acoustic phase response of the aluminium and diamond tweeters are compared. Below 20kHz the two responses are similar but the aluminium shows anomalies above this frequency. The phase differences apparent in the structural measurements (figures AI.6 and 7) are not so obvious in the acoustic response.

The acoustic impulse response

Finally in figure AI.12, the acoustic impulse response for aluminium and diamond tweeters is shown. Whilst at first glance this looks like convincing evidence that the diamond is better than the aluminium; the leading edge of the main pulse seems to be steeper than that of the aluminium that could be equated with a 'faster' sound. The faster rise time would also equate with more HF information. However when considering figure AI.10, it might be concluded then that the aluminium tweeter would have the fastest rise time.

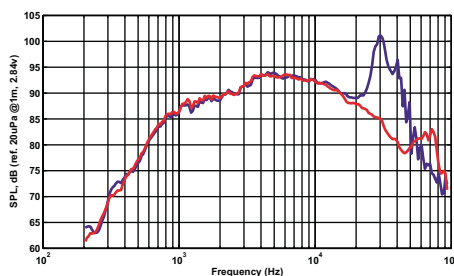
When the responses shown in figure AI.12 are low pass filtered to 20kHz (not shown) the resulting impulses look largely the same. The conclusion then is that the differences in rise times are the result of ultrasonic frequencies – though it is possible to argue that this result is curious looking at figure AI.11. Thus the responses in figure AI.12 are misleading and are shown here just for completeness.

Distortion Measurements (an aside)

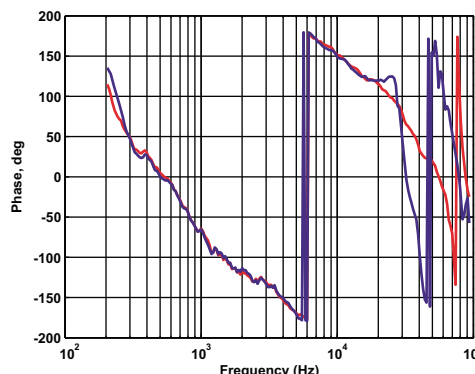
Other than the removal of the distortion features that result from the 30kHz aluminium tweeter break-up, there is no real reason that diamond should be more linear than aluminium. THD+N measurements for diamond and aluminium are shown in figure AI.13, for reference. Below 3kHz, which is better depends on the frequency considered and this variability is thought to be more to do with manufacturing differences than anything else (and this manufacturing variability confounds all detailed comparisons of distortion).

Appendix I continued

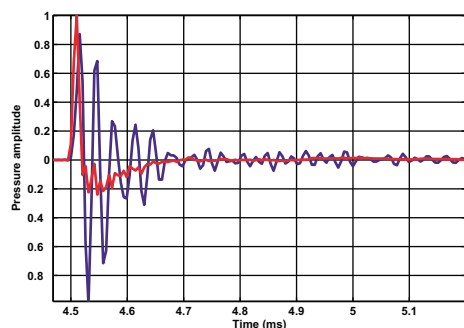
Diamond Dome Tweeter



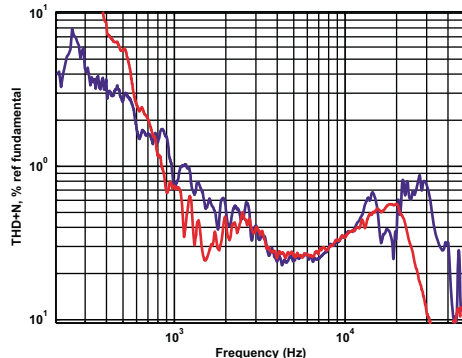
AI.10 Blue – aluminium, Green – diamond acoustic frequency response



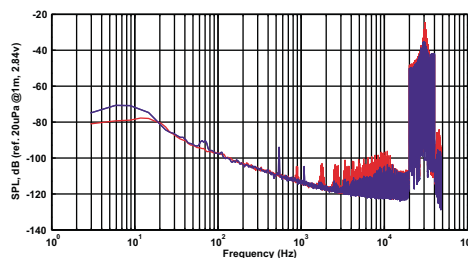
AI.11 Aluminium (blue) and diamond (red) phase response



AI.12 Impulse response of aluminium (blue) and diamond (red)



AI.13 THD+N for aluminium (blue) and diamond (red)



AI.14 Intermodulation distortion resulting from a multi-tone stimulus 2-40kHz. aluminium tweeter with a roll surround (Blue) and a foam surround (Red).

However both the aluminium and diamond tweeters have greatly improved distortion compared to the Nautilus 800 tweeters or even the Signature 800 tweeters. This is thought to be firstly because the coil position has been adjusted slightly to be correctly centred in the gap and secondly because of the use of the new roll surround. Over the important range, from 3kHz –10kHz the distortion maximum is 0.4%, with dips as low as approximately 0.26%.

On standard CD programme, there is little information above 20kHz and almost none at 22kHz. However, with high definition audio, information up to 96kHz can be present. Thus considerable effort was made to differentiate between diamond and aluminium when applying a multitone excitation from 20-40kHz and measuring the resulting intermodulation distortion. Unfortunately, without applying excessive power, little difference could be found.

However, in figure AI.14, the distortion resulting from a 20-40kHz multitone excitation applied to a Nautilus 800 Series tweeter with a foam surround and a new aluminium tweeter with roll

surround. The new tweeter gives up to 12dB lower distortion at some frequencies.

On High Frequency Audibility

An excellent paper that touches on the issues of high frequency audibility and high sampling rates and which is also a good source of references is (2, especially 117-132). Much of the following is paraphrased from this paper:

The advent of higher sampling rate formats such as DVD-A and SACD have provoked a debate over high frequency audibility. It is generally accepted that higher sampling rate formats sound better. Is this really because high frequency components (above 20kHz) are directly audible or because the increased sampling rate gives a bigger gap than 44.1kHz sampling, between 20kHz and the sampling frequency, thus allowing for less severe filters and/or less aliasing?

It is undoubtedly true that musical instruments contain ultrasonic components. For example a cymbal, which is said to have more content above 20kHz than any other instrument, has 40% of its power in this range (3). However is this audible?

It is worth first recalling briefly the function of the ear. See figure AI.15 for a cross section of an ear showing the three main sections; the outer, middle and inner ear. The frequency response of the outer and middle ear has a fast cut-off rate owing to the combined action of the acoustics of the ear canal and mechanical transmission loss (4), typified by the well-known Fletcher-Munson Curves (note the non-linearity).

The cochlear, the main structure of the inner ear, behaves as a bank of mechanical filters with the highest frequency filter closest to the eardrum (the membrane separating the middle from the outer ear). The centre frequency of the highest filter is approximately 15kHz and data suggests it has a bandwidth of 2kHz (5,6). There is some evidence that supersonic information that does manage to get to the cochlear (by bone-conducted sound rather than through the filters of the outer and middle ear), ends up in the high frequency bin. However,

there is no known credible evidence that airborne sound can be perceived above 25kHz.

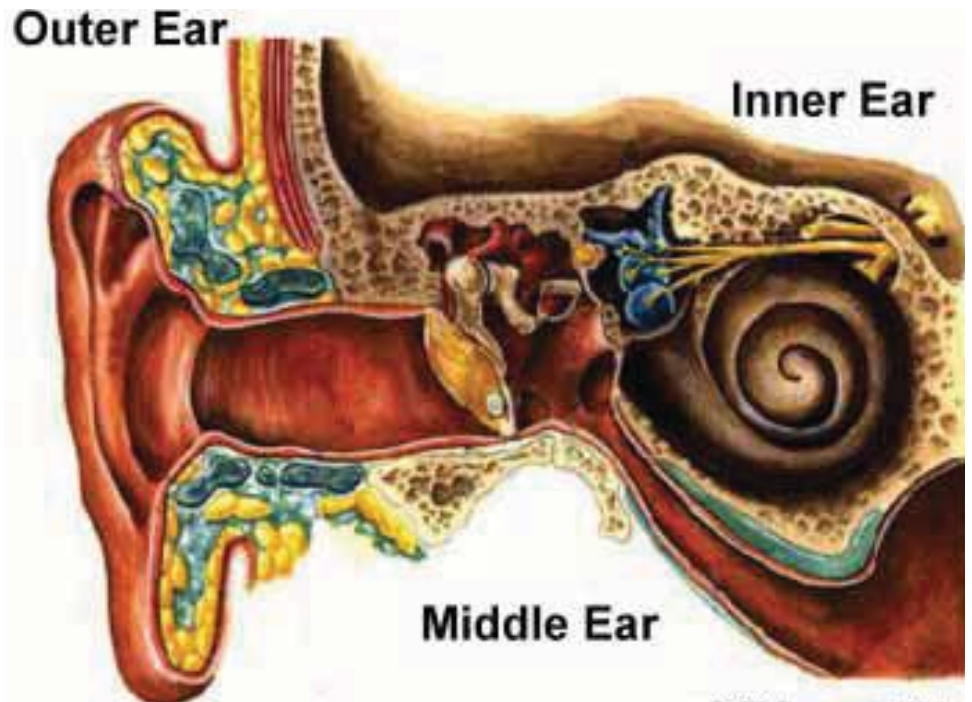
Against this background, there are a number of controversial works that challenge the established conclusions. In particular in (7), it is concluded that ultrasonic information modifies measurable brain response. This is not the same as normal auditory perception. Instead it is postulated that ultrasound could have a direct impact on the brain. This work is the subject of debate.

Undoubtedly further experiments will be carried out in this area, although convincing conclusions will be difficult to make. Such experiments are very difficult to carry out owing to the problem of keeping a like-for-like comparison before and after addition of ultrasonic information. One big problem is that of intermodulation resulting from speaker nonlinearity. Remember, another issue that confounds this debate is the fact that the ear is not linear (see figure AI.16) and therefore does not perform a perfect Fourier transform.

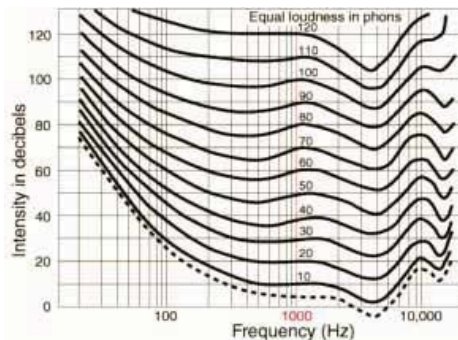
So far, the bandwidth of the ear has been discussed. Although related in a linear system at least, there is some debate over whether our hearing system can resolve very small time differences. Two cases are to be considered. Firstly, events that are closely separated in time, implying fine monaural resolution and consequently high bandwidth. Secondly, binaural time difference errors, such as differential dispersion or delay between channels that help build up the auditory scene. A number of investigations conclude that the lowest limit of temporal resolution for both monaural and binaural events is approximately 10µs (8-10).

So, on the one hand the audibility of ultrasonic frequencies is not accepted by the audio community, but on the other, 10µs time discrimination is, which in a linear system (which the ear is not) would imply a 50kHz audible bandwidth.

As an aside, could the 10µs time discrimination limit be an explanation as to why the diamond tweeter sounds better than the aluminium tweeter? In section 3.1 it was discussed that,



AI.15 The ear



AI.16 The Fletcher-Munson Curves

Appendix I continued

Diamond Dome Tweeter

at 20kHz, the structural phase response of the two tweeters differs by 4 degrees (although this difference is not apparent in the acoustic phase response). A 4 degree phase difference at 20kHz relates to a timing error of approximately 0.5 μ s – well below the established threshold.

Discussion

Undoubtedly the diamond tweeter is a significant improvement over the aluminium tweeter in terms of audibility. Words and phrases that are used to describe the performance of the diamond tweeter are effortless, detailed, producing a realistic sound stage, the tweeter disappears and the tweeter being well integrated with the system.

From an objective point of view the diamond can be demonstrated to give a response more like a perfect dome tweeter than the aluminium. This is particularly evident when considering the acoustic or structural magnitude response of the system. There are smaller differences with the structural phase response. Despite considerable effort to demonstrate a difference in time measurements (below 20kHz), little could be found.

At this stage the detail as to why the diamond sounds better than the aluminium tweeter is not clear. Whilst we can say the diamond's response is more perfect in the sense it is closer to an infinitely rigid tweeter (and this is quite compelling), the actual reason in terms of factors we normally consider, such as phase, timing etc is not clear. Are the relatively small differences more significant than established wisdom would suggest or are we looking in the wrong direction? Could, for example, the perceived improvement in performance be something to do with radial modes? Experiments will continue.

References

- 1 Bazley, E.N. (1976) Absorption in Air at Frequencies up to 100kHz. NPL Acoustics Report Ac 74
- 2 Stuart, J.R. (2004) Coding for High-Resolution Audio Systems, Journal of the Audio Engineering Society, 52 (3)
- 3 Boyk, J. (2003) There is life above 20kHz! A Survey of Musical Instrument Spectra to 102.4kHz, www.cco.caltech.edu/~boyk/spectra/spectra.htm
- 4 Moore, B. J. C. Frequency Selectivity in Hearing, Academic Press, New York
- 5 Moore, B.J.C and Patterson, R.D. (eds) (1986) Auditory Frequency Selectivity, Buus, S. et al. Tuning Curves at High Frequencies and Their Relation to the Absolute Threshold Curve, Plenum Press, New York).
- 6 Shailer M.J. et al. (1990) Auditory Filter Shapes at 8 and 10 kHz, J. Acoustic Soc. Am., vol 88 141-148.
- 7 Oohashi et al. (1993), On the mechanism of Hypersonic Effect, Proc. Int. Computer Music. Conf., Tokyo, Japan.
- 8 Nordmark, N.O. (1976) Binaural Time Discrimination, J.Acoust Soc. Am., Vol 35 870-880.
- 9 Henning, B. G. (1974) Detectibility of Interaural Delay in High-Frequency Complex Waveforms, J. Acoust Soc. Am. Vol 55 84-89
- 10 Klump, J.O and Eady, H.R. (1956) Some Measurements of Interaural Time Difference Thresholds, J. Acoust. Soc. Am., Vol 28 859-860
- 11 Krumbholz, K. and Patterson, R.D (2003) Microsecond Temporal Resolution in Monaural Hearing without Spectral Cues? J. Acoust. Soc. Am., Vol 113 2790-2800

Appendix II

The FST Midrange Driver

At first sight 'perfect piston' drive units, (ie those that move rigidly without bending and with a total freedom from resonances), would appear to satisfy the ultimate requirement for perfect sound reproduction. However, there are two limitations to this approach. Eventually, even very stiff materials exhibit break-up and, when they do, the resonances tend to be very severe due to the low inherent damping of stiff materials. Thus, one must ensure that the low-pass filter of the crossover to the next higher drive unit can be set at least 1.5 and preferably 2 octaves below the first resonance frequency. One must also have regard to the fact that the loudspeaker has to convert a one-dimensional electrical signal into a three dimensional sound field. Beaming or directivity effects limit the useful bandwidth of the drive unit. Much research has shown that a wide and uniform directivity pattern is important in creating a more realistic sound image and enabling off-centre listeners perceive a correct balance. In order to maintain a more uniform off-axis response, one must normally restrict the unit's bandwidth to below that frequency where the wavelength is equal to the circumference of the diaphragm.

In the 800D, a single midrange drive unit is required to cover the range 350Hz to 4kHz, with useful output outside this bandwidth. At the lower limit, the cone must be large enough to radiate high sound pressure levels without an excessive amount of excursion that would compromise non-linear distortion. A very stiff cone of that size would then exhibit the resonance and beaming limitations outlined above at the top end of the range. One must therefore opt for the controlled break-up approach and use a more flexible cone material.

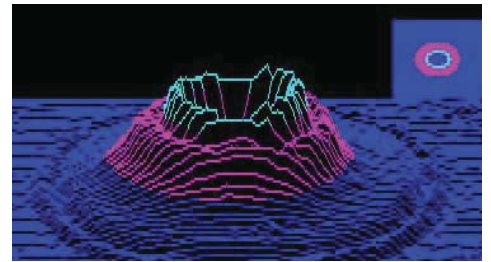
The break-up pattern of woven Kevlar® has proved beneficial for use in midrange and bass/midrange units, being superior to many other materials, not only because of the inherent properties of Kevlar, but also because the woven cone is not axi-symmetric. We have used laser interferometry to examine the motion of the surface of cones. In the illustrations, the basic shape of the cone is not evident, because velocity and not absolute position is being measured.

In figure AII.1, there are two impulse progression plots relating to a homogeneous plastic cone (a) and a woven Kevlar® cone (b). In each case, the drive unit voice coil is fed an electrical impulse. In flexible materials, a bending wave is initiated at the centre and moves out towards the rim of the cone. Here we are looking at this bending wave shortly after the impulse has been applied and motion is still restricted to the area immediately around the centre, but already the wave front in the Kevlar® cone has begun to take up a square shape imposed by the weave, as the speed of the bending waves in the direction of the fibres is significantly different from that at 45° to them.

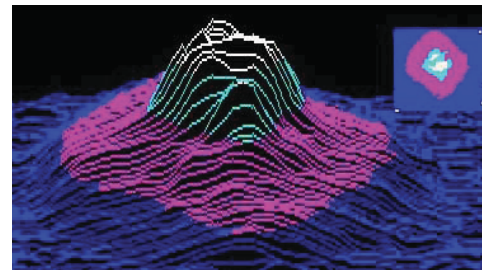
As the bending wave progresses, the circular form is maintained in the plastic cone. When the wave hits the roll surround, most of the energy passes into the surround, but because of the surround's different mechanical impedance, some of the energy is reflected back down the cone. Further reflection takes place where the surround is glued to the chassis and at the centre of the cone where it joins the voice coil, both again due to changes in mechanical impedance. This wave motion up and down the cone continues until internal damping dissipates the energy as heat and, because the concentric waves are efficient in radiating sound, the motion is heard as delayed coloration.

In the woven Kevlar® case, these reflections still occur, but at different times in different radial directions. The non-symmetrical motional pattern is less efficient at radiating sound, because there is an almost equal area moving forwards as there is moving backwards. So, although there is cone break-up going on, there is much less audible delayed coloration as a result and the Kevlar® cone drive unit sounds cleaner. (figure AII.2)

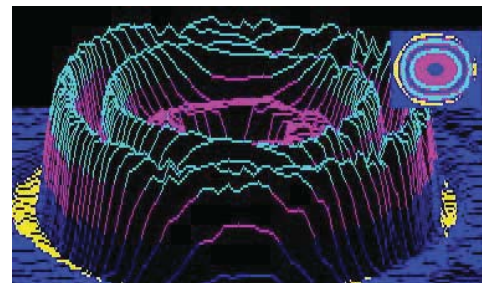
Up to now, we have examined cone behaviour when excited by an impulse. If steady state sine wave signals are applied, individual resonance frequencies may be identified as the wave reflections set up standing waves in the cone/surround combination whenever a whole number of half wavelengths exactly fits the out and back path. In a single continuous material, the standing wave patterns are the familiar shapes shown in figures AII.3a & b.



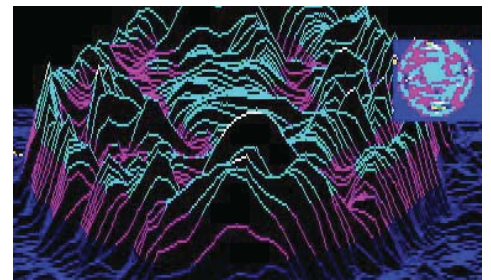
AII.1a



AII.1b Bending wave progression in plastic (a) and woven Kevlar® (b) cones shortly after an impulse signal has been applied.



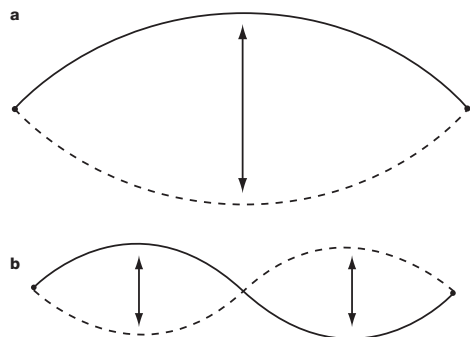
AII.2a



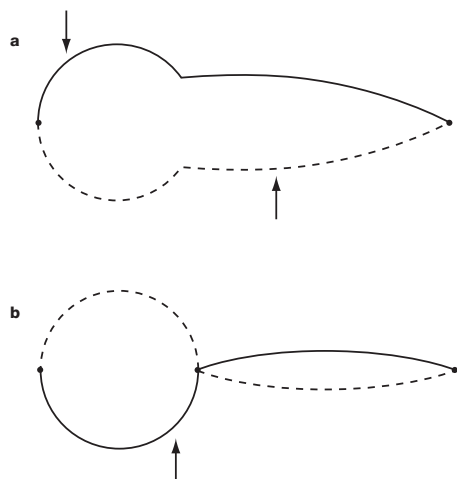
AII.2b Bending wave progression in plastic (a) and woven Kevlar® (b) cones after reflections at boundaries.

Appendix II continued

The FST Midrange Driver



AII.3 Standing wave patterns in a single continuous material Fundamental (a) and first harmonic (b) node



AII.4 Standing wave patterns in a combination surround and cone Fundamental (a) and first harmonic (b)



AII.5 Cone motion of plastic cone (upper) and FST (lower) drive units at 210Hz (a), 690Hz (b) and 1890Hz (c)

The proportions change somewhat in the case of a cone attached to a (mechanically different) surround. The cone is stiffer and will not bend as much as the surround and the bending wave velocity is much higher. The modified modal patterns are illustrated in figure AII.4. The node cusp shifts towards the cone to surround junction. The fundamental resonance results in a peak in the steady-state amplitude response, when the outer edge of the cone and the surround both move more than in the simple pistonic motion case. The first harmonic involves the cone moving more than it should in one direction, while the surround moves in the opposite direction. Whether this results in a dip, peak or no change in the amplitude response depends on the relative area velocity of the cone and surround, but more often than not it is a dip, often referred to as the surround dip.

These standing wave patterns can be modified if attention is paid to the mechanical impedance of both the surround and the voice coil. If these can be matched to the mean mechanical impedance of the outer rim and neck of the cone respectively, bending wave reflections can be reduced in magnitude, with a consequent reduction in the level of delayed energy coloration. The situation is a mechanical analogy of the electrical practice of terminating a coaxial cable with a resistor of a value equal to the characteristic impedance of the cable.

It was found difficult fully to address both of these criteria in a bass/midrange drive unit, where the need to have a large excursion at low frequencies imposes specific demands on the design of both the surround and the voice coil. If, however, one restricts the bandwidth to midrange frequencies, there is much more freedom to address the mechanical impedance requirements.

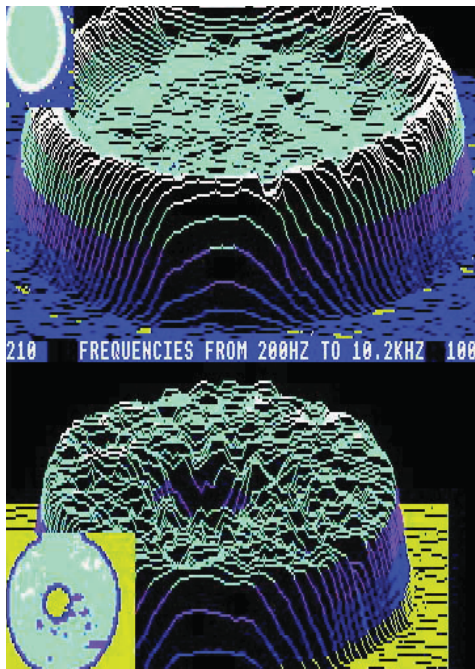
In the case of the voice coil, this involves setting the correct mass, which needs to be less than that of a typical long-throw coil. In the case of the surround, the solution was found by replacing the normal half roll surround by a foam polymer edge support that sits under the rim of the cone and is compressed or stretched as the cone moves back and forth (see figure AII.5). The woven nature of the Kevlar® cone does mean that the cone's mechanical

impedance is not the same at all points on the circumference, but the particular support material specification was chosen to have an impedance as close as possible to the mean value of the cone and to be highly resistive. Thus not only does more bending wave energy pass into the support, but much of it is dissipated as heat before reflection can take place at the boundary with the chassis.

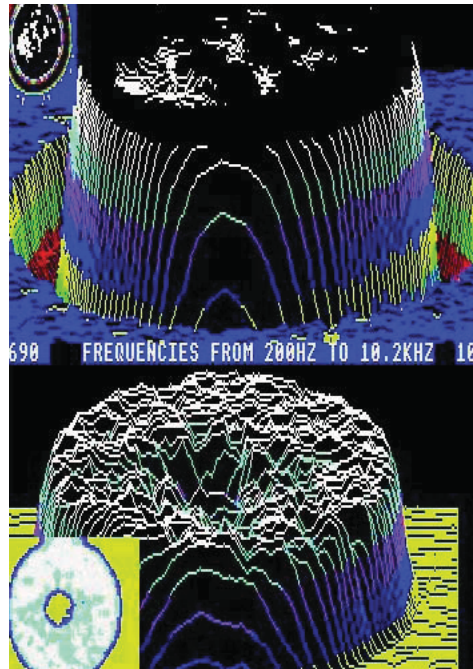
This is the basis of the FST (Fixed Suspension Transducer) midrange drive unit. Laser measurements of the motion of the diaphragm and support of the FST Kevlar® unit compared to the motion of a plastic cone with rubber roll surround are shown at three significant frequencies in figure AII.4. In each case, the FST drive unit is the lower of the two plots.

At 210Hz (figure AII.6a) we have the fundamental standing wave shown clearly in the case of the plastic cone, where the surround is moving in the same direction as the cone, but with excessive amplitude. At 690Hz (figure AII.6b), the plastic cone is showing the first harmonic and the surround is moving in the opposite direction to the cone. At both these frequencies, the FST cone is moving as a coherent whole. The hole in the middle is simply a consequence of the unit having a fixed central phase plug and so there is no motion.

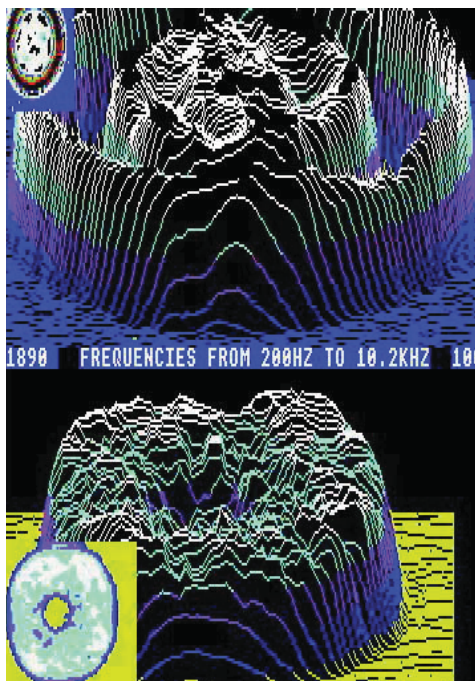
At 1890Hz (figure AII.6c), the plastic cone is exhibiting a higher mode resonance. The Kevlar® cone is beginning to break up and one can detect the four-fold peak pattern at the outer edge that is a consequence of the material's woven nature. Like in the case of the bending wave progression plot, this pattern builds in the outer part of the cone to be largely self-cancelling, leaving a smaller inner region as the major sound radiating area. The effective radiating area has roughly halved by 4kHz and halved again by 6kHz, with a consequent improvement in off-axis response compared to a rigid piston.



AII.6a



AII.6b



AII.6c Cone motion of plastic cone (upper) and FST (lower) drive units at 210Hz (a), 690Hz (b) and 1890Hz (c)

The use of Rohacell® in loudspeaker cones

Introduction

For the Nautilus 800 bass unit a combination of paper and Kevlar fibres with a high resin content was used for the diaphragm material. This combination of materials resulted in a very stiff cone. For the 800D, the bass performance has been improved further by using of a sandwich of 8mm Rohacell between two layers of carbon fibre. In this report, measurements are presented that show the differences between Rohacell/Carbon Fibre and Paper/Kevlar cone bass units.

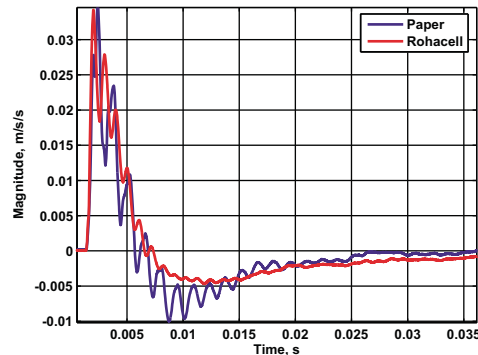
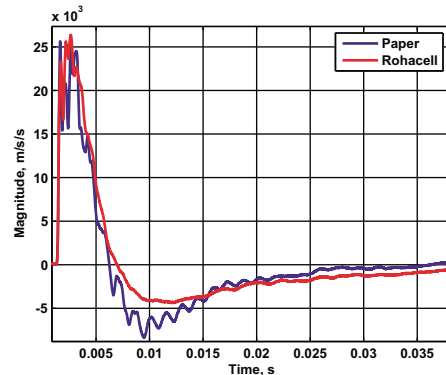
Material Considerations

Rohacell® is a polymethacrylimide- (PMI-) hard foam, that is used as a core material for sandwich constructions. It shows outstanding mechanical and thermal properties. In comparison to all other foams it offers the best ratio of weight and mechanical properties as well as highest heat resistance. It comes in different forms, but the material we are using (Rohacell 31) has low density (31kgm^{-3}) though with low Young's modulus (36MPa compared to paper in the region of 2000MPa). It has favourable (ie high) damping.

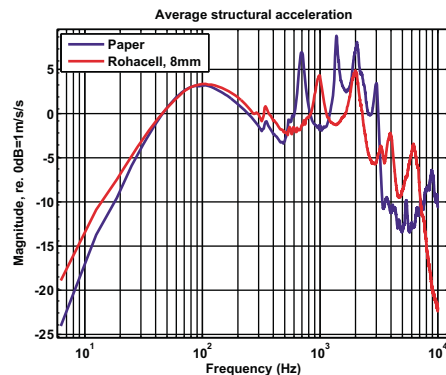
At first glance it might be thought that Rohacell would be a worse material to use than paper. The standard measure of dynamic stiffness that we use is the ratio of stiffness to density. Rohacell is very approximately six times worse than paper according to this measure.

However, because the material is of such low density, it is possible to use carbon fibre skins while not adding excessive mass. These skins, together with the Rohacell, result in a composite that has high stiffness and damping, as will be demonstrated in the following measurements.

Another important point to note is that the transmission loss through the resulting composite is higher than for paper. This is because a relatively thick cone can be used, owing to the low density of Rohacell.



AIII.1 The velocity responses of paper (blue) and Rohacell (red) cone bass units to an impulse measured at (top) the neck of the cone and (bottom) the edge of the cone.



AIII.2 Average structural acceleration response

Structural Measurements

The Structural Impulse Response

In figure AIII.1 the structural velocity response of paper and Rohacell to an impulsive excitation is compared. These plots highlight several advantages of Rohacell over paper. The most obvious difference is the higher damping level, indicated by a response with fewer wiggles. More generally the Rohacell response indicates fewer resonant features and a faster impulse (apparent when looking at the response, both consistent with improved stiffness of the composite).

Frequency responses and scans

In figure AIII.2, the average acceleration frequency response of all the points comprising a surface scan is shown for a paper and a Rohacell cone. This clearly shows that the first main break-up frequency for the Rohacell cone is higher than that for the paper cone. Both graphs have a common feature at approximately 320Hz, which requires further investigation. Above this frequency the paper has resonance frequencies at approximately 700Hz and 1300Hz and the Rohacell at approximately 1000Hz and 2000Hz.

The graph in figure AIII.2 clearly demonstrates that the Rohacell is stiffer. In figure AIII.3, scans at a number of frequencies are shown for the two cases. At low frequency the Rohacell bass unit is clearly more pistonic than the paper. Another obvious feature at higher frequencies is that the Rohacell bass unit rocks less than the paper.

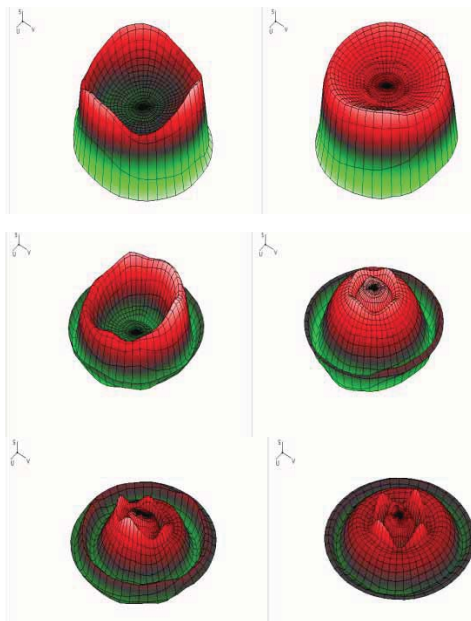
Time-Frequency Representations

In figure AIII.4, the wavelet transform has been used to produce a time-frequency plot of velocity at the edge of the cone in the two cases. Once again the greater stiffness and damping of the Rohacell is clear.

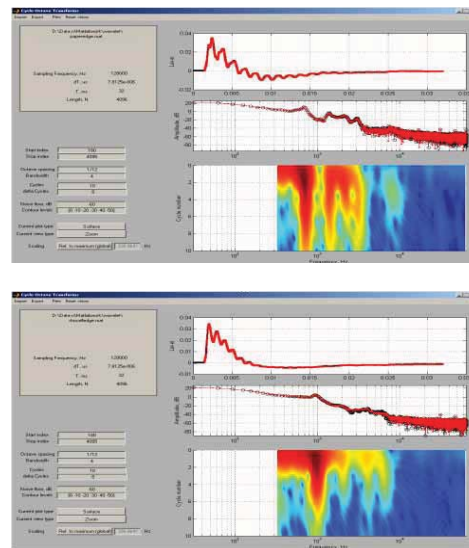
Acoustic Measurements

SPL Measurements

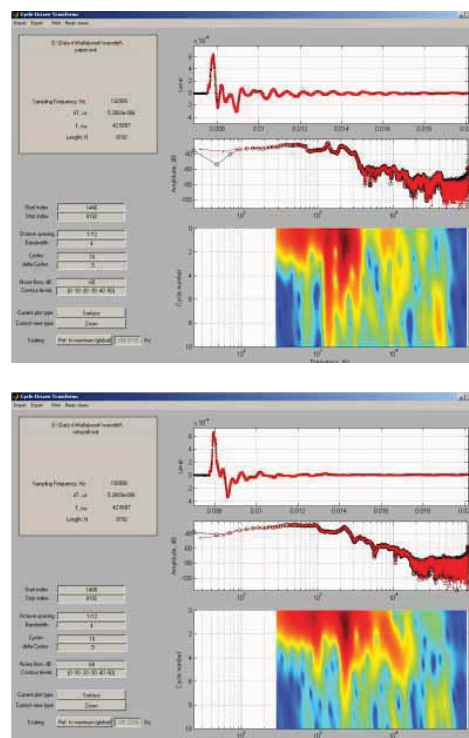
In figure AIII.5, the acoustic impulse and frequency responses are shown, together with the time-frequency plot for the paper and Rohacell cones. These plots do not really tell us any more than the structural plots shown in Section 3. Once again the Rohacell is clearly stiffer and better damped than the paper. In the paper case (figure AIII.5, top) the 700Hz and 1300Hz modes are clearly visible. In the



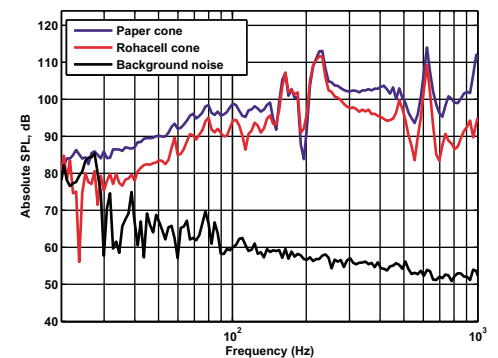
AIII.3 Scans of Paper (left) and Rohacell (right) at 350Hz, 1375Hz and 2000Hz



AIII.4 Cycle-Frequency plots created using the Wavelet Transform for (top) paper and (bottom) Rohacell cones.



AIII.5 Impulse (upper), frequency (middle) and time-frequency (lower) plots of a paper cone (top) and Rohacell cone (bottom) obtained using the Wavelet transform



AIII.6 Frequency response exterior to a clamped cone, excited via an internal speaker

Rohacell case the mode at 1000 Hz is clearly visible, though curiously the higher 2kHz mode seems to have increased in frequency to approximately 2.2kHz.

Transmission Loss

To assess the transmission loss for the paper and Rohacell cones the following experiment was carried out. An 8-inch driver was placed in an enclosure, a whole cut in the outside of the box and samples of 15-inch cones in the two materials were rigidly mounted in the hole (both at the edge and the neck of the cone). The hole in the centre of the cone was blocked. A measurement of the SPL was taken for the two cones in the same position, approximately 1cm from the surface of the diaphragm.

In figure AIII.6, the measured responses clearly show that the Rohacell has higher transmission loss than the paper. For example, the transmitted response through the Rohacell cone is approximately 7dB lower at 300Hz than for the paper cone.

Conclusions

A Rohacell/Carbon Fibre diaphragm is stiffer, better damped and has higher transmission loss than a Paper/Kevlar Diaphragm.

Appendix IV

Tapered tube theory

Finite Element Analysis Abstract

The Finite Element Method was used to analyse the interior acoustic field of an inverted horn system. The finite element model was verified by comparing simulated and measured sound pressure level responses at an interior point. Contours of equal pressure phase were used to visualise the interior acoustic field. It is concluded that the frequency range over which the system can be used, is restricted by an upper frequency which is dependent on the diameter of the horn.

Introduction

A common source of distortion in loudspeaker systems is internal acoustic resonances of the cabinet. High pressures can build up behind drivers at internal resonance frequencies of the cabinet, which affect the movement of the driver and thus colour the far-field sound. A solution to this problem is to use an inverted horn. A carefully designed inverted horn offers a smooth change in acoustic impedance which, when used in conjunction with an absorbent material, can result in a cabinet structure free of internal acoustic resonances.

In this paper, the results of Finite Element Analysis (FEA) of a prototype inverted horn designed for use in conjunction with an upper midrange dome are reported. Initial listening tests of the prototype revealed distortion occurring at approximately 10kHz. The Finite Element Method (FEM) was used to isolate the cause of this distortion.

The finite element model is described in 'The Finite Element Model'. In 'Verification of the Finite Element Model' the model is verified against the sound pressure level (spl) frequency response measured at an interior point. Finally, in 'Analysis of the Internal Pressure Field' the interior sound field is analysed in more detail.

The Finite Element Model

The FEM is a mathematical technique that can be used to produce approximate solutions to partial differential equations. By utilising the FEM it is possible to carry out computer simulations of structural and acoustic systems. This paper is not intended to explain the FEM in detail. For detailed descriptions of the FEM applied to loudspeaker design see (Refs1+5), for example.

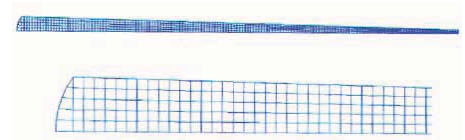
The main point is that by applying the FEM, a virtual prototype can be constructed on a computer that can reflect the real world with sufficient accuracy to be useful in the design and analysis of loudspeaker systems. In this case a commercial FE package called PAFEC FE (Refs 6-7) was used to carry out the analysis.

The real prototype was composed of a 43mm diameter aluminium dome driver and an exponentially decreasing horn of length 680mm. The interior of the horn was filled with polyester fibre wadding, a material commonly used to absorb unwanted sound. Figure AIV.1a shows the FE model of the inverted horn prototype. Note that the model was axisymmetric.

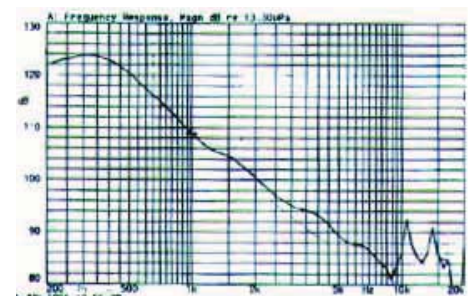
The model was composed of both structural and acoustic finite elements. Structural finite elements were used for the horn sides and the dome driver. The structural break-up of the dome driver was not modelled in detail and rigid motion (constant acceleration) was imposed. Detailed modelling of this component was considered unnecessary as initial measurements discounted structural break-up to be the cause of distortion occurring at 10kHz. Acoustic finite elements were used to model the wadding. (figure AIV.1)

Verification of the Finite Element Model

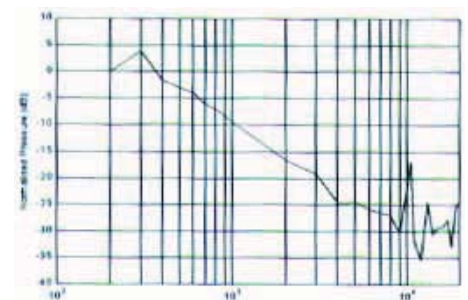
To gain confidence in the accuracy of the FE model a measurement of the spl response at an on-axis point approximately 50mm from the back of the driver was made using a microphone inserted through the side of the horn. This is compared to the simulated spl response at the same point in figure AIV.1b. Clearly the general trend is the same in both cases – after an initial rise the responses decrease with frequency to approximately 10kHz where a spike occurs.



AIV.1 The Finite Element Model
Upper – the entire mode,
Lower – close-up of the driver end



AIV.1a Interior SPL responses measurement



AIV.1b Interior SPL responses simulation

The differences between the measurement and the simulation probably arise because of:

- Small differences in measurement position.
- The simulated response being taken at a point whereas the microphone essentially averages over an area.
- Simplification of the geometry in the FE model.
- Uncertainty as to the acoustic impedance of the wadding.

However, the correspondence between the simulated and measured spl response is generally good and it is therefore assumed that the whole of the interior acoustic field is modelled with sufficient accuracy.

Analysis of the Internal Pressure Field

To gain insight into the nature of the interior acoustic field, animations of equal pressure magnitude and equal pressure phase were made. Such animations are a powerful means of visualising the interior acoustic field. Contours of equal pressure phase especially are significant because wave fronts move in directions normal to these. Snap shots of equal-pressure phase animations are shown in figure AIV.2.

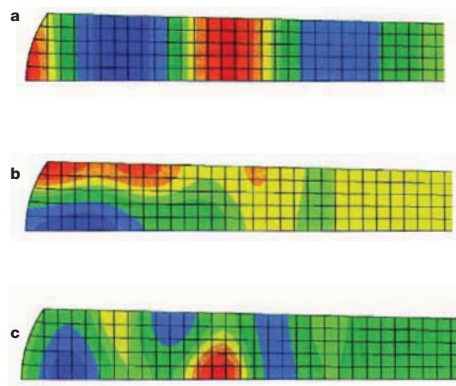
At 5kHz it is clear that the inverted horn is behaving as expected – the direction of propagation is down the tube. However, at 10kHz there is clear evidence of a resonance across the diameter of the tube. This ties in well with the spl responses shown in figure AIV.2 a-b, where a spike is visible at approximately 10kHz. At 11kHz, it is apparent that the main direction of propagation is down the horn but with a component across the diameter (this is very clear in animations).

Concluding Discussion

The problem cross-diameter resonance could be removed or the effects reduced by using:

- a more effective wadding
- a tube placed inside the horn
- a flatter radiator which would not excite diameter modes so strongly.

Each of these cases were analysed using the FEM and all resulted in either removing or reducing the 10kHz spike. However, none offer a realistic solution to the problem.



AIV.2 Simulated results showing contours of equal pressure phase a 5kHz, b 10kHz and c 11kHz

It is clear from the results presented in this paper that inverted horns are only effective up to a certain frequency dependent upon its diameter at the throat. This is perhaps an obvious result but by using the FEM the effects can be quantified and clearly visualised.

Sound Propagation down Nautilus™ Tubes (Phases & Frequencies)

- a** Top plot shows a plane wave moving smoothly down a Nautilus™ tube at low frequencies.
- b** Middle Plot shows the wave at the cut-on frequency of the first-order mode of propagation. This occurs as a resonance across the tube width.
- c** Bottom plot shows the propagation above the cut-on frequency. Energy then moves down the tube as a combination of plane waves and first order modes.

Note: all pipes and ducts will allow plane-only waves to pass down them below a certain frequency that depends on their cross sectional dimensions. Above a first critical cut-on frequency waves can also propagate in a zig zag fashion along the tube. The angle of the zig and zag changes with frequency and is at right angles to the length of the tube at the cut-on frequency – which therefore shows up as a cross mode. Higher-order modes of propagation also have their own cut-on frequencies, which will also show up as cross resonances at higher and higher frequencies. For best effect therefore, Nautilus™ tubes can only be used

up to the cut-on frequency of their first higher-order mode. Ref: Book 'Mechanical Waveguides' by Martin Redwood.

References

- 1 Jones, C.J.C (1986) Finite Element Analysis of Loudspeaker Diaphragm Vibration and Prediction of the Resulting Sound Radiation, PhD Thesis, Brighton Polytechnic.
- 2 Jones, M.A, Henwood, D.J. and Fryer P.A. (1992) A Computer Model of the Vibration and the Sound Radiated by Loudspeaker Models and its Validation, Acoustics Letters, 15(8)
- 3 Henwood, D.J. (1993) The Boundary Element Method and Horn Design, The Journal of the Audio Engineering Society, 41(6).
- 4 Geaves, G.P. (1995) Modelling and Optimal Design of Loudspeaker Diaphragms Using Numerical Methods, PhD Thesis. University of Brighton.
- 5 Geaves, G.P. (1996) Design and Validation of a System for Selecting Optimised midrange Loudspeaker Diaphragm Profiles, The Journal of the Audio Engineering Society, 44(3).
- 6 PAFEC Limited. (1984) PAFEC Theory
- 7 PAFEC Limited (1995) PAFEC-FE Acoustics User Manual Level 8.1

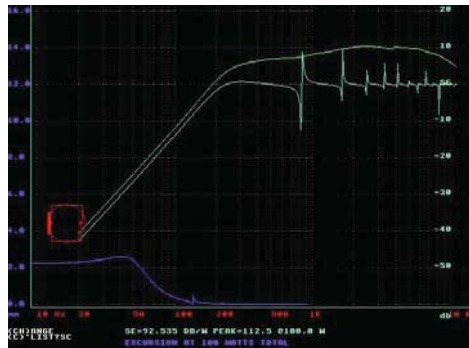
Appendix V

Sphere/Tube Midrange Enclosure

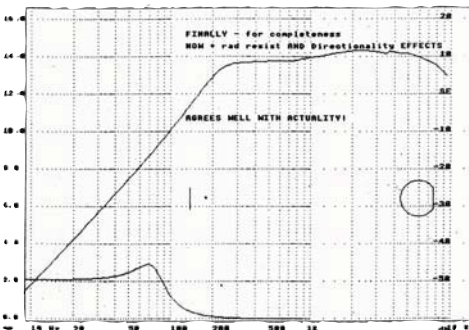
It was known that a simple Nautilus™ tapered tube would not work well over the bandwidth required of the drive unit (see appendix II), so other enclosure configurations were investigated. In particular, a sphere is well known to give a smooth diffraction-free exterior shape. Initial experimentation was directed at investigating how the performance was affected by the size of the sphere and how the drive unit was mounted in it. In all cases, the spheres were constructed from a GRP outer shell, lined on the inside with Fibrecrete. A sphere of around 300mm proved to be the best size. Any larger and imaging seemed to be impaired. Any smaller and the unit sounded ‘closed in’. This is a difficult phrase to explain succinctly, but is akin to having traces of the effect obtained by cupping the hands round one’s mouth when speaking. The same effect is heard if tubes are used above the frequency of the onset of cross modes and this gave a clue as to what was happening in the sphere.

In fact the way the drive unit chassis fitted into the sphere was found to have a similar effect, which was only removed if both the inside and outside surfaces of the sphere blended smoothly with the rim of the chassis. This involved the sphere having a thin wall close to the unit and so to maintain overall stiffness of the enclosure, internal and external spherical profiles were offset, with the internal sphere centre being brought forward.

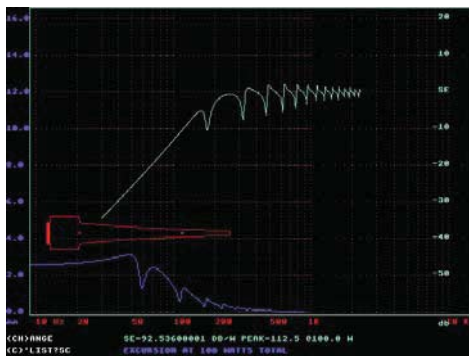
The sphere supports strong internal cross modes, evident in delayed response waterfall plots. These could only be damped by using copious amounts of wadding inside the sphere. Listening tests, however, revealed a loss of transparency with this approach, even when the waterfall plots apparently indicated a good result. The combination of a sphere and an inverse horn was then investigated both experimentally and theoretically. Measurements were made of spheres closed and open, with and without absorption being present and then with an added Nautilus™-style rear tube, which had an open end and was either empty or filled with absorption. Meanwhile some theoretical predictions of these systems were made to see which tallied with the reality.



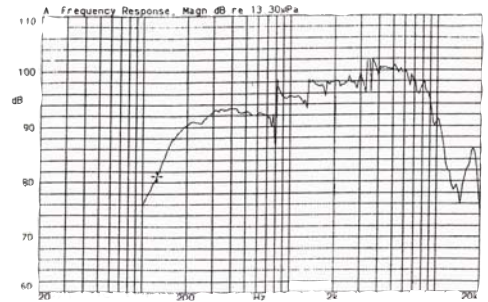
AV.1 Box and Sphere Internal & External Effects



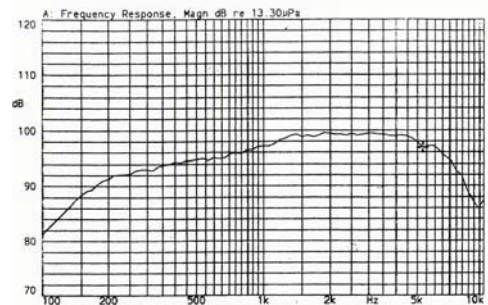
AV.2 Prediction of simple sphere and piston response including external acoustic effects



AV.3 Long Rear Inv Horn + short Tube



AV.4 New Midrange Unit (measured)
In a Sphere – no absorption present – 1/24 Octave



AV.5 New Midrange Unit (measured)
In a Sphere with a Tube with absorption in Sphere and Tube

To a reasonable degree of approximation a sphere can be modelled internally by a pipe of length and diameter equal to the diameter of the sphere and having the same volume. When this is done, the simulated cone output agrees remarkably well with the measured output for a cone in a closed sphere or cubical box. The only difference between the box and the sphere appears to be in the frequencies of the harmonics. In a sphere these follow Bessel function zero crossings, which are spaced differently from those in a pipe, whose resonances essentially follow a sine wave’s zero crossings. However, the form and amplitude of the response shape is remarkably similar. Exact analytic modelling of a sphere adds only a little extra accuracy to these features.

When a tube is added to the back of the sphere, the combination might be expected to behave like two tubes in series. To model this involved the modification of existing modelling routines to allow for a change in diameter at the intersection of the two tubes. Previously there had only been the possibility of a smooth join,

with the end of the first tube having the same diameter as the beginning of the second tube. However, when this routine was used to simulate a sphere (modelled as a real box) with a pipe attached, the theoretical results did not tally with the experimental results at all. The resonances in the real example corresponded only to those found in the pipe part of the combination, rather than to those of the box and the pipe taken separately, and to those of the combination of the two – which the theoretical modelling showed. (figures AV.1, 2, 3)

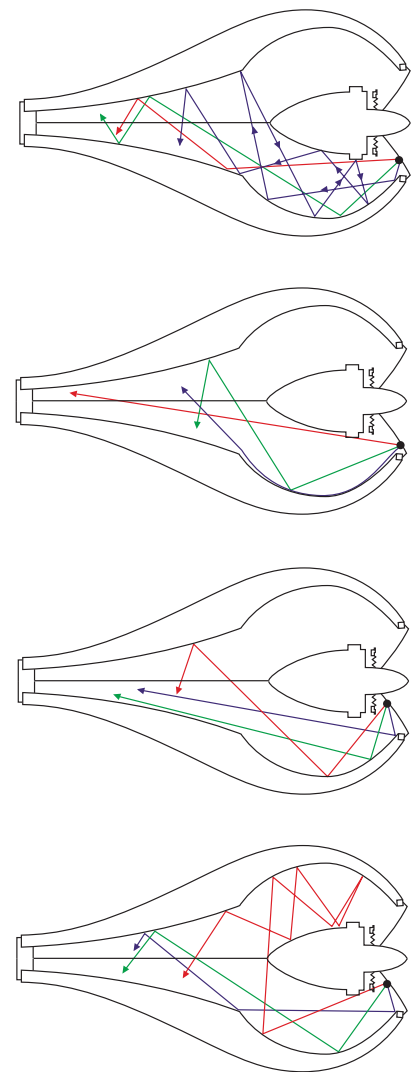
Changing the modelling of the sphere to a simple lumped parameter volume, but keeping a ‘proper’ tube plugged into this, gave much more realistic results, which agreed closely with experiment. It seems that an empty sphere, on its own, at the rear of the speaker acts as a high Q resonance with Bessel function harmonics. However, as soon as a hole is cut into the sphere, particularly if it has the same diameter as the driver, and a Nautilus™-style tube is plugged into it, the sphere resonance is greatly defused. The sphere then behaves almost completely like a lumped parameter spring, even with no absorption present in either sphere or pipe. We are then only left with traces of the resonances due to the length of the pipe alone. Merely cutting a hole in the sphere, with no tube present, gives rise to a classic Helmholtz resonator, which has the usual low frequency resonance, but which does not stop the sphere’s internal resonances at high frequencies to anything like the same extent.

The next step, having proved that the analytic modelling tallies remarkably well with the measurements (figures AV.4, 5), was to see how much the various dimensions of the tube could be pared down. Reducing the length to around 300mm and increasing the taper rate from -3 to -11 gives similar results to the long tube with minimal absorption present, though now the fundamental tube resonance frequency is shifted into the region where the ‘shorting effect’ of the lumped parameter volume reduces its amplitude. If the diameter of the large end of the tube is reduced to be smaller than that of the driver, the effect of this appears to be deleterious. This is because the acoustic impedances of the near end of the tube and of the matching section of the sphere both have

to be matched to the impedance of the driver opposite to them in the sphere for maximum power transfer from sphere to tube. Also, if the taper rate is increased further, the horn cut-off frequency will be correspondingly increased, and with it the changes in acoustic impedance that this represents. So these changes will intrude into the pass band such that the beneficial effects may be expected to decrease. Furthermore, a closed-end horn appears to be better than an open ended horn, partly because the fundamental is at a higher frequency and is therefore shorted out more by the sphere. (figures AV.6)

The combination of GRP and Fibrecrete used to construct the experimental enclosures did not lend itself to mass production and so an alternative material was required. It had to be stiff and heavy to minimise vibration levels in the walls and be mouldable into the complicated shape required. The material chosen – Marlan®, a synthetic resin – proved ideal for the application when used with the decoupling techniques described below.

It appears, then, that the combination of a sphere plus a tapering tube is greatly superior to a simple sphere or a tube on its own. Furthermore, when an easily achievable value of absorption is placed in both the sphere and the tube, closed at the far end, the remaining small resonance effects present with the empty sphere and tube combination are removed. The ability to reduce the amount of internal wadding maintains transparency on listening.



AV.6 Some simplified vector representations of the radiation from a diaphragm visualised as a number of omnidirectional high frequency virtual point sources. This shows how the sphere/tube combination minimises reflections back to the diaphragm.

Note: lossy wadding is placed in sphere and tube and diaphragm’s rear suspension disperses/absorbs coil area reflections

Appendix VI

Matrix™ cabinet



The phenomenon of cabinet radiation has been recognised for as long as loudspeakers have been used in boxes. In theory, the function of the box is to act as a perfect obstruction to the acoustic field generated within it by the rear radiation from the drive units. Even vented enclosures rely on the panels containing, without deflection, the pressure element of the resonant action of the port.

Of course, real materials have finite loss and stiffness and hence will deflect in an acoustic field, and the problem has been to minimise this movement by judicious use of the available materials within the constraints of economics and ergonomics.

In general, at low frequencies the stiffness of the walls dominates their behaviour, while at high frequencies it is their mass which rules. Between these two extremes they interact in a resonant manner which can grossly magnify and time smear the transmission at certain frequencies. This situation is rendered tolerable by resistive losses or damping.

In general one is trying to maximise all these variables, although at times it can make more sense to ensure that a resonance is outside the frequency band to be used than it is to keep it subdued with the use of mass or damping.

The stiffness of a panel for a given mass can be increased dramatically by curving it. Hence axially loaded tubes and spheres have long been recognised as the most efficient users of materials, though in our rectilinear society they have usually been relegated to more exotic designs.

The mass of panels can be increased simply through the use of dense material. Bricks, lead and sand layers all offer increasing attenuation with frequency, but these are all definitely for the DIY enthusiast.

In the real world, cabinets were made of wood with various degrees of panel bracing and damping, like bituminous mats and suchlike, which also helped increase the mass. By increasing both the mass and the stiffness, the lowest point in the curve corresponding to the minimum transmission loss may be brought up to reasonable levels. (figure AVI.1) In 1983

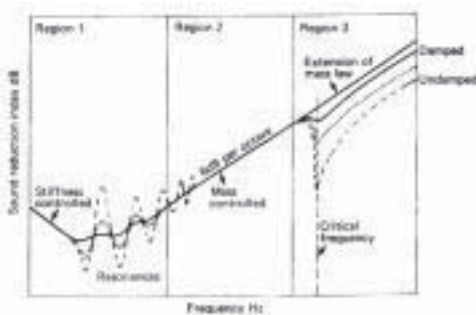
Celestion revealed their SL600, which for the first time used Aerolam™ panels in which two sheets of material are separated by a honeycomb structure. This structure makes the best of a given mass and thickness of material by ensuring that all forces act in the plane of its sheet components. This greatly increases the transmission loss at low frequencies by extending the stiffness region of the curve upwards in frequency. The result was a stiff rather than light enclosure, with high frequency resonances near the coincidence critical frequency, which required damping with thin pads. Aerolam™ is, however, rather costly and difficult to work with, and the lightness of the panels makes the mass law part of the curve lower than usual, which allows high frequencies to be transmitted through the cabinet panels.

The Matrix™ approach to the problem is to extend the honeycomb principle of Aerolam™ to the full width of the enclosure. The walls are then being supported across their full area and, in the limit, require no bending stiffness at all, the displacement being entirely dependent on the longitudinal stiffness and acoustic velocity in the honeycomb.

To provide the support of the three pairs of walls, an orthodox structure is preferable to the honeycomb. A wine box inspired the final structure of the Matrix™ which has now become a standard feature in all the high-end B&W models.

The result when using wood is a cabinet that exceeds the stiffness of Aerolam™ for low frequencies, has a higher mass for better high frequency transmission loss, and the high inherent damping of wood composites over aluminium significantly damps the inevitable resonances, which now occur at much higher frequencies. The overall mass of the cabinet is higher than that of Aerolam™, which is an essential element in a decoupled driver configuration, where it acts as a seismic mass arrangement.

The B&W CM1 for instance traded mass for stiffness by using a rigid phenolic resin cabinet, which shifts the resonances well out of band. Other ideas like moulded trays or 3-dimensional weaving have all been examined but the original 'low-tech' solution still offers the simplest and



AVI.1 Mass Law + Stiffness + Coincidence

cheapest answer.

Conclusion

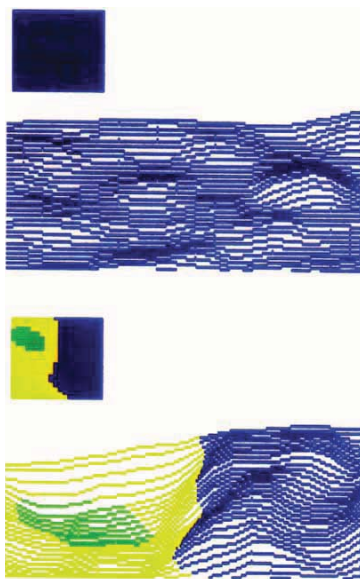
B&W's patented Matrix™ enclosure reinforcement system was used in the Matrix™801 to greatly reduce cabinet vibration effects. Even when using very strong and massive laminated wood enclosures such as those found for instance in the Signature™800, there will always be cabinet panel resonances in evidence without Matrix™ stiffening. These, though they may have been reduced in magnitude by the cabinet's own mass and stiffness and by the judicious use of strategically placed bracing members, will still radiate to some extent. This radiation is compounded by the much larger area that the whole cabinet represents when compared with the area of the drive unit diaphragm itself. This means that unwanted movement of the cabinet's surface must be reduced to the smallest levels achievable. This is where the Matrix™ system comes into play as shown in the next few pictures.

Effect of Matrix™ Technology.

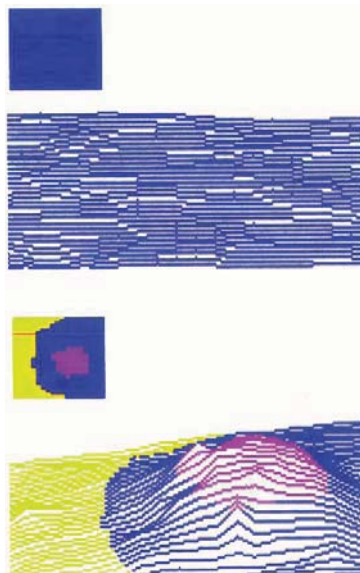
Cabinets damaging sound
(Impulse Plots, figure AVI.2a, b etc)
Lower image shows cabinet side without Matrix™.
Upper image shows effect of Matrix™ on cabinet side vibrations.

The lower picture shows the effect of an impulse being fed into a speaker on the right hand side, (not seen), at right angles to the side we are looking at. Initially we see the impulse spreading over the visible cabinet side and ringing on for a very long time after that.

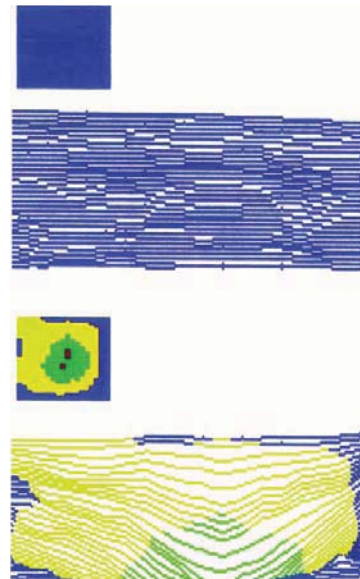
The upper picture shows the same speaker and cabinet side, but now there is a Matrix™ present. The effect of the Matrix™ is to virtually remove all traces of the cabinet vibration except immediately behind the speaker unit. The vibrations have been reduced by at least 45dB. In this illustration, the cabinet was made of thick MDF material, (glued compressed sawdust), often used in speaker cabinets.



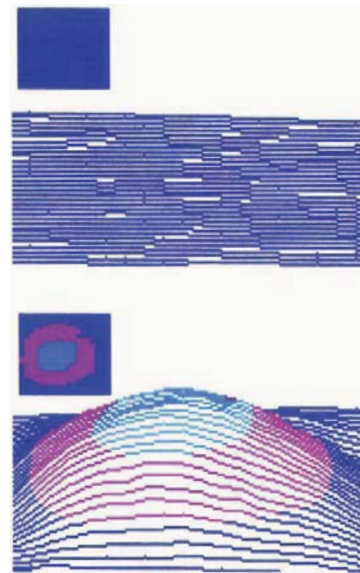
AVI.2a Whole Cabinet side Impulse Progression Plot, at 480 u-sec



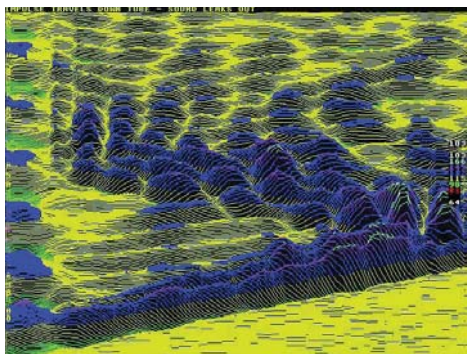
AVI.2c Whole Cabinet side Impulse Progression Plot, at 2010 u-sec



AVI.2b Whole Cabinet side Impulse Progression Plot, at 1740 u-sec



AVI.2d Whole Cabinet side Impulse Progression Plot, at 3330 u-sec



AVI.3 Single Slice Impulse Progression Plot – Box Side

Points to note are

- A Matrix™ completely prevents the box sides vibrating where it connects to them
- A Matrix™ damps out any remaining vibrations in the much smaller unsupported regions
- Cabinet radiation is reduced by at least 45dB relative to no Matrix™ present

Effect of Insufficient Transmission loss inside to outside (Impulse Plot) figure AVI.3

The plot shows the transmitted vibration of the side of a long tubular cabinet in response to an input impulse fed to a drive unit at the left hand side. So we have distance from left to right, and time moves away from us up the page.

Points to note are:

- The initial impulse moves from the speaker at the left, along the tube from left to right
- It is reflected at the right hand side and moves back again along the tube from right to left
- The wave speed can be determined from the acute angle of the initial movement to the x axis
- This is the speed of sound in air, not in the material of the box

This clearly shows that the box is not massive enough to stop the sound from leaking out through the material of the box itself.

Note: that a vibration in the chassis of the driving speaker can be seen at the left hand side.

The Effects of the Decoupling Spring on Speaker Performance

The effects of the decoupling spring between the magnet chassis and the speaker box have been investigated theoretically and experimentally verified. The main results of this are hardly surprising – the resonance frequency of the magnet plus chassis on the decoupling spring stiffness should be as low as possible to avoid any undesirable effects on the speaker's response in its pass band. Also, if the resonance frequency of the magnet plus chassis on the decoupling spring, is the same as that of the speaker cone on the combined stiffness of its suspension and the air in the box, then there is no effect on the speaker's response. This latter effect would drift in production and is probably not a desirable solution to the decoupling problem. The effects of the spring losses on the response have also been investigated.

Method

As in time honoured style, an equivalent circuit was derived by inspection for the three masses and three springs and one force generator, all fully floating, which this complete system comprises. The fact that all three masses were fully floating contributed to the difficulty of finding the correct equivalent circuit, because a reference to ground is always required for equivalent circuit analysis. Once a mechanical circuit had been derived, the 'voltage' electrical model was derived from that mechanical circuit with capacitors being equivalent to masses and inductors to springs. Then the dual of that circuit was produced to form the 'impedance' model, (inductors = masses, capacitors = springs), which was analysed to produce the volume velocities (ie currents) flowing into all the parts of the system. These are used to give the output response taking everything into consideration.

Verification

A simple speaker system was built comprising of a magnet and a cone of the same mass as the chassis plus the magnet. This was suspended on rubber bands to comprise a fully floating system. The nearfield sound pressure output of the cone was measured

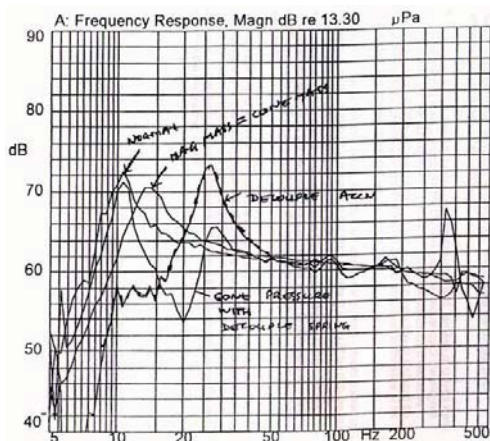
- with the magnet equal to the cone mass and
- with the magnet being much heavier than the cone (which is the normal situation)

Next, the whole system was supported on a large lump of rubber and this constituted the 'decoupling spring' of a more normal speaker system (this test system had no box of course). The acceleration at various places in the system was also measured with a small accelerometer. The frequency responses of the accelerations of these parts of the system are related to the frequency response shapes of the volume velocities of the same parts and thus to any radiation which may take place.

Of course, parts like the decoupling spring will not actually do any radiating, but other parts like the speaker cone itself will. Thus accelerations of the parts of the system may be compared with each other, just like the acoustic outputs of some parts may be. (figure AVII.1)

Points to note are:

- The shift of 1.414 in the basic resonance of the system when the magnet mass changes from 'large' to the same as the speaker cone.
- The dip followed by a peak in the cone output with decoupling spring present. The dip occurs at the frequency at which the magnet plus chassis resonates on the stiffness of the spring.
- The output of the cone at high frequencies remains unchanged over a wide range of magnet masses. This occurs because the voice coil produces a force, which it exerts equally in both directions, ie into the cone and into the magnet system. They then exhibit an appropriate acceleration according to $F = ma$ with F being the same in both directions and the magnet and cone masses determining the accelerations and hence the radiation from both directions.



AVII.1 The results show a high degree of correspondence between the measured system and an equivalent theoretical system

The effect of the decoupling spring losses was then investigated. As expected when the losses are total (ie $Q(\text{decouple})$ very small) the system defaults to a normal speaker plus chassis plus enclosure. As $Q(\text{decouple})$ is increased, the dip and peak in the response become more and more pronounced. The effective Q of the lump of test rubber was approximately 20, which gave the correct ratio between peak and dip in the response. Next, a more normal speaker system was investigated and families of curves were produced varying such parameters as $Q(\text{decouple})$, the frequency of the magnet resonating on the decoupling spring, and so on. From these curves it becomes apparent that either the decoupling resonance should be very low, or it should be the same as that of the cone mass resonating on the combined stiffness of its suspension and the air in the enclosure. In the interests of maintaining consistency of performance with variations in the driver fundamental resonance frequency, the former option was adopted.

Finally, the volume velocity being fed into the cabinet was plotted – this of course is the reason for decoupling the magnet in the first place and it should be reduced as much as possible within the pass band. Curves are shown with the decouple frequency being 1Hz and $Q(\text{decouple})$ being 20. It is seen that very little volume velocity is being fed into the cabinet. Comparing this when $Q(\text{decouple})$ is small and $F(\text{decouple})$ is 20 shows the size of the relative problem that proper decoupling will solve.

So decoupling is effective if it is correctly applied, the big danger being that the resonance of the magnet on the decoupling spring may fall within the pass band. If that is the case, there will be a peak and a dip in the response the size of which depends on the decoupling spring losses. Of course, the larger the losses the less effective the decoupling will be.

Use of decoupling in the 800D

The 800D uses extensive vibration isolation to minimise cabinet resonances and driver interactions in a similar way to the previous Nautilus 801 and Signature 800. The techniques used have drawn from B&W research work, which has shown, both theoretically and

practically, the benefits of decoupling. This work has also shown how and where decoupling is best applied, as well as the problems that can arise if performed incorrectly.

Good isolation between components is relatively easy to achieve on the laboratory bench, but engineering it into a rugged product would have been far more difficult without the application of a new material. It is vital to ensure that the fundamental spring /mass resonance of any reliable decoupling scheme is below the operating frequency range of the speaker drive unit. If this is achieved then any damping control is unnecessary and even undesirable. To achieve the lowest resonance the spring must be soft and the mass must be high. The trouble has always been getting a soft spring to support a high mass within tolerances. The midrange driver isolation of the Nautilus™801, duplicated in the 800D, was a particular challenge and one that drove the search for new materials.

Despite the huge mass and stiffness of the midrange enclosure, decoupling the midrange driver from it produces huge reductions in cabinet vibration. However, there must be a complete seal that fits within the required acoustic shape and point contacts (fixing screws are undesirable because they unnecessarily excite higher order modes). A tensioned rod system was devised to hold the driver against the cabinet with complete axisymmetry. It was then necessary to find a very compliant material to mate them.

Foams were easily soft enough but unable to support a load long-term. Heavily plasticised materials could be found with the low Shore hardness required, but leached or crept in the long-term and were often too lossy to be effective across the band. Unfortunately, a fairly large gulf separated the hardness of these materials from the usable, homogenous, stable rubbers – even the softest silicones. Armed with an idealised specification, the purchasing team succeeded in a more extensive search for super-soft rubber suppliers.

The material finally chosen was an ultra-soft, thermoplastic rubber, injection moulded using cross-linked gel techniques. This material is effectively a liquid suspended with complete

stability in a polymer molecular matrix. Its mechanical properties are a reflection of this structure. It is very compliant in shear and stretch but has poor compressibility when confined, much like a liquid but unlike conventional elastomers. And while it is freely elastic at low frequencies, it exhibits more viscoelastic behaviour at much higher frequencies (it has a high $\tan \delta$ product) giving it a useful transmission loss. The gel is thus employed in an L-section gasket on the rim of the midrange chassis. The mass is supported by the thin edging, which provides shear freedom, and the tension is held against a thicker compressive region, the unconstrained edge of which follows the critical internal profile of the midrange cabinet. The gel is also employed at the other end of the tensioned rod to provide a fully floating assembly with the required single degree of freedom at a frequency well below the pass band.

Additional mass is coupled to the midrange magnet to further lower the resonance frequency and reduce chassis displacement, this being of additional importance because the cone impedance matching relies on the chassis as a virtual ground. The high loss of the gel at these elevated frequencies is thus invaluable, because it provides damping control of any structural modes in the chassis itself. To ensure that low-frequency vibration from the bass driver does not excite the midrange decoupling resonance, and to shift cabinet on cabinet resonances below the bandwidth of the bass driver, the weighty midrange head is supported on a bed of the gel at its base and at the rear of the tailpipe.

A similar scheme is employed for the tweeter/head interface. The tweeter motor is satisfactorily isolated from the heavy cast housing by conventional rubber O rings, but the entire housing is decoupled by a sculpted gel interface. Isolation is provided by shear freedom, but a ribbed surface profile is employed to improve compressibility and thus ensure that even the rocking modes are well below band, yet kept marginally above the midrange cabinet's fundamental resonance frequency.

It will of course be noted that the bass drivers are not decoupled from the cabinet. This design decision follows from the Nautilus™801 and was made fairly early in that speaker's development stage, because the complications necessary to do the job correctly would have been impractical and perhaps unwarranted. Unlike the midrange and treble drivers, a bass driver reacts against a large air stiffness, so any orthodox compliance scheme would involve losses or in-band resonances unless the mass of the magnet was unreasonably high. In passing, note that limited magnet excursion has no effect on the acoustic output of a mass-controlled diaphragm, as in the mid and treble schemes.

However, decoupling cannot be ignored because it will occur in a mechanical system at some frequency whether it is desired or not. If that frequency cannot be brought below band then it is best to raise it above. To this end, the hugely stiff bass chassis are bolted firmly into the rigid Matrix™ cabinet, which ensures that the first chassis/cabinet resonance is just above band and that there is minimal lost motion between the two. The Matrix™ construction of the cabinet has long been proven to be acoustically inert, so any vibration energy imparted on the cabinet has no serious panel modes to excite and is quickly dissipated. Lost motion to the acoustic environment is also minimised because the cabinet and plinth assembly is massive enough to become a virtual earth for the driver to react against.

Introduction

Much work at B&W over the years has resulted in proprietary Finite Element and Boundary Element code capable of accurately predicting the vibration and acoustic behaviour of axisymmetrical shapes using Finite and Boundary Element Analysis. Papers listed (refs) include several on this topic. B&W proprietary code runs at more than 10 times the speed of any commercially available package and allows in-house optimisation packages based on 'simulated annealing' to find the global minimum of any target function we may like to specify. The result of this is that a computer may be left to search through the whole relevant design space to find the best model that will fit our requirements – and it will not be trapped in any local minima along the way.

When non-axisymmetric modelling is needed, commercial Finite Element packages have to be used and one of these, PAFEC, allowed the modelling of the total acoustics of normal Nautilus™ rearward inverted horns, though not the coupling of a lumped parameter speaker model at the near end. The tube was therefore excited with an 'ideal' forced diaphragm for this exercise. As expected, this shows up the onset of the first higher order cross mode of propagation as a resonance across the mouth of the horn (ie where the speaker is situated). This graphically illustrates that rearward Nautilus™ horns may not be used on their own above this cut-on frequency, as this transverse mode is clearly audible through the speaker diaphragm.

The following report from Gary Geaves covers the analysis of this phenomenon:

B&W Loudspeakers Ltd and Computer Simulation

Computer simulation based on the Finite Element and Boundary Element methods has been widely exploited in many diverse scientific and engineering applications. The Finite Element Method was developed in the 1950s to aid in the design of aircraft structures. Since then it has been applied to structural, thermal, electromagnetic, fluid flow and acoustic problems. In many industries, such as the automotive, it has been long regarded as an essential design tool. However, it is only

relatively recently that sufficient computer power has become readily available and the underlying mathematical techniques sophisticated enough to be of use in the design of loudspeakers.

Engineers at B&W were quick to spot the potential of computer simulation in the design of loudspeakers, first becoming involved through collaborations with academic institutes in the mid 1980s. At that time, if one wanted to carry out simulation of an acoustic system, it was necessary to develop and code the algorithms from scratch. For this reason, B&W has proprietary code, written in the Fortran programming language, to solve a specific class of problem. This code is used routinely and is being constantly enhanced. It has also been used as the basis for an optimisation system that will automatically select designs fulfilling specified design criteria.

Recently, especially in the last five years, commercial, off the shelf systems have become available that allow simulation of acoustic systems to be performed. With the introduction of such systems, computer simulation in the loudspeaker industry is becoming increasingly important, with many other companies investing in the area. More recently, the task of porting the Fortran code to Matlab, a popular high level scientific programming language, has commenced at B&W. Though Matlab code is slow to execute in comparison to Fortran code, it has numerous high level features and in-built graphics routines that make it an ideal test bed for quickly trying out new ideas.

A detailed description of B&W Loudspeakers' research into and application of computer simulation to the design of loudspeakers may be found in the references section.

References

- 1 Jones, C.J.C (1985) Finite Element Analysis of the Effect of Damping in the Piston and the Outer Suspension of a Loudspeaker Diaphragm, Proc spring Conf of the Institute of Acoustics, York Univ.
- 2 Jones, C.J.C (1986) Finite Element Analysis of Loudspeaker Diaphragm Vibration and Prediction of the Resulting Sound Radiation, PhD Thesis, Brighton Polytechnic
- 3 Jones, M.A. and Henwood, D.J. (1991) Finite Element Modelling of Loudspeaker Drive Units, In IMACS '91, Vol. 4, ed. R. Vichnevetsky & J. J. Miller. Criterion Press, Dublin
- 4 Jones, M.A, Binks, L.A. and Henwood, D.J. (1992) Finite Element Methods Applied to the Analysis of High Fidelity Loudspeaker Transducers, Computers and Structures. 44
- 5 Jones, M.A, Henwood, D.J. and Fryer P.A. (1992) A Computer Model of the Vibration and the Sound Radiated by Loudspeaker Models and its Validation, Acoustics Letters, 15(8)
- 6 Henwood, D.J. (1993) The Boundary Element Method and Horn Design, The Journal of the Audio Engineering Society, 41(6)
- 7 Geaves, G.P. (1994) An Investigation using the Boundary-Element Method into the Acoustic Field Resulting from Concave Loudspeaker-Type Structures, Acoustics Letters, 18(6)
- 8 Geaves, G.P. and Chakrabarti, R. (1995) Modelling and Optimal Design of Tweeter Loudspeakers, In Proceedings of Vibration and Noise 95, 25th-27th April, Venice
- 9 Geaves, G.P. (1995) The Simulation of midrange Loudspeakers using Numerical Methods, In Proceedings of the IEE Audio Engineering Colloquium, 1st May, London, Digest No: 1995/089
- 10 Geaves, G.P. (1995) Modelling and Optimal Design of Loudspeaker Diaphragms Using Numerical Methods, PhD Thesis. University of Brighton
- 11 Kirkup, S.M. and Jones, M.A. (1996) Computational Methods for the Acoustic Modal Analysis of an Enclosed Fluid With Application to a Loudspeaker Cabinet, Applied Acoustics, 48(4)
- 12 Geaves, G.P. (1996) Design and Validation of a System for Selecting Optimised midrange Loudspeaker Diaphragm Profiles. The Journal of the Audio Engineering Society, 44(3)
- 13 Geaves, G.P. (1996) Horn Optimisation using Numerical Methods, Presented at the 100th Convention of the AES, Copenhagen, pre-print 4208 (J-5).
- 14 Geaves, G.P (1998) Finite Element Analysis of an Inverted Horn. B&W Loudspeakers Ltd White Paper

Appendix IX

Laser Interferometry

Introduction

Various laser test methods have been extensively used in the development of speakers at B&W. There now follows an introduction to the armoury of laser test methods available.

B&W was the first speaker company to use a Harwell interferometer to make the vibrations in cones visible. Over the years there have been several significant improvements to the system, and one entirely new technique has been invented, which has great potential for helping to improve the design of cones and surrounds. Lasers are being used routinely during the development of new cones and surrounds at B&W.

The four main ways that a laser may be used to show cone and cabinet vibrations are:

- Single Slice single frequency plots (phase-sensitive or rectified)
- Single Slice multiple frequency plots (phase-sensitive or rectified)
- Impulse Progression Plots (single slice animated or as a 3-D plot)
- Whole cone plots of frequencies or impulses (as individual plots or computer animated)

In addition, each of these techniques may be applied to the air itself in front of the cone and the speaker enclosure by utilising a very light diaphragm to represent the movement of the air in response to the sound radiated from the driver and the cabinet.

Computer animation techniques may be used to produce movies showing either the phase response at any single frequency over the whole cone or the progression of an impulse as it spreads out from the cone neck.

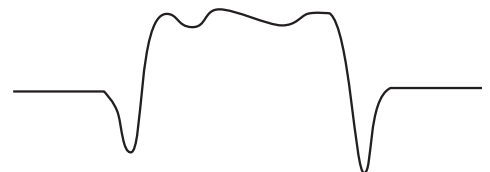
Single Slice – single frequency – phase-sensitive or rectified

The laser is used to plot single slices across the middle of the cone

A diameter across the cone is scanned with the laser beam to produce two distinct types of plot as shown in figures AIX.1a and b. This is done at a single frequency of interest. On reflection from a moving object, the frequency of the laser light is changed by the cone movement due to the Doppler effect. The motion of the object is derived from that frequency shift by using what is in effect an FM radio. The output of this FM radio is then compared with the input signal to the speaker. If they are in phase with one another the result is plotted upwards on the screen. If they are out of phase it is plotted downwards. The resulting phase-sensitive plot shows which parts of the cone are moving in the same direction as the voice coil and which parts are moving in the opposite direction – that is, it shows which parts are totally out of phase with the voice coil. The disadvantage of this type of plot is that those regions which are 90° out of phase with the voice coil do not show up at all. To overcome this disadvantage we have the 'rectified' plot, which disregards phase and always plots upwards if there is any cone movement at all. Clearly there is a need for both types of single slice plot for a complete picture of cone movement to be obtained.

Full speaker surface scan – single frequency – phase-sensitive or rectified

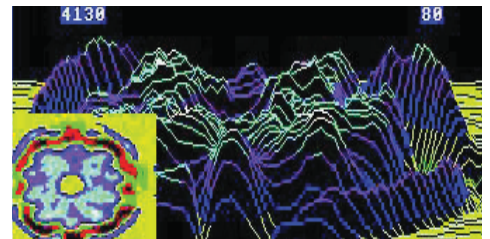
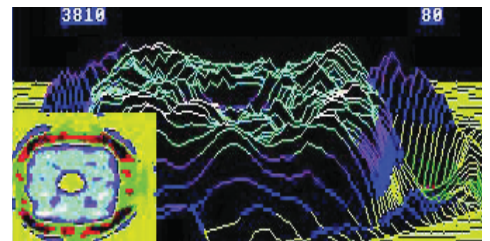
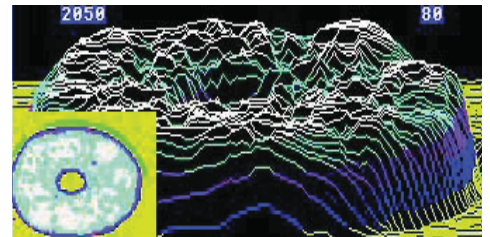
The second type of plot is produced by scanning the whole surface of the speaker, still at a single frequency of interest. On reflection, the frequency of the laser light is still changed by the cone motion because of the Doppler effect. The motion is derived as before from the frequency shift by using the FM radio principle and the resulting information is now displayed in 3-D, producing mountain like plots as shown in figures AIX.2 and 3. A perfect piston-like cone gives 'top hat' pictures, with every point on the cone moving exactly the same amount with so-called 'piston' motion. The hills and dales produced by less than piston-like motion are easy to see, but are possibly less easy to interpret, and greatly aid the design and development process. Figure AIX.2 shows a classic cone surround mode where the whole surround is moving out of phase with the cone causing a dip in the resulting frequency response. Figure AIX.3 shows a totally symmetrical break-up pattern where for every region going upwards there is an equal



AIX.1a Phase Sensitive Slice Plot – Surround out of Phase



AIX.1b Rectified Slice Plot – No Phase Information



AIX.2 Whole Cone Single Frequency Plots. Top Picture at Low Frequency, Bottom at high Frequency.
Note: 4-way symmetry and smoothly reducing central area

and opposite region going downwards. The net result of this is that air is merely shunted around in the near field and very little sound energy finds its way into the far field. What we are then left with is any underlying perfect piston motion and the radiation from the central regions, which are still moving pistonicly. When the hills and dales are equal in number and height, we have what is in effect a multipole source which, when the wavelength of sound in air is greater than that in the material, is very inefficient at radiating. Just as with single frequency single slice plots, the scans may be done with phase-sensitive detection or with a rectified output. The surround resonance shows up as a characteristic 'flan dish' shape with phase-sensitive detection, whereas with rectified plots only a slight difference will be seen from perfect piston motion.

Phase animated – single frequency – full-surface scan

The full-surface phase-sensitive detection method is used for this type of plot except that, instead of just one whole surface scan, a set of up to 20 surface scans are carried out, each one being at a different phase though the vibration cycle. When these 20 pictures are placed in the computer's memory, a second programme allows all twenty pictures to be repeatedly mapped onto the screen. This gives the impression of animation and can often show up features in a speaker's response not clearly visible from a single frozen-phase whole-cone scan. For IBM PCs these can be produced as 'AVI' files which may be played with the standard Windows™ media viewer programme.

Phase Animated Single Frequency Plot (20 Phases) figure AIX.3

- Complete single-frequency phase-sensitive plot over whole cone
- A bell mode is evident, giving peaks and dips around cone's circumference
- A resonance in the surround can clearly be seen – it is the first harmonic
- The surround pulls tight at top dead centre (see single slice at the top left)
- The picture shown here is from top dead centre

Note: The bell mode has an equal number of sectors going upwards and downwards. These are also of equal amplitude and therefore their radiation cancels out in the near field (it's an 'acoustically fast' multipole source). The surround resonance is not cancelled out by anything and is responsible for a major peak and dip in the speaker's response. The surround pulling tight will cause distortion in the resulting output sound.

Frequency animated full-surface scan

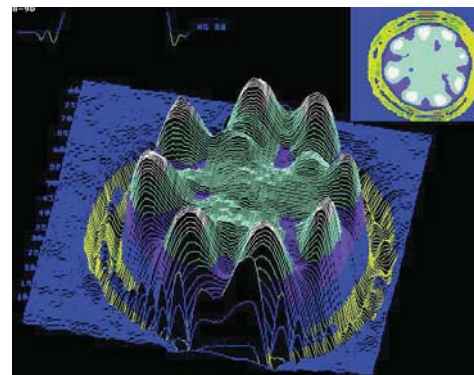
Either the phase-sensitive full-surface or the rectified full-surface type of plot is used for this technique, except that instead of just one whole surface plot being carried out at a single frequency, a set of 256 separate frequencies are used from 200Hz to 20kHz, spaced at approximately 80Hz intervals.

In this case, the scanning mechanism leaves the laser spot at each of 126 x 126 positions on the cone surface, while 256 measurements are taken smoothly from 20kHz down to 200Hz at each of the 256 separate frequencies. The results are stored on a computer disc and the spot is then moved on to the next position. Complete surface plots for each frequency are disentangled from the set of results at a later date, using specially written software.

Just as with phase animated plots, the set of 256 separate frames can be projected onto the computer screen as a movie, graphically showing the development of surround and one resonances which sweep in and out of view as the frequency is changed. The differences between the behaviour of say a Kevlar® cone with a bending wave impedance matched surround and a plastic cone with a conventional surround is very striking when both animated full-surface scans are visible on the screen at the same time.

Frequency Slice Plots

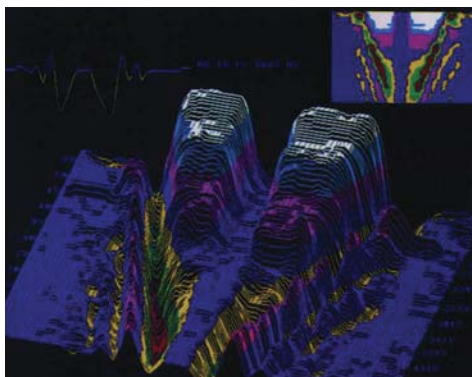
In this case instead of the whole surface of the cone being raster scanned at a single frequency like a TV picture, a single strip of the cone from edge to edge through the middle is repeatedly scanned. Starting at the rear of the plot and at a low frequency, the frequency is increased for each succeeding sweep plotting in front of the previous one, and the resulting 3-D plot shows



AIX.3 Phase sensitive whole cone plot. Peaks and dips cancel out, surround sound resonance does not.

a frequency history of the behaviour of that slice of cone as can be seen in figure AIX.4. Once again this may be done using either phase-sensitive detection or the rectified method. Resonances and other problems may be seen at a glance, particularly if the cone is axisymmetric. This may be the only kind of laser plot that is necessary to show everything that is wrong (or right) with the speaker cone/surround/coil combination.

The results of Finite Element Analysis are often plotted in this way as well, so it forms a very convenient test for the accuracy of finite element predictions of cone vibration behaviour.



AIX.4 Phase Sensitive Frequency

Phase Animated Frequency Slice Plots (figure AIX.4)

Just as with the slice plot above, a complete set of scans is done from a low frequency to a high frequency at each of 20 different phases. The resulting 20 plots are then animated, revealing each slice's behaviour as it moves through a complete vibration cycle. This rather curious 'frequency normalised' phase animated frequency slice plot shows the same 20 phases for each frequency, so the animation proceeds at the same rate for 20kHz as it would for 200Hz. Another form of plot, as yet to be produced, would cycle through the phases at 20kHz at 100 times the rate that they are cycled at 200Hz. It is doubtful though whether such a plot would be of any use. The frequency-normalised phase-animated slice plot gives the impression that energy passes down the plot from low frequencies to high frequencies, but this is merely an artefact of the normalisation.

Plots such as these show in graphic detail phenomena such as the progression of energy from the voice coil to the surround at high frequencies, just like waves moving down a length of rope being shaken up and down at one end. Also often seen is the surround lagging behind the movement of the otherwise piston-like cone by 90°.

Phase Animated Frequency 'Slices' (20 Phases) (figure AIX.4)

- Rear Slice is a scan across the middle of the cone at 0.5kHz
- Front Slice is a scan across the middle of the cone at 5.5kHz
- Each frame is at a different phase through a complete cycle at each slice's frequency
- This is a very bad cone, showing major resonances and poor surround behaviour
- The single frame from the sequence shown here illustrates the surround phase lag at the rear

Note: The slice at the front, at 5.5kHz, is just like a rope being waved at one end. No sound will be radiated at this frequency. Even the slice at the back, at 0.5kHz, shows that the surround lags behind the cone (otherwise behaving like a piston) by 90°. Thus the surround radiation will cancel and reinforce the cone sound differently depending on the direction. On axis there will be little effect, but the directional pattern will suffer peaks and dips as a result. The major resonances produce peaks and dips in the speaker's response in all directions.

Impulse Progression Plots – in cones and in the air – slices or full cone

The latest technique in the formidable armoury of laser-based measurement techniques available to B&W engineers is called the Impulse Progression Plot.

In this case, the laser beam is pointed at a position on the cone and the speaker is fed with an impulse, rather than either a single frequency or a sequence of frequencies as in the previous methods. The resulting impulse response of the point is stored in the computer and the beam is moved on to the next point, where its impulse response is translated into digits.

For the single slice impulse progression plot, just a single line of impulse responses is used. For the whole cone case obviously, impulse responses from the whole cone surface have to be translated for processing later.

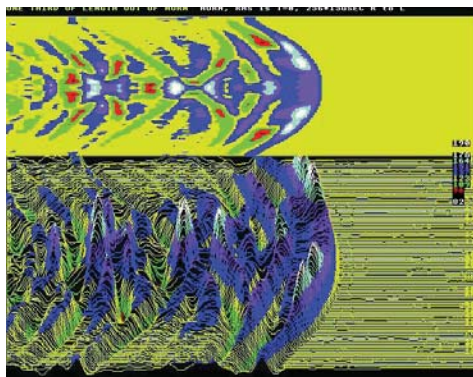
With a single line of impulses, a plot is produced across the whole diameter for each time interval of the sampling of the individual impulse responses. Each succeeding time

interval may be produced as a 3-D plot, with time equals zero placed at any edge of the page (usually at the left hand side). The resulting cone behaviour is then displayed in 3-D as a time history from left to right (or whatever).

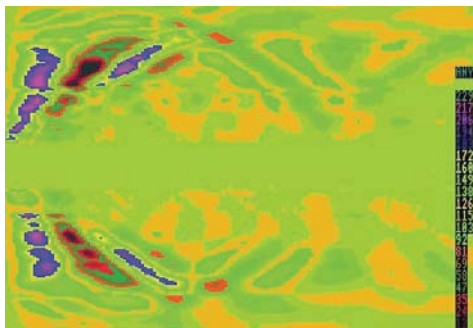
Alternatively, the single line may be displayed on the computer as a movie, and the line then appears to waggle up and down as the impulse progresses back and forth along it. However, perhaps the most useful presentation technique for the single slice impulse progression plot is as a coloured contour plot, with time equals zero at the left hand side – time therefore progresses from left to right, with the voice coil in the middle and the surround at top and bottom. An example of this is shown in figure AIX.5.

This sort of presentation immediately reveals that there are several different types of wave motion conveying energy from the voice coil to the surround and back again. The most significant of these are bending waves and compression waves, the latter travelling much more quickly than the former. Figure AIX.6 shows the impulse coming in at the voice coil in the centre. The cone begins to follow it and the wave progresses outwards in both directions to strike the surround near the edges of the picture. This looks very much like ripples produced when a stone is dropped into a round pond.

A computer animated version of this picture shows in graphic detail how much of the incoming bending wave is taken into the surround and how much is reflected back down into the cone again to form standing waves or resonances. The impulse may also be seen moving about in the surround itself, all the while being absorbed and reflected during its travels. The cone can clearly be seen to behave like a transmission line for bending waves (and for other types of waves as well) and for best effect should be terminated in the characteristic impedance of that line at both ends. This will ultimately produce minimum reflections and maximum absorption and consequently fewer resonances and a cleaner sound output.



AIX.5 Wavefront Arrival Plot – Sound in the Air



AIX.6 Impulse Progression Plot – Cone Diameter

Generalisations

As with all the above single slice types of plot, this single slice impulse progression plot is especially applicable to axisymmetrical cone structures.

For materials such as woven Kevlar®, the whole cone impulse progression plot has to be used. In this case, a complete picture of the whole cone is built up from each of the sampled individual time elements making up the impulse responses at each point on the cone. These pictures are cycled from either the hard disc or the memory of the computer onto the screen, showing graphically an animation of the progression of the impulse across the whole of the cone surface.

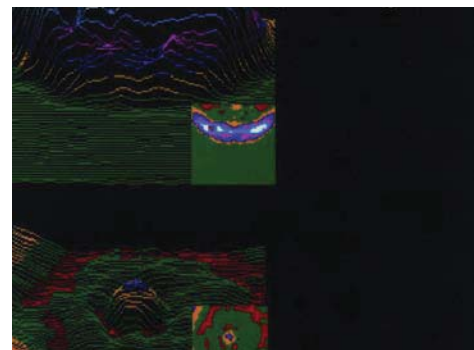
Plots of the motion of the air motion itself

As described in the paper 'Laser Techniques in Loudspeaker Design including the Impulse Progression Plot', B&W has a Laser Doppler Velocimetric technique for observing the passage of waves across the surface of a

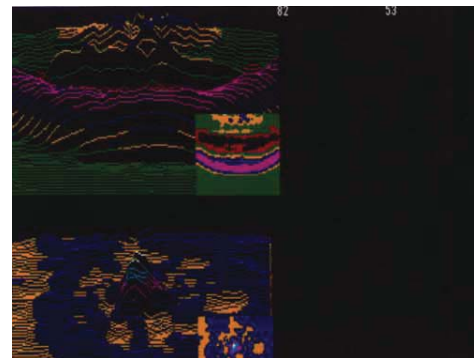
speaker cone. As further shown in the Paper 'New Pipe and Horn Modelling', this technique may be extended to measure air motion in order to discover which parts of the speaker cone do the radiating and which parts of the speaker box allow waves to be diffracted, so spoiling the resulting sound. The technique involves placing a very light, highly stretched clingfilm diaphragm, lightly dusted with talcum powder, in front of the driver. Although this diaphragm is like gossamer and is totally acoustically transparent, it does move with the passage of any sound wave, behaving almost like part of the air up to supersonic frequencies. Since it moves with the sound it may be observed with the Laser Doppler velocimeter, which therefore detects the movement of the air itself. (figure AIX.6)

This technique may be used in a number of ways. The most obvious is to scan a whole diaphragm placed in front of a cone or speaker box. This allows us to observe the progression of the impulse across the air in front of the cone and across the surface of the box. The second way is to place the diaphragm in a succession of positions further and further away from the speaker or box and measure either a slice across the diaphragm, or indeed the whole diaphragm at each position. Computer processing then allows the passage of the impulse in the air to be viewed as it passes through each successive diaphragm, either as a succession of 'stills' or as a computer animated movie. This is very useful for observing the transitions from near field behaviour close to the driver or speaker box to far field behaviour, which is what is usually perceived by the listener, and to pin point sources of diffraction and radiation within the total speaker system.

The passage of an impulse through a single diaphragm may be displayed as a 3-D plot, rather like the slice plot for displaying the behaviour of a single slice across a speaker diaphragm at different frequencies. In this case, the first arrival is plotted at the right hand side and subsequent arrivals are displayed from right to left. We thus see graphically with this 'wavefront progression plot' how energy comes along well after the original impulse has passed that point in space.



AIX.7 Phase Sensitive Frequency



AIX.8 Phase Sensitive Frequency

When observing the differences between the impulse behaviour of axisymmetric cones such as those made from plastic, with non axisymmetric cones made from woven Kevlar® fibres, the difference is striking. The sound energy radiated by the axisymmetric cone consists of an initial wavefront, which largely represents the music, followed by a series of other waves, which are not the same in all directions, representing the coloration of the cone and caused by the waves bounding backwards and forwards across the cone. Measuring the behaviour of the air can also be used to illustrate how cabinet edges really do produce copies of the original sound, but often out of phase with the original and delayed by the time it took for the sound to get from the driver to the diffracting sharp edge. (figures AIX.7 and 8)

B&W Bowers & Wilkins

B&W Loudspeakers Ltd T +44 (0) 1903 221800
Dale Road F +44 (0) 1903 221801
Worthing West Sussex info@bwspeakers.com
BN11 2BH England www.bwspeakers.com

B&W Group UK
T +44 1903 221 500
E uksales@bwgroup.com

B&W Group North America
T +1 978 664 2870
E marketing@bwgroup.us

B&W Group Asia
T +852 2 790 8903
E showroom@bwgroup.hk

Kevlar is a registered trademark of DuPont. Rohacell is a registered trademark of Röhm GmbH & Co. KG. Marlan is a registered trademark of Polylac Holland bv. Nautilus and Matrix are trademarks of B&W Loudspeakers Ltd. Copyright © B&W Loudspeakers Ltd. E&OE. Design by Thomas Manss & Company. Printed in the UK. B&W Loudspeakers Ltd reserves the right to amend details of specifications without notice in line with technical developments.

What's a **TEPEX**[®] Sandwich?

By Steve Mowry

TEPEX is the registered trademark of Bond-Laminates GmbH (www.bond-laminates.de/en). Since 2000 the industrial group CENTROTEC Sustainable AG (www.centrotec.com/index_e.php) has been a partner within Bond-Laminates. With the support of CENTROTEC, Bond-Laminates has established its industrial development and manufacturing facilities in Brilon, Germany. TEPEX sandwich is a combination of thin outer layers with a structural foam core. This family of materials is lightweight but very stiff/rigid. Alternating movements can also be absorbed due to the inherent properties of the sandwich composite structure. This makes the material particularly useful for loudspeaker woofer cone applications.

CONSTRUCTION

TEPEX sandwich is a material that consists of thin outer skins of TEPEX dynalite and a foam core (**Fig. 1**). This combination results in a very rigid but light material that can be formed three-dimensionally in a single operation. This is because the forming temperature for both the outer layers and the foam is the same. The forming temperature is approximately 190° C.



FIGURE 1: Illustration of molded sandwich composite construction, Focal "W" cone (www.uto-pia-be.com/Technology/Cone.htm).

A key component of Tepex sandwich is the Rohacell core (www.rohacell.com/en), which is a polymethacrylimide (PMI) hard foam that is used as a core material for sandwich composite

constructions. It exhibits outstanding mechanical and thermal properties. In comparison to all other foams, it offers the best ratio of weight and mechanical properties as well as the highest heat resistance of any structural foam. Rohacell is the registered trademark of Rohm GmbH, a subsidiary of Degussa AG, Düsseldorf, Germany, with distributors throughout the world.

I discussed sandwich composites in "Metal Sandwich Composite Cones for Pro Drivers" in the May 2006 issue of *Voice Coil*. There is an I-beam two-dimensional analogy associated with sandwich composites with the resultant distribution of loads inherent in the skin/foam core configuration, where a composite is simply a specific combination of two or more materials that improves the properties of the individual components. Nature itself has demonstrated the principle that high-strength fibers are the most suitable lightweight material for absorbing forces. Wood, plant leaves, muscles, and bones are just a few examples of composite structures that occur naturally.

These fibers critically determine the mechanical characteristics of the composite, such as its strength and rigidity. The materials generally used are glass and carbon fibers. The matrix material, too, performs a crucial function, transferring the forces between the fibers. The utilization of thermoplastics such as TPU and PA12 offer clear advantages in terms of forming

properties, shelf life, and ease of recycling over thermoset plastics.

TEPEX sandwich can readily be formed into straight cones. The fundamental stages involved are heating the semi-finished cone, forming and subsequently cooling the part in the mold, then removing and finishing the cone including trimming and attaching the surround. Process heating by means of infrared radiation is the preferred method; however, contact heating can also be used. The typical components are carbon, glass and/or aramid fibers, the binding resin, and Rohacell. The process and raw materials are much easier to control than paper cone manufacturing. Once removed from the mold, the properties are stable and environmentally robust. "Quality is designed-in."

There are several grades of TEPEX sandwich composites that are well suited to loudspeaker woofer and mid-base transducer applications.

TEPEX sandwich 106-FG50—0.07mm 28% Glass Fiber Reinforced Nylon 12 (Polyamid) skins/2-10mm Rohacell LS foam core.

TEPEX sandwich 106-FG200—0.17mm 45% Glass Fiber Reinforced Nylon 12 (Polyamid) skins/2-10mm Rohacell LS foam core.

TEPEX sandwich 106-FG290—0.25mm 45% Glass Fiber Reinforced Nylon 12 (Polyamid) skins/2-10mm Rohacell LS foam core.

TEPEX sandwich 108-FG200—0.17mm 45% Glass Fiber Reinforced Thermoplastic Polyurethane skins/2-10mm

TABLE 1 Material properties of TEPEX skins

Material	28% Glass/PA12	45% Glass/PA12	45% Glass/TPU	45% Carbon/TPU	50% CARBON/PPS
Modulus	11.6 GPa	17.5 GPa	23 GPa	41 GPa	40 GPa
Density	1600kg/m ³	1800kg/m ³	1900kg/m ³	1500kg/m ³	1550kg/m ³
Poisson's #	0.3	0.3	0.3	0.3	0.3
Damping	0.010	0.010	0.010	0.010	0.010
Max Temp	105°C	105°C	90°C	90°C	220°C

TABLE 2 Material properties of Rohacell cores

Material	Rohacell 71XT	Rohacell 71LS	Rohacell 51LS	Rohacell 31LS	Coated Paper
Modulus	105 MPa	90 MPa	68 MPa	35 MPa	6.0 GPa
Density	75kg/m ³	75kg/m ³	52kg/m ³	32kg/m ³	683kg/m ³
Poisson's #	0.4	0.4	0.4	0.4	0.33
Damping	0.10	0.10	0.10	0.10	0.020
Max Temp	230° C	170° C	170° C	170° C	N/A

Rohacell LS foam core.

TEPEX sandwich 108-FG290—0.25mm 45% Glass Fiber Reinforced Thermoplastic Polyurethane skins/2–10mm Rohacell LS foam core.

TEPEX sandwich 208-C190—0.25mm 45% 12k Carbon Fiber Reinforced Thermoplastic Polyurethane skins/2–10mm Rohacell LS foam core.

TEPEX custom high temp sandwich—0.25mm 50% 12k Carbon Fiber Reinforced Polyphenylene Sulfide skins/2–10mm Rohacell 71XT core.

Note that Rohacell LS refers to Loud-Speaker applications and XT refers to eXtended Temperature application. The safe operating temperature of TEPEX is directly related to the resin utilized. TPU applications have the friendliest low temperature processes. PA12 requires slightly higher process temperature, while PPS requires high temperature processes.

SIMULATION

The mechanical material properties of the skin materials are listed in *Table 1*. The mechanical material properties of various Rohacell core materials and for a base line simulation, treated/coated paper are listed in *Table 2*.

Figure 2 illustrates the cone geometry used in all simulations. Only the thicknesses and material properties change.

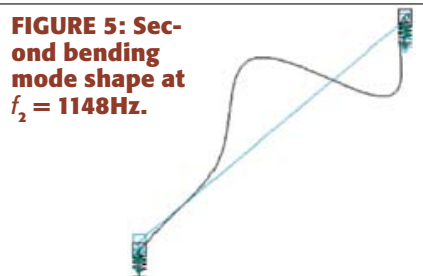
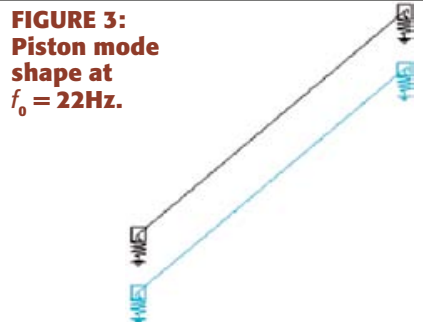
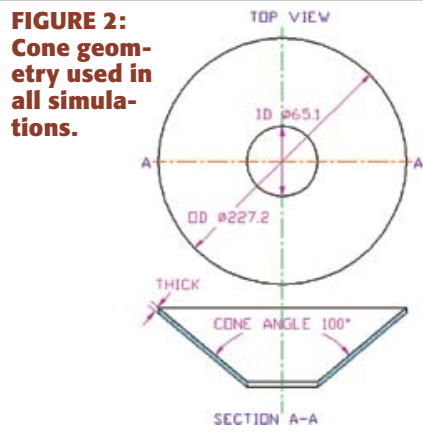
I will simulate all models with S. M. Audio Engineering's proprietary linear dynamic one-dimension composite axisymmetric shell finite element natural frequency analysis with lumped boundary conditions. The assembly boundaries are free to move only in the $\pm y$ -direction, the direction of operation. The voice coil, spider, surround, neck joint, et al. are replaced with two spring and two mass elements. The appropriate values for these are an input to this analysis and can be based on measured data or other simulations. The air load was ignored. This simplifies the FEA. Ironically, the typical "Composites Engineer" is not familiar with harmonic analysis techniques. Their analysis is focused on structural criteria.

First I will simulate a moving assembly containing a 1.3mm thick hard pa-

per cone. The assembly models remain constant throughout this discussion except for the cones. A summary of the results is listed here and the mode shapes are illustrated in *Figs. 3-6*.

MODE	FREQUENCY (Hz)	GENERALIZED Mmd (g)	MODAL DAMPING
f_0	22	77	
f_1	973		0.02
f_2	1148		0.02
f_3	1297		0.02

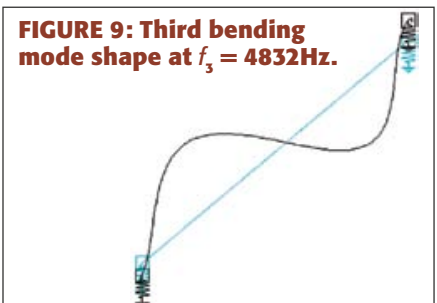
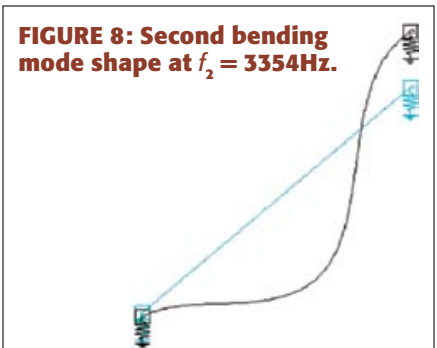
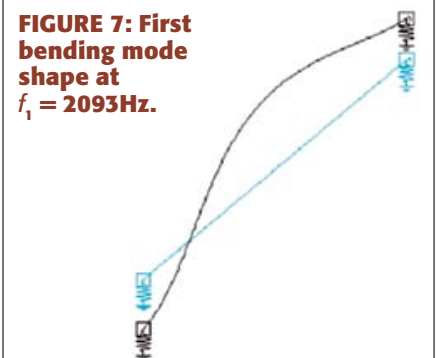
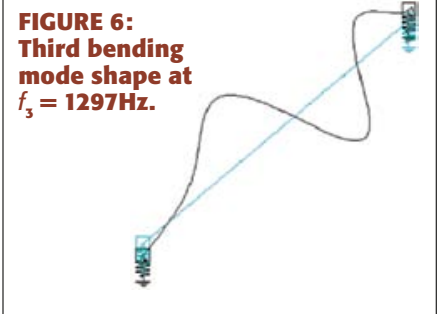
The piston mode shape in *Fig. 3* is the



same for all models. All points move in phase. The frequencies of the piston mode, f_0 , vary due to the mass of the respective cone.

The first bending mode is reasonably well damped, but that is what is expected from paper.

A moving assembly containing a 0.25mm 45% Carbon-TPU/8.0mm Rohacell 31LS/0.25mm 45% Carbon-TPU TEPEX sandwich cone was simulated. A summary of the results is listed here, and the first three bending mode shapes are illustrated in *Figs. 7-9*.



MODE	FREQUENCY (Hz)	GENERALIZED Mmd (g)	COMPOSITE MODAL DAMPING
f_0	21	83	
f_1	2093		0.02
f_2	3354		0.03
f_3	4832		0.03

The cone model illustrated in **Figs. 8-10** is similar to the cones used in B&W's 250mm woofers in the 800D loudspeakers (www.netcomposites.com/news.asp?2865). It is no wonder that this topology and materials are the best all-around performing of all the simulations.

A moving assembly containing a 0.25mm 50% Carbon-PPS/2.0mm Rohacell 71XT/0.25mm 50% Carbon-PPS was simulated. A summary of the results is listed here, and the bending mode shapes are illustrated in **Figs. 10-12**. This is a high temperature cone, good to 220° C with reasonable mass and stiffness along with good damping. This appears to be a good candidate for professional low-frequency transducer applications.

FIGURE 10: First bending mode shape at $f_1 = 1722\text{Hz}$.



FIGURE 11: Second bending mode shape at $f_2 = 2483\text{Hz}$.

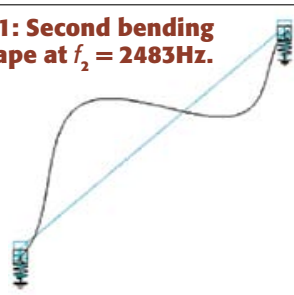
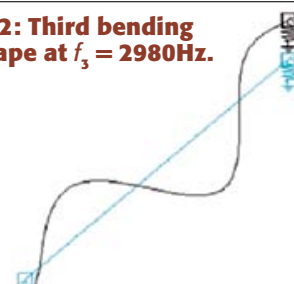


FIGURE 12: Third bending mode shape at $f_3 = 2980\text{Hz}$.



MODE	FREQUENCY (Hz)	GENERALIZED Mmd (g)	COMPOSITE MODAL DAMPING
f_0	22	79	
f_1	1722		0.02
f_2	2483		0.02
f_3	2980		0.02

A moving assembly containing 0.07mm 28% Glass-PA12/4.0mm Rohacell 71LS/0.07mm 28% Glass-PA12 TEPEX sandwich was simulated. A summary of the results is listed here, and the first three bending mode shapes are illustrated in **Figs. 13-15**. This is an ultra-light cone but with less stiffness than paper.

MODE	FREQUENCY (Hz)	GENERALIZED Mmd (g)	COMPOSITE MODAL DAMPING
f_0	25	60	
f_1	690		0.04
f_2	1210		0.06
f_3	1364		0.05

The cone illustrated in **Figs. 13-15** seems to utilize skins that are just

FIGURE 13: First bending mode shape at $f_1 = 690\text{Hz}$.

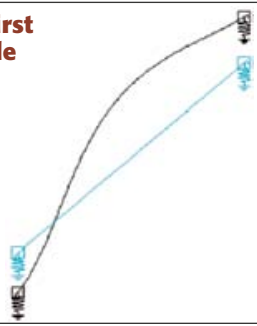


FIGURE 14: Second bending mode shape at $f_2 = 1210\text{Hz}$.

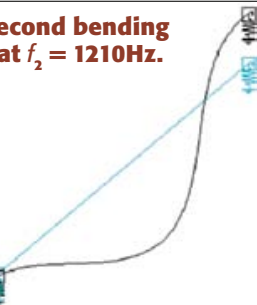
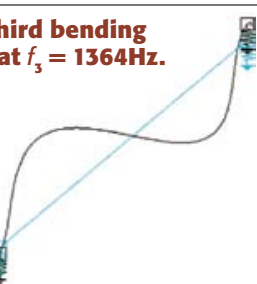


FIGURE 15: Third bending mode shape at $f_3 = 1364\text{Hz}$.



too thin and with too little glass fiber. In this case, the cone tends to the characteristics of Rohacell; the core properties dominate. The next simulation increases both the thickness of the skins but also simulates the increase in glass fiber content from 28-45%. The results indicate a cone with low mass and higher stiffness. This is similar to the Focal "W" cone (**Photo 2**).

A moving assembly containing a 0.17mm 45% Glass-PA12/4.0mm Rohacell 31LS/0.17mm 45% Glass-PA12 TEPEX sandwich was simulated. The results are listed here, and the bending mode shapes are illustrated in **Figs. 7-9**.

MODE	FREQUENCY (Hz)	GENERALIZED Mmd (g)	COMPOSITE MODAL DAMPING
f_0	23	70	
f_1	1098		0.02
f_2	1819		0.03
f_3	2131		0.02

A moving assembly containing a 0.17mm 45% Glass-TPU/2.0mm Rohacell 51LS/0.17mm 45% Glass-TPU TEPEX sandwich was simulated. The results are listed below, and the bending mode shapes are illustrated in **Figs. 19-21**.

MODE	FREQUENCY (Hz)	GENERALIZED Mmd (g)	COMPOSITE MODAL DAMPING
f_0	23	70	
f_1	1156		0.02
f_2	1708		0.02
f_3	2016		0.02

OBSERVATIONS

The paper cone initially bends somewhat locally at the outside diameter (**Fig. 4**) and works inward as frequencies are increased (**Figs. 5 and 6**). The sandwich composite cones tend to distribute the bending load throughout the cone and bends more as a system at all modes. When the core thickness was in the range of 4-8mm, there was a simplifying of the mode shapes. When the core was less than 4mm thick, f_2 resembled f_3 in cones with a core of 4-8mm, illustrating improved damping. Furthermore, the modes (bending frequencies) were spaced farther apart

than with the single laminate hard paper cone, and even farther apart as the core thickness was increased.

The transmission loss through the TEPEX sandwich cone is greater than with paper. This is due to the thickness and low-density, high air cell content, Rohacell core of the structure. This applies to sound pressure inside the enclosure.

This type of composite sandwich cone offers a high degree of inherent design flexibility to the loudspeaker engineer/designer. By changing skin thickness and/or material and/or core thickness and/or grade of Rohacell, a fairly wide range of cone characteristics can be realized.

The cost of TEPEX sandwich type composite cones depends on quantity and material selection; however, clearly this type of composite cone will be more costly than the best paper cone. Carefully designed molded TEPEX sandwich composite cones offer an exciting high-performance alternative to single laminate paper, plastic, or metal cones. Development of new

cones such as these is best done in Asia to help minimize cost and thus offer the technologies to a broader end-user base.

Photos 1 and 2 show two examples of implementation of the types of cones that were presented here, and they are among the most highly respected loudspeaker manufacturers within the industry.

There is additional information available on the development of this 250mm woofer's sandwich composite cone in B&W's 800D development whitepaper, www.bwspeakers.com/downloadFile/technicalFeature/800_Development_Paper.pdf, pages 8, 9, 24, and 25. Frankly, the entire paper is a must read and includes discussions on several other exciting technologies and cutting-edge loudspeaker engineering. **M**

Steve Mowry, president of SM Audio Engineering, has a BS, Business Administration, from Bryant College, and a BS and MS, Electrical Engineering, from URI with high-

est distinction. Steve has worked in R&D at BOSE, TC Sounds, EASTTECH, and P.Audio. Steve is currently an independent consultant/lecturer in project management/transducer and system design. His website is www.s-m-audio.com.

FIGURE 16: First bending mode shape at $f_1 = 1098\text{Hz}$.

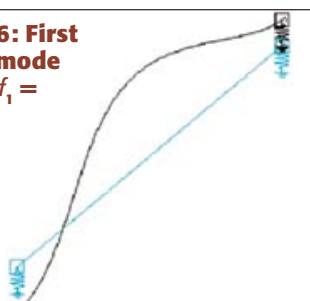


FIGURE 17: Second bending mode shape at $f_2 = 1819\text{Hz}$.

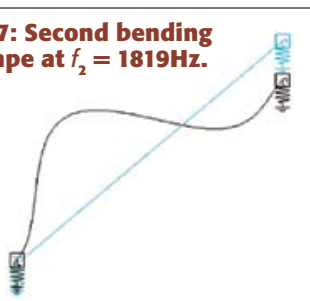


FIGURE 18: Third bending mode shape at $f_3 = 2131\text{Hz}$.

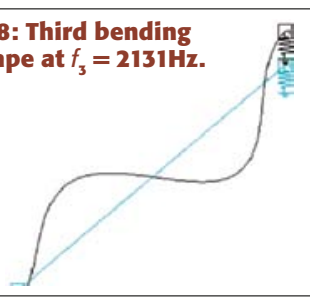


FIGURE 19: First bending mode shape at $f_1 = 1156\text{Hz}$.

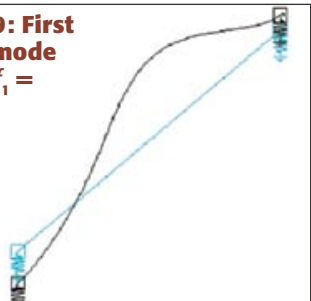


FIGURE 20: Second bending mode shape at $f_2 = 1708\text{Hz}$.

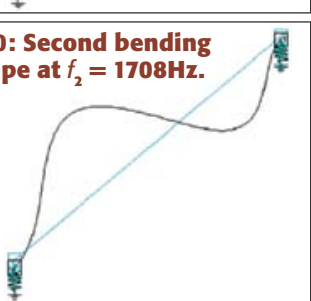


FIGURE 21: Third bending mode shape at $f_3 = 2016\text{Hz}$.

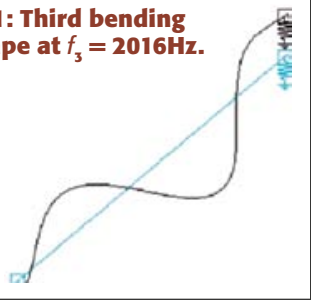


PHOTO 1: B&W 250mm woofer with TEPEX sandwich type Carbon Fiber-TPU/8mm Rohacell 31LS/Carbon Fiber-TPU composite cone.



PHOTO 2: Focal 325mm woofer with sandwich type glass fiber-polymer resin/Rohacell/glass fiber-polymer resin composite "W" cone.



US006219432B1

(12) **United States Patent**
Fryer et al.

(10) **Patent No.:** **US 6,219,432 B1**
(45) **Date of Patent:** **Apr. 17, 2001**

(54) **LOUDSPEAKER DRIVE UNIT**

FOREIGN PATENT DOCUMENTS

(75) **Inventors:** **Peter Alexander Fryer, W. Sussex;**
Stuart Michael Nevill, Kent; Stephen
Philip Barnham Roe, Sussex, all of
(GB)

(73) **Assignee:** **B&W Loudspeakers Limited,**
Worthing (GB)

(*) **Notice:** Subject to any disclaimer, the term of this
patent is extended or adjusted under 35
U.S.C. 154(b) by 0 days.

(21) **Appl. No.:** **09/214,623**

(22) **PCT Filed:** **Jul. 2, 1997**

(86) **PCT No.:** **PCT/GB97/01773**

§ 371 **Date:** **Jan. 11, 1999**

§ 102(e) **Date:** **Jan. 11, 1999**

(87) **PCT Pub. No.:** **WO98/02016**

PCT Pub. Date: **Jan. 15, 1998**

(30) **Foreign Application Priority Data**

Jul. 9, 1996 (GB) 9614395
Apr. 30, 1997 (GB) 9708874

(51) **Int. Cl.⁷** **H04R 25/00**

(52) **U.S. Cl.** **381/398; 381/423; 181/171**

(58) **Field of Search** **381/398, 405,**
381/184, 423, 428, 432, FOR 153; 181/164,
169, 171, 172; 367/174, 163

(56) **References Cited**

U.S. PATENT DOCUMENTS

3,684,052 8/1972 Sotome .
3,862,376 1/1975 White .
4,433,214 2/1984 Jasinski .
4,517,416 * 5/1985 Goossens 381/428
4,547,631 10/1985 Nieuwendijk et al. .
4,821,330 * 4/1989 Pfeleiderer 381/184
5,608,810 * 3/1997 Hall 381/398

0 492 914 A2 7/1992 (EP) .
885501 12/1961 (GB) .
1 270 033 4/1972 (GB) .
1491080 11/1977 (GB) .
1 563 511 3/1980 (GB) .
1604934 12/1981 (GB) .
2087688 5/1982 (GB) .
2 122 453 1/1984 (GB) .
2 153 629 8/1985 (GB) .
2 182 823 5/1987 (GB) .
59-94996 5/1984 (JP) .
59-108500 6/1984 (JP) .
60-192497 9/1985 (JP) .
61-195100 8/1986 (JP) .
5-161193 6/1993 (JP) .
406165291 * 6/1994 (JP) 381/FOR 153
7-015791 1/1995 (JP) .
7-222280 8/1995 (JP) .
WO 83/01884 5/1983 (WO) .

OTHER PUBLICATIONS

M Colloms, "High Performance Loudspeakers", 4th edition,
published 1991, Pentech Press, pp. 166-168.

* cited by examiner

Primary Examiner—Curtis Kuntz

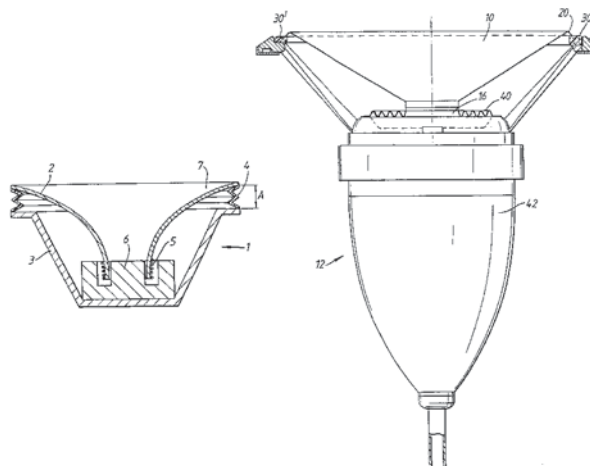
Assistant Examiner—Suhan Ni

(74) *Attorney, Agent, or Firm*—Burns, Doane, Swecker &
Mathis, L.L.P.

(57) **ABSTRACT**

A loudspeaker drive unit (1) comprises a diaphragm (2), a chassis member (3) and a surround (4) connecting the outer portion of the diaphragm to the chassis member in which (i) substantially all parts of the surround (4) located between the diaphragm (2) and the chassis member (3) and capable of radiating sound are arranged parallel or at an acute angle with respect to the longitudinal axis of the loudspeaker drive unit (1), or (ii) the surround is made of a body of foam material (30) arranged to be compressed against the chassis member (32) when the diaphragm (10) moves towards the chassis member, or (iii) the bending wave impedance of the surround (30) is matched to the bending wave impedance of the diaphragm (10).

22 Claims, 3 Drawing Sheets



LOUDSPEAKER DRIVE UNIT

BACKGROUND OF THE INVENTION

1. Field of the Invention

This invention relates to loudspeaker drive units.

2. Description of Related Art

Known loudspeaker drive units comprise a diaphragm of which the outer portion is connected to a chassis member by way of a flexible surround.

The surround stops sound radiated by the rear surface of the diaphragm from passing round the outer edge of the diaphragm and thus cancelling out radiation from the front surface of the diaphragm. The surround allows the cone to move freely in an axial direction but restrains movement of a rocking kind or in a non-axial direction.

The surround thus has an important role in the operation of a loudspeaker drive unit, particularly, if the drive unit is to be used in a hi fi audio system.

In fact, both the surround and the diaphragm influence the quality of sound reproduction from a loudspeaker drive unit and it is exceedingly difficult to come close to an "ideal" loudspeaker drive unit using currently available materials.

OBJECTS AND SUMMARY

It is an object of the invention to provide a loudspeaker drive unit with an improved surround.

In one aspect thereof, the present invention provides a loudspeaker drive unit comprising:

a diaphragm made of a first material;

a chassis member; and

a surround made of a second, different, material connecting the outer portion of the diaphragm to the chassis member; wherein the bending wave impedance of the surround is substantially equal to the bending wave impedance of the diaphragm.

The surround provides mechanical damping to waves of bending that travel up the diaphragm and enter the surround and it reduces the possibility that these waves will be reflected back down into the diaphragm again. This first aspect of the invention is based on the realisation that when the bending wave impedance of the diaphragm is substantially equal to the bending wave impedance of the surround, the matching of the two impedances can avoid the reflection of waves back into the diaphragm again because the diaphragm is correctly "terminated".

The characteristic impedance of a medium is the velocity of the type of wave in question multiplied by the density of the medium. For a bending wave the velocity is given by the following formula:

$$(1.8f^3h)^{0.5}(e/\rho)^{0.25}$$

where ρ =density, e =Young's modulus, h =thickness and f =frequency.

If, for the sake of example, the thickness of the surround was equal to the thickness of the diaphragm but the density of the surround was $\frac{1}{8}$ the density of the diaphragm, and the Young's modulus of the surround was $\frac{1}{8}$ the Young's modulus of the diaphragm, then the bending wave velocity would be the same in both the surround and the diaphragm but the bending wave impedance of the surround would be $\frac{1}{8}$ that of the diaphragm. If the thickness of the surround were now made instead 8×8 (=64) times the thickness of the diaphragm, matching of the bending wave impedances would be achieved.

When bending waves are reflected back into a diaphragm, standing waves tend to appear and the diaphragm seems to "break up" into sections instead of acting uniformly. This "break up" can be avoided by matching the bending wave impedance of the surround to that of the diaphragm.

According to another aspect thereof, the present invention provides a loudspeaker drive unit comprising:

a diaphragm;

a chassis member; and

a surround connecting the outer portion of the diaphragm to the chassis member; wherein the surround is made of a body of foam material arranged to be compressed against the chassis member when the diaphragm moves towards the chassis member.

In such a construction, axial movement of the diaphragm alternately compresses and decompresses the material of the surround rather than bending it as in a conventional surround.

The use of a surround made of a body of foam material arranged to be compressed against the chassis member when the diaphragm moves towards the chassis member provides a particularly effective and practical solution to avoiding sound radiation from the surround and one which lends itself particularly well to matching of the bending wave impedances as in the first-mentioned aspect of the invention.

Preferably, substantially all parts of the surround located between the diaphragm and the chassis member and capable of radiating sound are arranged parallel or at an acute angle with respect to the longitudinal axis of the loudspeaker drive unit.

This aspect of the invention is based on the realization that the surround has its own resonant frequencies and that by arranging that substantially all parts of the surround located between the diaphragm and the chassis member and capable of radiating sound are arranged parallel or at an acute angle with respect to the longitudinal axis of the loudspeaker drive unit the adverse effect of these resonances can be reduced. In such an arrangement sound is not radiated forwards from the surround with the sound from the diaphragm but is directed away to the side or at an angle. The effect of resonances of the surround is therefore less objectionable to a listener positioned in front of the loudspeaker drive unit.

The invention may be applied to either an active loudspeaker drive unit, that is, for example, one with a magnet system and voice coil for driving the diaphragm, or to a passive radiator, that is, a unit in which there is no direct electromagnetic drive to the diaphragm. Passive radiators, sometimes called "drone cones" are used in ports of loudspeaker enclosures.

Preferably, the outer portion of the diaphragm lies axially beyond the chassis member. The diaphragm then lies closest to the listener and the surround is located behind it.

The surround may be joined to the diaphragm at a location spaced from the periphery of the diaphragm. Such a construction enables the diaphragm to be made larger than the surround.

Advantageously, the surround is of integral construction with the diaphragm. By that means problems of making a connection between the surround and the diaphragm can be avoided.

The surround may be made of a resilient polymeric material, for example, rubber, for example, silicone rubber. A surround made of such material has particularly good flexibility.

The surround may be made of a foam material, for example, foam plastics material or foam rubber material. A surround made of such a material has particularly good damping properties.

3

The surround may be made of plastics material.

The surround may be made of a woven material.

Advantageously, the surround is corrugated. That is a simple way of giving the diaphragm freedom to move.

The surround may be substantially "C"-shaped in cross-section and preferably the open mouth of the "C" faces the said axis.

The surround may be substantially ">"-shaped in cross-section and preferably the point of the ">" faces the said axis. Such a construction comprises in effect two straight sections joined by an integral hinge portion.

The surround may be of square cross-section, two opposite sides of the square running substantially parallel to the said axis and the two remaining sides being joined to the diaphragm and chassis member respectively. Such a construction is particularly simple to realize using foam material. The surround may be rectangular instead of square in cross-section.

The surround may be in the form of bellows running substantially parallel to the said axis.

The surround may be in the form of a ring, preferably a ring of hollow cross-section.

The ring may be of circular cross-section or of elliptical cross-section.

The interior of the ring when of hollow form may be sealed and optionally the interior of such a ring is filled with a gas, for example, air. Optionally, the gas is under pressure. Such constructions provide a cushioning effect somewhat analogously to the inner tube of a bicycle tire.

The interior of a hollow ring may instead be open to ambient air by way of slits or holes.

Preferably, the diaphragm is cone-shaped and the periphery of the cone is joined to the flange by a re-entrant portion. Such a construction is particularly well-suited to matching of the bending wave impedances.

The re-entrant portion simply makes an annular indentation in the foam material when it compresses it towards the chassis member.

Preferably, the re-entrant portion makes a circumferential line contact with the body of foam material. Such a construction ensures that very little of the foam material is put into motion by the diaphragm.

The foam material may extend radially further outwardly of the line contact than it does radially inwardly thereof. By that means it is possible to provide a good mounting for the re-entrant portion and to ensure that there is sufficient foam to dissipate the energy of bending waves entering it from the diaphragm.

Preferably, the re-entrant portion is an integrally-formed part of the diaphragm.

Preferably, the diaphragm is made of a resin-impregnated woven plastics material.

As in the first aspect of the invention, the bending wave impedance of the surround is preferably substantially equal to the bending wave impedance of the diaphragm.

The use of the material and dimensions specified in the next five paragraphs, particularly in combination, enables an exceptionally good loudspeaker drive unit, with virtually no "break up" owing to the reflection of bending waves, to be produced.

The plastics material may be Kevlar.

Preferably, the foam material has a Shore hardness in the range 20 to 30.

The diaphragm may have a diameter in the range 100 to 180 centimetres.

Preferably, the thickness of the diaphragm is in the range 0.5 to 1.0 millimeters inclusive.

4

The thickness of the body of foam material may in the range 2 to 10 millimeters inclusive, preferably in the range 3 to 6 millimeters inclusive.

BRIEF DESCRIPTION OF THE DRAWINGS

Loudspeaker drive units constructed in accordance with the invention will now be described, by way of example only, with reference to the accompanying drawing, in which:

FIG. 1 is a diagrammatic cross-section through a first loudspeaker drive unit in accordance with the invention;

FIGS. 2 to 5 show diagrammatically modifications to the drive unit of FIG. 1;

FIG. 6 shows a further modification applied to the drive unit of FIG. 5;

FIG. 7 is a diagrammatic cross-sectional representation of the diaphragm of a second loudspeaker drive unit embodying the invention shown in FIG. 10;

FIGS. 8 and 9 are diagrammatic cross-sectional representations of alternative surrounds for the drive unit of FIG. 10; and

FIG. 10 is a diagrammatic, partly sectional view, of the second loudspeaker drive unit, the right hand side of the figure corresponding to FIG. 9 and the left hand side corresponding to FIG. 10.

DETAILED DESCRIPTION OF THE PREFERRED EMBODIMENTS

Referring to the accompanying drawings, a loudspeaker drive unit 1 is shown in FIG. 1 and comprises a diaphragm 2, a chassis member 3 and a corrugated surround 4. The diaphragm 2 is a cone-type diaphragm and is provided with a voice coil 5 located in an annular gap of a magnet system 6. The central portion of the diaphragm 2 is supported by a so-called "spider" not shown in the figure. The outer portion 7 of the diaphragm lies axially beyond the chassis member 3 by the spacing A.

The surround 4 is in the form of cylindrical bellows running parallel to the central axis of the drive unit 1 and thus effectively all parts of the surround located between the diaphragm 2 and the chassis member 3 and capable of radiating sound are arranged at an acute angle or parallel with respect to the longitudinal axis of the loudspeaker drive unit.

The cylindrical bellows surround 4 is made of any suitable material, for example, plastics, silicone rubber or woven material.

FIG. 2 shows an arrangement in which the bellows surround 4 is replaced by a surround 4A in the form of a ring of hollow circular cross-section. The interior of the ring 4A is sealed and filled with air under pressure.

FIG. 3 shows an arrangement in which the bellows surround 4 is replaced by a surround 4B of integral construction with the diaphragm 2. The surround 4B is substantially "C"-shaped in cross-section and the open mouth of the "C" faces the central axis of the drive unit 1.

FIG. 4 shows an arrangement in which the bellows surround 4 is replaced by a surround 4C that is ">"-shaped (or "V" on its side) in cross-section, the point of the ">" facing the said axis.

FIG. 5 shows an arrangement in which the bellows surround 4 is replaced by a surround 4D of square cross-section, two opposite sides of the square running substantially parallel to the said axis and the two remaining sides being joined to the diaphragm 2 and chassis member 3 respectively. The surround 4D is made of a foam plastics material.

5

FIG. 6 shows a modification to the arrangement of FIG. 5 in which the surround 4D is joined to the diaphragm 2 at a location spaced from the periphery of the diaphragm. This variation may be applied to the surrounds shown in any of FIGS. 1 to 4.

FIG. 7 shows the diaphragm 10 of the loudspeaker drive unit 12 shown in FIG. 10. The diaphragm 10 is made of resin-impregnated woven Kevlar (registered Trade Mark) which is a polyaramide made by Dupont. Suitable discs of resin-impregnated woven Kevlar are available from Messrs Fothergill and Harvey (also known as Cautaults) under the reference D)208/030/9022. Such discs have a weight before resin application of 20 grams per meter and a solvent to resin ratio of 3:2 is used. The resin-impregnated woven Kevlar discs are pressed into the cone-shape shown in the figure and heat treated to harden the resin and lock the cone into shape.

The diaphragm 10 comprises a throat portion 14 for attachment to the voice coil 16 (FIG. 10), a cone portion 18 of 120° conical flare, and a re-entrant portion 20. The overall diameter of the diaphragm 10 is approximately 140 millimeters.

The periphery diaphragm 10 is mounted in the loudspeaker drive unit 12 by either the surround 30 and chassis member 32 shown in FIG. 8 or the surround 30' and chassis member 32' shown in FIG. 9. In FIG. 10, the right hand side of the figure shows the use of the arrangement of FIG. 8 and the left hand side that of FIG. 9.

The surrounds 30 and 30' each comprise an annulus made out of foam material of rectangular section. The foam material used is a low density, very soft foam PVC with a strong acrylic pressure-sensitive adhesive on each of two opposite sides sold, under the trade name Techniseal 110, by Messrs Technibond Ltd, The Valley Centre, High Wycombe, Bucks. Such foam has a Shore 00 hardness of 25, requires a force of 1.5 Newtons per square centimeter to compress it, exhibits a compression deflection of 0.5 Newtons per square centimeter and a compression set of 10% maximum.

The surround 30 is of rectangular section 4.5 millimeters thick and 6 millimeters broad and the surround 30' is of rectangular section 3 millimeters thick and 6 millimeters broad. The surround 30, because of its greater thickness, has a greater bending wave impedance than that of the surround 30' and is also capable of allowing a greater excursion of the diaphragm 10. The surrounds 30 and 30' are suitable for matching the bending wave impedance of a diaphragm 10 which has a thickness in the range 0.5 to 1 millimeters and is of the diameter and shape given above.

The re-entrant portion makes a circumferential line contact with the surround 30, 30' to which it adheres by virtue of the adhesive provided on the foam. As can be seen in FIG. 10, the foam material extends radially further outwardly of the line of contact than it does radially inwardly thereof.

The loudspeaker drive unit shown in FIG. 10 further includes a diaphragm-type suspension 40 for the voice coil 16, an aero-dynamically shaped magnet assembly 42, and a rear support tube 44.

In all of the above constructions, the bending wave impedance of the diaphragm is preferably made substantially equal to that of the surround by an appropriate choice of materials and dimensions. If, however, a less high quality loudspeaker drive unit is all that is required, it is possible to leave the bending wave impedances unmatched.

The invention is also applicable to loudspeaker drive units with dome-type diaphragms.

The first material of which the diaphragm is made may be chemically the same as the second material of which the

6

surround is made but treated differently to modify its physical properties in order to provide stiffness for the diaphragm and flexibility for the surround. For example, the diaphragm may be of a non-foamed plastics material and the surround of the same plastics material in a foamed form.

What is claimed is:

1. A loudspeaker drive unit comprising:

a diaphragm made of a first material;

a chassis member; and

a surround made of a second, different, material connecting the periphery of the diaphragm to the chassis member, the surround being made of a body of foam material arranged to be compressed against the chassis member when the diaphragm moves towards the chassis member; wherein:

the diaphragm is cone-shaped and has a first, narrow end and a second, broad end,

the periphery of the broad end of said diaphragm is joined to the foam by a re-entrant portion, said re-entrant portion extending in a direction toward said narrow end;

the area over which the re-entrant portion makes contact with the body of foam material is substantially a line of contact between the circumference of the diaphragm and the foam material, said line of contact being defined by the re-entrant portion of said diaphragm making contact with said foam material at an angle.

2. A loudspeaker drive unit as claimed in claim 1, wherein the foam material extends radially further outwardly of the line of contact than it does radially inwardly thereof.

3. A loudspeaker as claimed in claim 1, wherein the foam material is a low density, very soft PVC foam material.

4. A loudspeaker drive unit as claimed in claim 1, wherein the diaphragm is made of a resin-impregnated woven plastics material.

5. A loudspeaker drive unit as claimed in claim 1, wherein the surround is of substantially rectangular cross-section and two opposite sides of the rectangle run substantially parallel to the longitudinal axis of the drive unit, and the two remaining sides are joined to the diaphragm and chassis member respectively.

6. A loudspeaker drive unit as claimed in claim 1, wherein substantially all parts of the surround member located between the diaphragm and the chassis member and capable of radiating sound are arranged parallel or at an acute angle with respect to the longitudinal axis of the loudspeaker drive unit.

7. A loudspeaker drive unit as claimed in claim 1, wherein the outer portion of the diaphragm lies axially beyond the chassis member.

8. A loudspeaker drive unit comprising:

a chassis member;

a magnet system mounted on said chassis member;

a cone-shaped diaphragm made of a resin-impregnated woven plastics material, said diaphragm having a first, narrow end and a second, broad end;

a voice coil located on said narrow end of said cone-shaped diaphragm and located in the magnetic field of said magnet system;

a surround member made of a body of low density foam material located on said chassis member; and

a peripheral return portion of said diaphragm directed backwardly generally towards said narrow end and joining said broad end of said diaphragm to the body of foam material and making contact with the body of

7

foam material over a narrow line-like path defined by an angled meeting of the peripheral return portion of said diaphragm with said foam material;

said peripheral return portion and said surround member connecting the broad end of said cone-shaped diaphragm to the chassis member so that said foam material is compressed against the chassis member when the diaphragm moves towards the chassis member.

9. A loudspeaker drive unit as claimed in claim 8, wherein the return portion is an integrally-formed part of the diaphragm.

10. A loudspeaker drive unit as claimed in claim 8, wherein the plastics material is a polyamide plastics material.

11. A loudspeaker drive unit as claimed in claim 8, wherein the surround member is of oblong cross-section.

12. A loudspeaker drive unit as claimed in claim 8, wherein substantially all parts of the surround member located between the diaphragm and the chassis member and capable of radiating sound are arranged parallel or at an acute angle with respect to the longitudinal axis of the loudspeaker drive unit.

13. A loudspeaker drive unit as claimed in claim 1, wherein the outer portion of the diaphragm lies axially beyond the chassis member.

14. A loudspeaker drive unit comprising;

a chassis member;

a magnet system mounted on said chassis member;

a diaphragm;

a voice coil located on said diaphragm and located in the magnetic field of said magnet system; and

a surround member made of a body of low density foam material located on said chassis member;

said surround member connecting the outside of said diaphragm to the chassis member so that said foam material is compressed against the chassis member when the diaphragm moves towards the chassis mem-

8

ber and said foam material providing a terminating impedance so matched to the bending wave impedance of the diaphragm as to prevent bending waves traveling in the diaphragm from being reflected back into said diaphragm by said foam material.

15. A loudspeaker drive unit as claimed in claim 14, wherein said diaphragm is cone-shaped and a peripheral return portion of said cone joins the outer end of said cone to the body of foam material and makes contact with the body of foam material over a narrow line-like path.

16. A loudspeaker drive unit as claimed in claim 14, wherein the foam material has a Shore hardness in the range 20 to 30.

17. A loudspeaker drive unit as claimed in claim 14, wherein the surround member is of square cross-section.

18. A loudspeaker drive unit as claimed in claim 14, wherein substantially all parts of the surround member located between the diaphragm and the chassis member and capable of radiating sound are arranged parallel or at an acute angle with respect to the longitudinal axis of the loudspeaker drive unit.

19. A loudspeaker drive unit as claimed in claim 14, wherein the surround member is made of foam plastics material.

20. A loudspeaker drive unit as claimed in claim 14, wherein the diaphragm is made of a resin-impregnated woven plastics material.

21. A loudspeaker drive unit as claimed in claim 14, wherein the outside of said diaphragm contacts said surround member at an angle to define a line of contact therewith.

22. A loudspeaker drive unit as claimed in claim 14, wherein said diaphragm has first and second ends, said outside is at the second end of said diaphragm, and said outside of said diaphragm comprises a portion directed generally backwards towards said first end of said diaphragm.

* * * * *

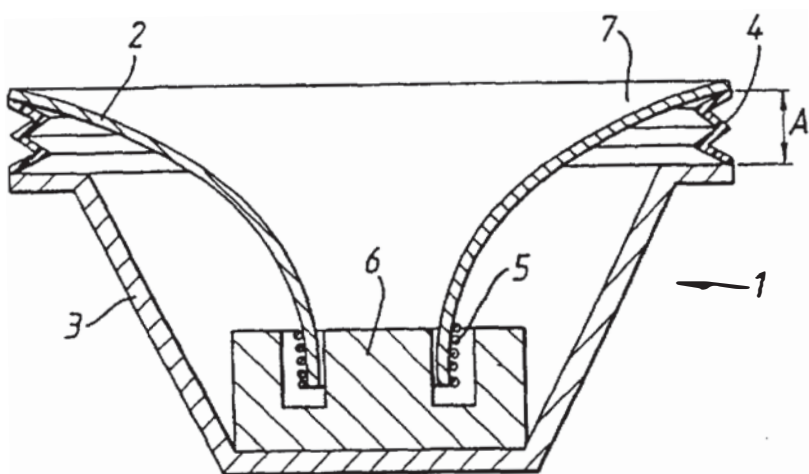


Fig. 1

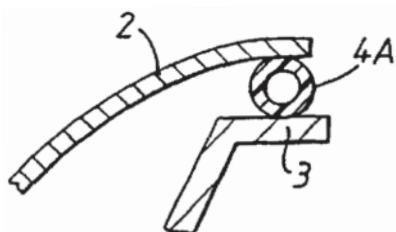


Fig. 2

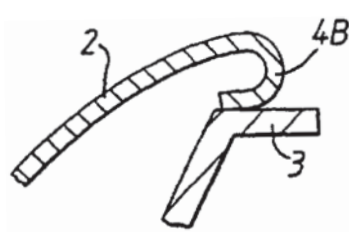


Fig. 3

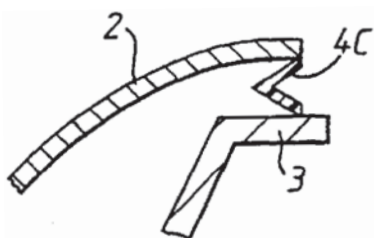


Fig. 4

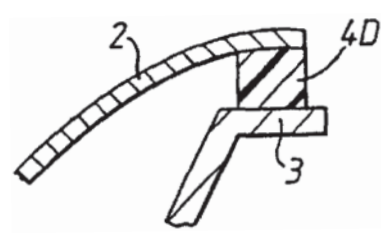


Fig. 5



Fig. 6

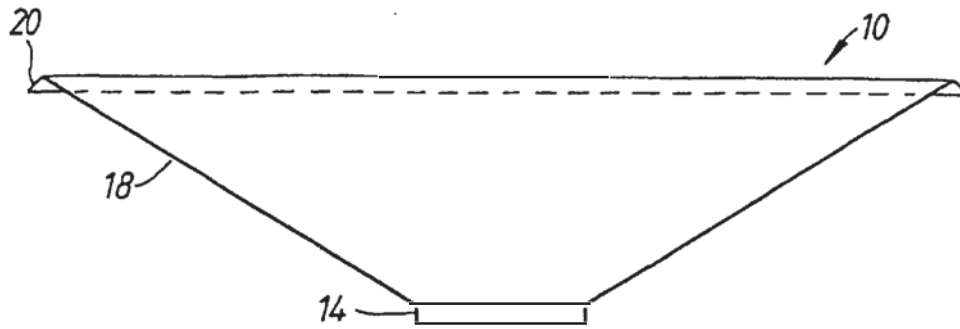


Fig. 7

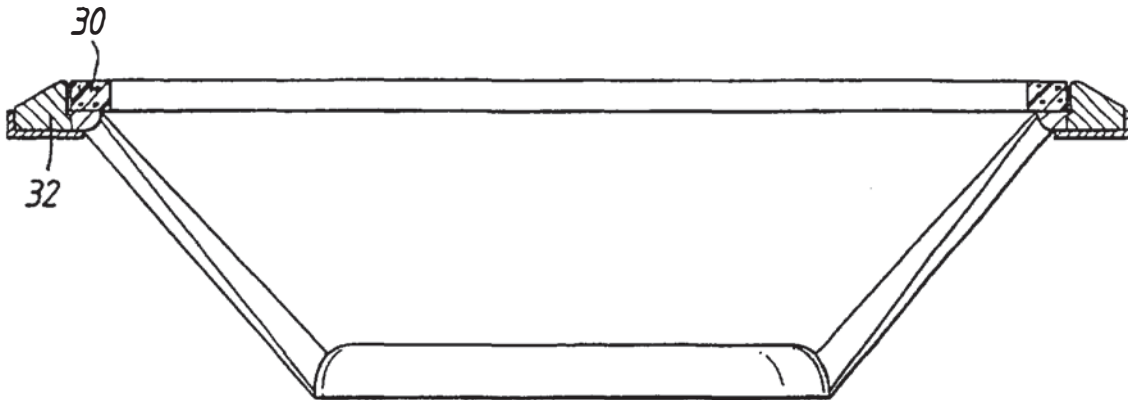


Fig. 8

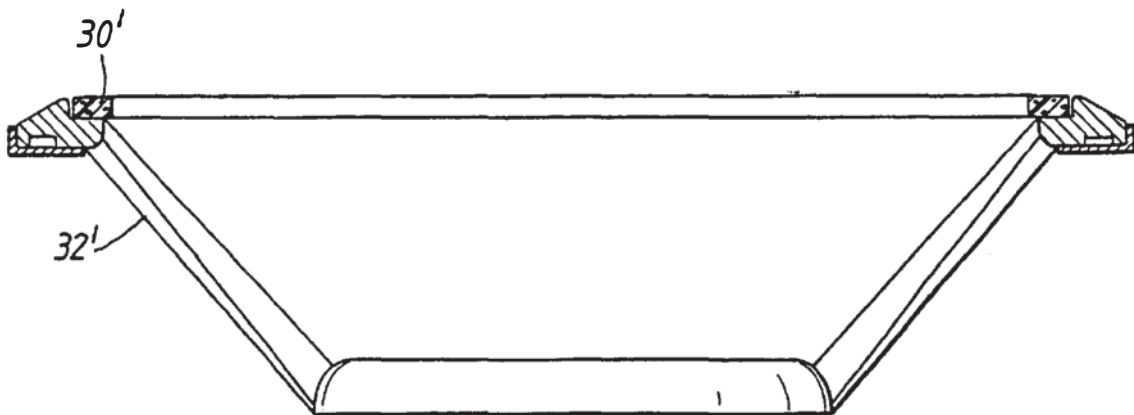


Fig. 9

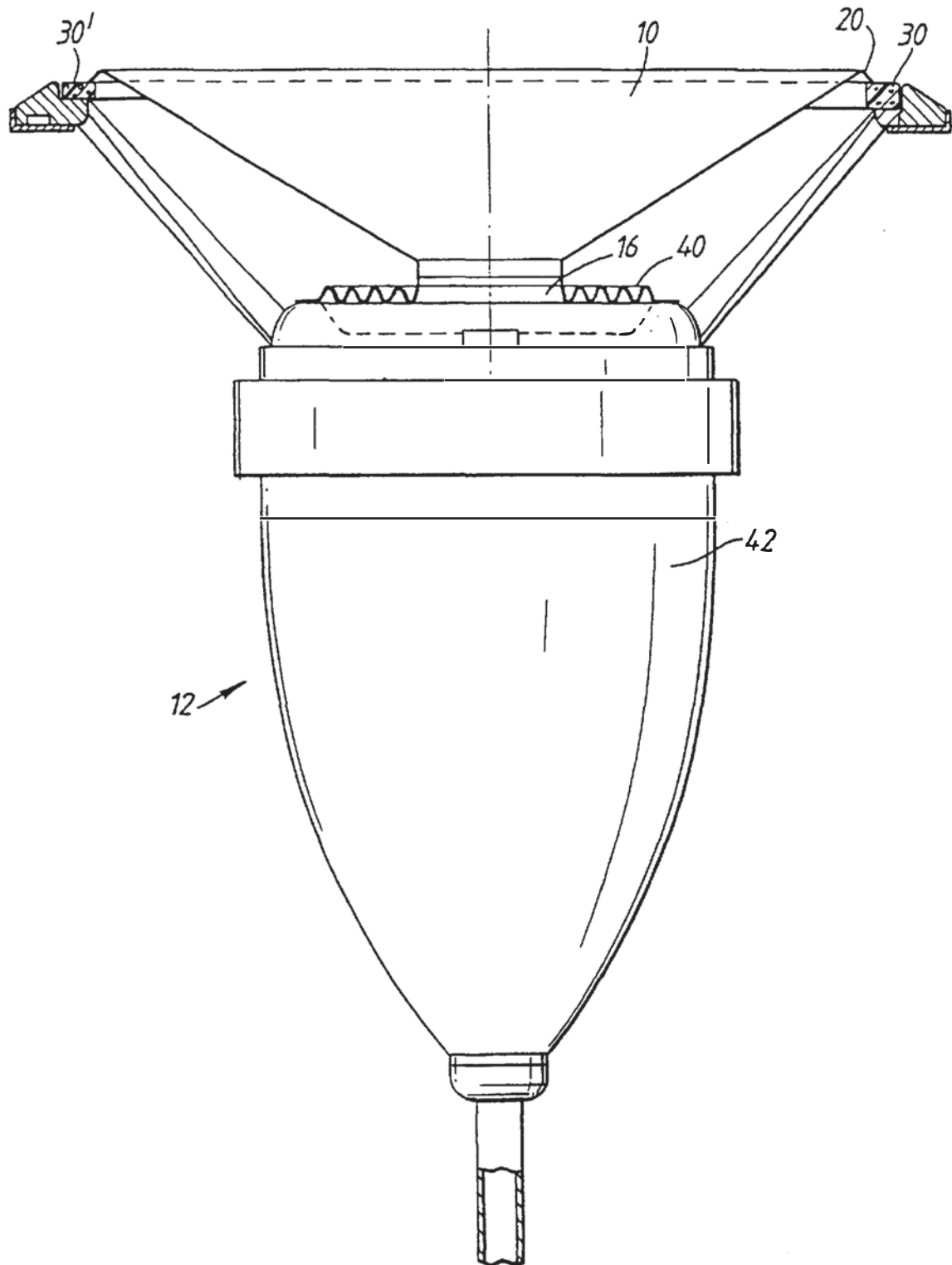


Fig.10

Diamond loudspeaker cones for high-end audio components

E. Wörner^{1*}, C. Wild¹, W. Müller-Sebert¹, P. Koidl¹ and A. Bankewitz²

¹ Fraunhofer-Institut IAF, Tullastr. 72, 79108 Freiburg, Germany

² Thiel & Partner GmbH, Kantstr. 1, 50259 Pulheim, Germany

eckhard.woerner@iaf.fraunhofer.de

Keywords: CVD diamond, membrane, loudspeaker, acoustical simulation

Abstract

Conventional loudspeaker membranes made of metal or synthetic material such as fabric, ceramics or plastics suffer from nonlinearities and cone breakup modes at fairly low audio frequencies. Due to their mass, inertia and limited mechanical stability the speaker membranes made of conventional materials cannot follow the high frequency excitation of the actuating voice-coil. Low sound velocity causes phase shift and sound pressure losses due to interference of adjacent parts of the membrane at audible frequencies.

Therefore, loudspeaker engineers are searching for lightweight but extremely rigid materials to develop speaker membranes whose cone resonances are well above the audible range. With its extreme hardness, paired with low density and high velocity of sound, diamond is a highly promising candidate for such applications.

We report on the realization of dome shaped CVD diamond membranes by deposition on curved silicon substrates. Domes with diameters between 20 and 65 mm and with a thickness ranging from 50 to 120 μm were prepared. After deposition, the substrate is dissolved and the rim of the diamond dome is cut by laser scribing. Free standing diamond membranes are mounted onto dynamic voice coils and integrated into tweeter and/or midrange driver chassis. Extended tests and optimisations led to loudspeaker systems that show a second and third harmonic distortion behaviour in the important frequency range between 3 to 10 kHz that is reduced by 40% in comparison to already excellent established values obtained with sapphire membranes. Cone resonance frequencies of CVD diamond membranes are increased by a factor of two, as predicted by simulations.

Introduction

Diamond membranes – in theory – have always been the dream of loudspeaker engineers since the mechanical properties of diamond are close to those of an ideal hypothetical material which would have an infinite Young's Modulus and – at the same time – a vanishing density. However, since nature doesn't offer diamond in the shape of membranes and the *High Pressure High Temperature* synthesis only provides small crystallites, acoustic engineers were compelled to use ordinary materials like aluminium or sapphire for high end tweeters.

With the development of CVD technologies to produce large area diamond discs with properties matching those of the best natural diamonds [1,2] and molding techniques to deposit CVD diamond on preshaped substrates [3,4,5], diamond domes for loudspeaker applications became feasible. After early suggestions by Sumitomo [6] no further development was done until in 1999 when Fraunhofer IAF and Thiel & Partner GmbH, an audio equipment manufacturer specialized in hard material loudspeaker membranes, entered a cooperation aiming to develop a novel high frequency tweeter with a diamond membrane. This cooperation succeeded in launching its first commercial tweeter system in the year 2000. Nowadays leading audio system manufacturers such as Avalon Acoustics (USA), Lumen White (Austria), Mårten Design (Sweden) and Kharma (Netherlands) are using these tweeters for their high end loudspeaker systems

In this paper we describe the deposition and machining of a diamond membrane, its mounting on a voice-coil and its integration into tweeter chassis. We will assess the mechanical and acoustical properties of these systems by FEM simulations and compare their result with sound pressure measurements. Finally we will discuss the effect of frequencies above the audible range (>20 kHz) on the auditor.

Preparation of CVD diamond tweeter membranes

To prepare dome shaped diamond membranes, polycrystalline CVD diamond is deposited onto preshaped substrates. The possibility to make three dimensional diamond devices by simply replicating a substrate has been used by a number of scientists to create for example anti reflection structures by the moth eye effect [4] or optical diamond lenses e.g. for CO₂-laser surgery [3]. For these kinds of applications generally silicon is used as a substrate since it is easy to machine and polish, it enables the nucleation of diamond and is easily dissolved in acid after diamond deposition. Figure 1 illustrates the processing steps to prepare dome shaped CVD diamond membranes.

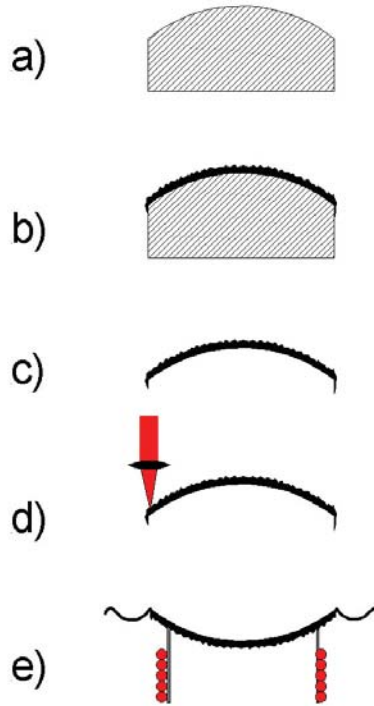


Fig.1: Processing steps to prepare dome shaped CVD diamond tweeter membranes. a) preshaped silicon substrate. b) substrate after deposition of CVD diamond. c) diamond dome after separation from the substrate. d) laser cutting of diamond dome. e) diamond membrane assembled with surround and voice coil former.

For growing thick free standing CVD diamond, a microwave plasma CVD reactor with ellipsoidal cavity [7] that provides stable deposition conditions is used. As standard growth conditions we use a microwave power of 6 kW at a frequency of 2.45 GHz, a substrate temperature between 700 and 900°C and a pressure ranging from 100 to 200 mbar. The feed gas is 1-2% methane in hydrogen. After CVD diamond deposition (Fig.1b) the silicon substrate is dissolved in acid (Fig.1c) and the rim of the now free standing membrane cut using a Nd:YAG laser scribe (Fig.1d). As a last step the completely machined membrane (Fig.1e) is mounted onto a voice-coil, fixed with a surround and integrated into a tweeter and/or midrange loudspeaker driver chassis (Fig.2).



Fig.2: Free standing dome shaped CVD diamond membranes (front) and a D20-tweeter from Thiel & Partner equipped with a CVD diamond membrane.

Mechanical and acoustic properties of diamond tweeters

To describe the acoustic properties of loudspeakers, a commercial finite element modeling program (*Finecone*) that calculates amplitude response and impedance in radial symmetry was used. As a matter of fact, there are also non axial-symmetric modes present, but since these are higher in frequency than the cone breakup (i.e. the first and dominant natural oscillation of the membrane voice coil configuration), these do not play a dominant role and therefore we do not want to go in further detail here. As a first approach and to check the reliability of these simulations, the resonance frequencies f_n of a flat membrane that are given analytically by [8]:

$$f_n = \frac{k_n}{2\pi} \sqrt{\frac{Et^3}{12\rho r^4(1-\nu^2)}} \quad (1)$$

were calculated.

In equation (1) r is the radius and t the thickness of the membrane, E its *Young's Modulus*, ν its *Poisson's Ratio* and ρ its density. k_n is the constant for the n^{th} natural oscillation ($k_1 = 10.2$, $k_2 = 21.3$, $k_3 = 34.9$, ...). According to equation (1) the natural frequencies are proportional to the square root of E/ρ , i.e. a good membrane should be stiff and light. For a flat 60 μm thick diamond membrane 20 mm in diameter with $E = 1140 \text{ GPa}$, $\nu = 0.1$ and $\rho = 3.51 \text{ g/cm}^3$, the first natural frequency occurs according to (1) at a frequency of as low as 5.09 kHz. For a simple rim-supported membrane the simulated result equals exactly the one analytically postulated. A real tweeter membrane however is not free standing but attached to a voice-coil former and clamped to a centralizing surround, both adding mass and increased damping to the whole structure. A cross section of a typical configuration used for simulations with *Finecone* is shown in figure 3.

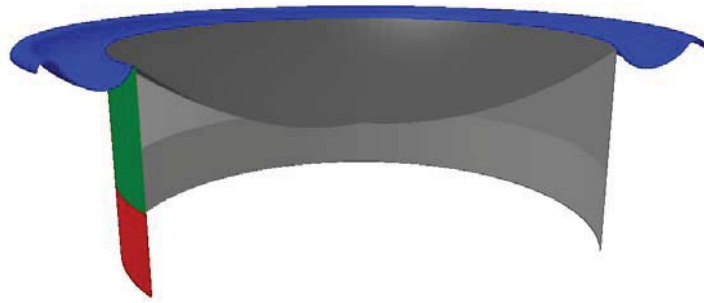


Fig.3: Cross section through a tweeter membrane attached to a former (green) on top of an actuating voice-coil (red) and clamped to a surround (blue).

For the fixed membrane, the cone breakup occurs at a lower frequency, basically due to the fact that combined oscillations of former and dome are lower in frequency than oscillations of the isolated dome itself. Besides the material of the membrane, also its geometry and the properties of the attached surround and voice coil former play a crucial role for its overall performance. The sag height of the membrane has a very strong influence on the sound pressure level (SPL). Figure 4 displays the frequency dependence of the calculated SPL for diamond tweeter membranes fixed as shown in figure 3 for various sag heights.

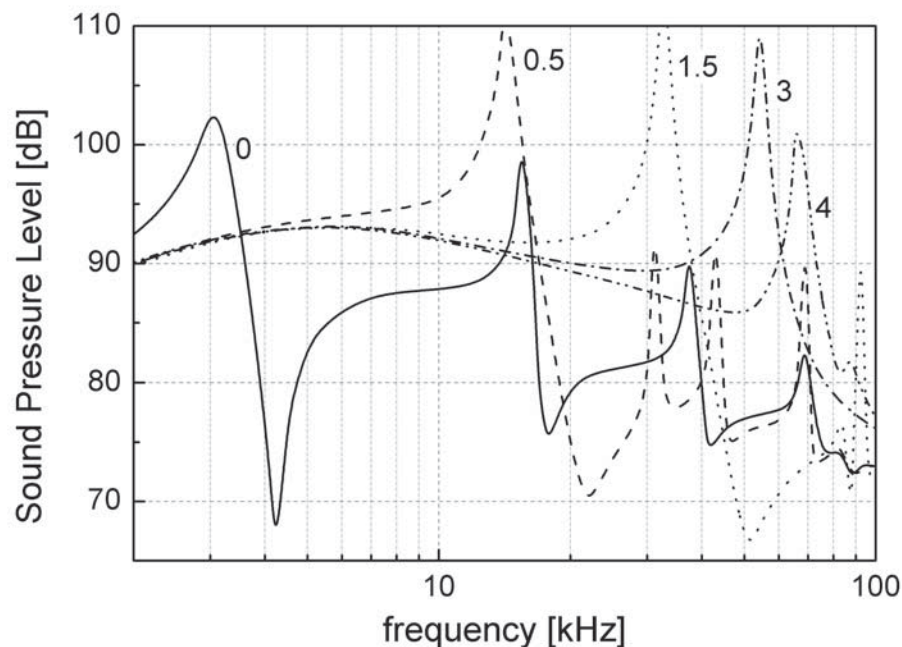


Fig.4: Sound pressure level (SPL) in a distance of 1m vs. frequency for a 20 mm diamond membrane with increasing sag height ranging from a flat membrane to a membrane with a sag height of 4 mm.

Although flat membranes would be highly desirable in terms of vanishing *phase loss* (see below) figure 4 clearly states that the sag height has a strong influence on cone breakup frequencies and high frequency SPL. A comparatively moderate sag height of 0.5 mm increases the frequency of the first cone breakup almost by a factor of 5 from 3 kHz to 14 kHz with further increase to almost 70 kHz given a sag height of 4 mm. Inversely proportional to the sag height appears the high frequency SPL and the peak energy of the cone breakup, suggesting an optimum of 3.0 to 3.5 mm sag height. Cone breakup modes are always associated with a significant increase in harmonic and non-linear distortion, also with undesired lobing of sound pressure. In terms of sonic quality therefore cone breakup modes should be pushed as far away as possible from the audible range to avoid any kind of subharmonic interference.

The membrane thickness has a moderate influence on the SPL, the thicker and thereby stiffer the membrane, the higher the cone breakup, which is desirable. However for a thicker and heavier membrane the total SPL is reduced; an optimum can be found for the D20-tweeter in between 50 and 60 μm . Figure 5 compares the SPL of an aluminium, a diamond and a infinitely stiff dome (\varnothing : 20 mm, $h = 3.5$ mm) of the same mass. Surprisingly at first sight is the fact that the infinitely stiff membrane shows a pronounced dip in the response around 90 kHz. This is a result of phase interferences or phase losses, i.e. for inverted dome shaped membranes matters that the sound generated at the centre of the membrane reaches the auditor later than the sound generated at the rim, thus enabling the sound waves to interfere and extinguish each other at certain frequencies. This effect is strongest if the competing regions have about the same area.

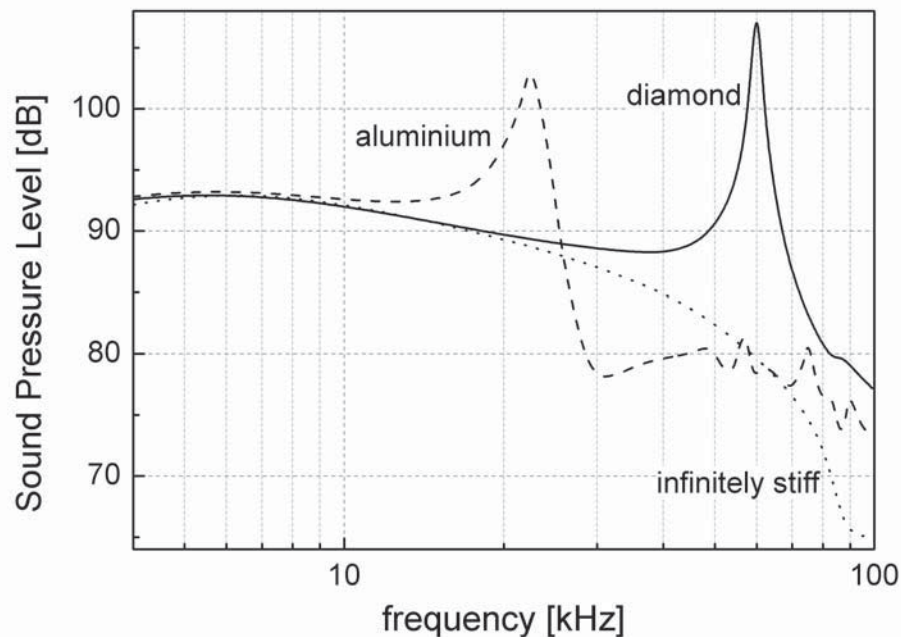


Fig.5: SPL vs. frequency for an aluminium, a diamond and an infinitely stiff membrane, all of the same mass.

In the case of diamond, the cone breakup at 60 kHz overrides phase losses and as a result prevents the sound pressure from decreasing. The aluminium dome suffers from cone breakup at a rather low frequency of 22 kHz although this is well above the audible range. We will discuss in the next section whether or not this has an influence on the auditor.

Figure 6 finally shows the measured sound pressure level and total harmonic distortion (THD) for D20-6 tweeter with a diamond membrane. As predicted by theory, the cone breakup occurs at a frequency of around 65 kHz.

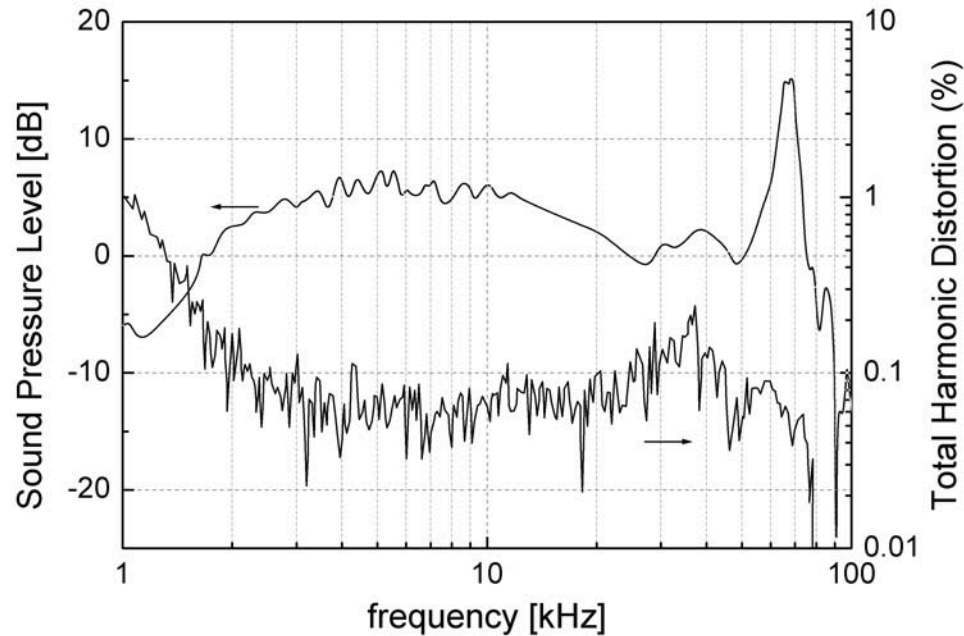


Fig.6: Sound Pressure Level and Total Harmonic Distortion vs. frequency of a D20-6 tweeter, measured with B&K 4138 microphone in app. 10 cm of distance and R&S UPD Analyzer processing.

One of the most crucial features of the diamond membrane is the fact that the harmonic distortion is greatly reduced as can be seen from figure 6. In the most important range from 3 kHz to 10 kHz, the total harmonic distortion in general is below 0.1 % with the exception of occasional spikes. The mean smoothed value is near 0.07 %, a value we have not been able to achieve with even the best conventional tweeters. Common THD values of ordinary tweeters are one order of magnitude higher.

Commercially available domes have sizes of 20 mm, 25 mm, 30 mm and 50 mm. Laboratory samples of 63 mm diameter have been produced. As expected, a similar picture as for the mentioned 20 mm domes appears with larger cones. Figure 7 shows measured and simulated SPLs of a 50 mm diamond and sapphire cone. In good agreement with the simulation, the cone breakup occurs for the diamond dome at about 30 kHz, almost one octave higher than for the sapphire cone of the same size. In addition the total harmonic distortion (THD) of a diamond cone is way better than with any kind of conventional membrane material, thus improving the sonic quality of mid frequencies.

Since the large diamond cone still has a bandwidth that reaches well above the audible range, it can be used as tweeter with a very low cross-over point. Frequencies as low as 400 Hz appear possible, thus coming closer to the ideal sound transducer: a single-point, time-coherent minimal-phase system covering the entire audio band.

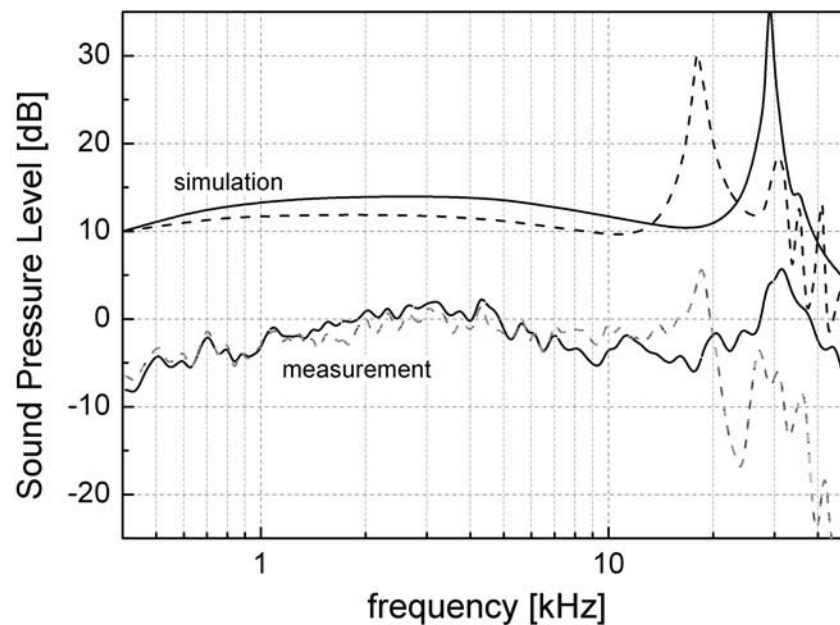


Fig.7: Measured and simulated (20 dB offset) SPL vs. frequency for a diamond (solid) and a sapphire midrange driver (dashed), both 50 mm in diameter.

Conclusions

Membranes made of CVD diamond enable audio frequencies of up to 100 kHz to be transmitted, values that are not achievable with any other material.

So far, the question whether or not frequencies above 20 kHz have any influence on the auditor had been of concern only for a few high end audiophiles, who do not use conventional CDs containing almost no acoustic information above 20 kHz. However the breakthrough for SACD and DVD audio format with sampling rates of 192 kHz or higher is only a matter of time. Do we all need to buy new speakers with diamond tweeters?

The perception of frequencies beyond 20 kHz has been lively discussed in the past. It is common understanding now among audiophiles that extended reproduction chains improve the overall performance. The degree of frequency extension and the influence on clarity, ambience and neutrality are still controversially disputed. However various researchers proved that orchestral music contains significant spectral energy in frequencies up to 100 kHz, Oohashi [9] provided evidence that inaudible high-frequency sounds have a significant effect on human brains. This has been called “the hypersonic effect”. Although more research has to be done on the influence of ultrahigh frequencies on the auditor, the audio community agrees on the fact that systems that are linear up to highest frequencies sound more detailed, effortless and produce a more realistic sound stage. This is mirrored by the steadily growing demand for speakers with diamond membranes.

References

-
- ¹ E. Wörner, Thermal Properties and Applications of CVD Diamond, Low Pressure Synthetic Diamond: Manufacturing and Application, eds. B. Dischler and C. Wild, Springer, Heidelberg, Germany, (1998) p. 165
 - ² C. Wild, CVD Diamond for Optical Windows, Low Pressure Synthetic Diamond: Manufacturing and Application, eds. B. Dischler and C. Wild, Springer, Heidelberg, Germany (1998) p. 189
 - ³ E. Wörner, C. Wild, W. Müller-Sebert and P. Koidl, Diamond Relat. Mater. Vol. 10 (2001) p. 557
 - ⁴ V. Ralchenkov, I. Vlasov, V. Konov, A. Khomich, L. Schirone, G. Sotgiu and A.V. Baranov, *Proc. Applied Diamond Conference / Frontier Carbon Technology'99*, eds. M. Yoshikawa et al., Tsukuba, Japan (1999) p. 128
 - ⁵ H. Björkman, P. Rangsten, U. Simu, J. Karlsson, P. Hollman and K. Hjort, *MEMS'98*, Heidelberg, Germany (1998) p. 34
 - ⁶ Japanese Patent Office: JP59143499A2
 - ⁷ M. Fünér, C. Wild and P. Koidl, Appl. Phys. Lett. Vol. 72 (1998) p. 1149
 - ⁸ W.C. Young: *Roark's Formulas for Stress and Strain* (McGraw-Hill Inc., New York, 1975)
 - ⁹ T. Oohashi et al, J. Neurophysiol. Vol. 83 (2000), p. 3548